mgen(doc)

BIAXIAL BENDING OF L-SHAPE REINFORCED CONCRETE COLUMN SECTIONS

by

MOHAMMED T. ABU AL-KHAIL

A thesis
presented to University of Ottawa
in partial fulfillment of the
requirements for the degree of
Master of Engineering
in
DEPARTMENT OF CIVIL ENGINEERING

ABSTRACT

A computer program was developed to determine the interaction curves and the isoload contours for L-Sections reinforced concrete columns. The program used the generally accepted assumption of plane sections remaining plane, but the maximum limiting concrete strain was a variable parameter. The isoload contours are relatively smooth curves with deviations only occurring in cases where the neutral axis is parallel to a major dimension of the section. This deviation from the general shape of the curve increases as the allowable concrete strain is increased and as the section is subjected to more compression. The ultimate biaxial moments increase by 3 to 6% (depending on the load level) when the maximum allowable concrete strain is increased from 0.003 to 0.004 . The ultimate biaxial curvatures increase by 35 to 48% (depending on the load level) when the maximum allowable concrete strain is increased from 0.003 to 0.004.

ACKNOWLEDGEMENTS

The author wishes to convey his sincere appreciation to professor N.J. Gardner for his guidance and interest during the course of this study. It has been a privilege and a pleasure to work under his supervision.

The author also takes this opportunity to thank all his teachers at Baghdad College (Baghdad-Iraq), Lisgar Collegiate Institute (Ottawa-Canada), and the faculty and staff members of the Department of Civil Engineering at the University of Ottawa (Ottawa-Canada).

Last but not least important, the author wishes to express his appreciation to his family for support and encouragement.

PREFACE

One of the program sessions at the 1981 American Concrete Institute fall convention held in Quebec city was on the behaviour of reinforced concrete columns. One paper presented by Mr. Mohammed Iqbal[1] entiled "NON-RECTANGULAR COLUMN AND SHEARWALL SECTIONS WITH BIAXIAL BENDING", dealt with the behaviour of columns of various cross-sections when subjected to biaxial bending. The paper used the well established numerical summation method[2] to develop interaction diagrams and isoload contours. Figure 8 of appendix A shows that the isoload contours of an L section show a sharp re-entrant discontinuity at the axis of symmetry. From the same FIGURE, it is seen that the magnitude of the discontinuity is of the order of 25 percent. This result would not be expected as it is untypical of the behaviour of more conventional cross-sections. Previous research on square column sections subjected to biaxial bending revealed that :-

1. For square column sections reinforced on four faces ;
   a) If bending resistance at a particular load level is constant for angles of eccentricity, the contour line would approach a circular arc.

---

[1] Refer to appendix A

[2] Also referred to as the finite method

b) Deviations from the circular arc appear to be largest in regions of maximum moments.

2. For square column sections reinforced on two faces ;

a) The isoload contours can be approximated by an elliptical arc.

b) The maximum deviations from the elliptical arc appear to be largest in regions of maximum moments.

Then one can expect the isoload contours for the L shaped column section to be of a less regular shape, but there is no apparent reason for expecting a sudden change in the value of the ultimate bending moment.

It is the purpose of this study to investigate the shape of the isoload contours for the same L shaped column section used by Mr. Mohammed Iqbal. Also the effects of changing the maximum allowable concrete strain on the ultimate biaxial bending moments and curvatures are investigated.

CONTENTS

Appendix

Chapter I

INTRODUCTION

1.1 FORWORD

Columns in reinforced concrete structures are usually cast in-situ and continuous with the beams and slabs comprising the floor components. Because of the resulting end constraint in two directions, the columns are almost invariably subjected to biaxial bending combined with compression. A good example for which the biaxial bending moments can be critical is the external corner column. The most commonly used cross-sections are the circular, the square, the rectangular, and the "L-shaped" sections.

Analysis and design of column sections subjected to biaxial bending are difficult because a trial and error procedure is necessary to find the inclination and location of the neutral axis that satisfies the equilibrium equations.

The strength of columns subjected to biaxial bending can be illustrated by interaction surfaces. By varying the inclination of the neutral axis, it is possible to obtain a series of interaction diagrams at various angles to the major axes of the section. A typical set of interaction diagrams is shown in FIGURE 1.1.1, and a complete set of diagrams for all inclinations of the neutral axis will describe

the interaction surface. Each point on this surface represents one particular set of axial load Pu, and moments about the major axes Mux, and Muy, which will together produce the failure surface of the section. It is well known that the interaction surface depends on the geometry of the section, the concrete strength, the steel strength, the steel arrangment, and the concrete cover.

If a horizontal section is taken through the interaction surface, the interaction line obtained gives the possible combinations of Mux, and Muy that would cause failure at a given axial load Pu. This line is a constant load (isoload) contour of the interaction surface.

1.2 REVIEW OF PREVIOUS WORK

1.2.1 Properties of Concrete

Concrete is a heterogeneous, viscoelastic material which can sustain compression but very little tension. To simplify analysis, concrete is generally idealised as a homogeneous isotropic material having no tensile strength, and creep buckling effects are not quantitatively considered. In flexural problems it is also generally assumed that the effect due to the strain gradient can be ignored, i.e. the stress strain behaviour in flexure is assumed to be identical with that for uniform compression. The actual non-linear and strain-softening nature of the curve must be considered when applying the general column theory to reinforced concrete columns.

The concrete stress-strain curve is non-linear and has a falling branch; it exhibits a distinct maximum stress after which the stress decreases while the strain increases. The initial modulus of elasticity and the maximum stress are generally related to the strength of standard test specimens; cubes, cylinders and prisms are all used. The stress-strain curve can be determined either indirectly from the flexure test of a reinforced concrete member, or directly from the compression test of a plain concrete specimen.

Tests on reinforced concrete beams have shown that the concrete on the compression face tends to crush and spall off at an ultimate strain lying between 0.003 and 0.004. Many investigators have assumed that this is the maximum compressive strain to which concrete can be subjected. From tests on vertically cast, short eccentrically loaded reinforced concrete columns, Hognestad deduced a stress-strain curve for concrete in flexure which has been used by most subsequent American workers. The rising branch of the curve is represented by a parabola and the falling branch by a straight line, with a cutoff at an ultimate strain of 0.0038. The maximum stress is taken as 85 percent of the cylinder strength and the initial modulus as a simple linear function of the maximum stress.

When plain concrete specimens are tested in compression, they tend to crush suddenly at a strain of 0.002-0.0025. It has been shown, however, that such failures are generally

due to a sudden release of energy from the testing machine, which is not suitably stiff, into the specimen as the concrete reaches the falling branch of the stress-strain curve.

1.2.2 Short Reinforced Concrete Columns Subjected to Biaxial Bending

Many investigations to determine the ultimate strength of reinforced concrete members subjected to biaxial bending with compressive force have been conducted in the last few decades.

In this section a review of some of the methods proposed for the analysis and design of biaxial bending of reinforced concrete columns will be summarized. It should be noted that all the methods which will be presented deal with relatively short columns for which the effect of lateral deflection on the magnitude of bending moments is negligible. Furthermore, effects of sustained loading and reversal of bending moments are not considered.

In 1958 Au presented a trial and error procedure for designing rectangular columns subjected to axial load and biaxial bending moments. The equations of equilibrium were derived for the three possible cases of the location of the neutral axis :

1. Section with the neutral axis intersecting opposite sides of the section (FIGURE 1.2.2.1a).
2. Section with the neutral axis intersecting adjacent sides of the section, the compression zone is less

than half the total area of the section (Figure 1.2.2.1b).

3. Section with the neutral axis intersecting adjacent sides of the section, the compression zone is greater than half the total area of the section (Figure 1.2.2.1c).

The compatibility equation is only required when the compression failure prevails, and is easily formulated by assuming a linear strain relationship. Since the problem involves solution of non-linear simultaneous equations in each case, the numerical computation in general is tedious, particularly if several repetitions are required. To avoid this problem Au provided charts for each of the three possible neutral axis positions to simplify the operation.

In 1960, Bresler suggested two approximate methods for calculating the failure load of short columns under biaxial eccentricities from the failure loads of the same section under uniaxial eccentricity. The first of these methods was called the reciprocal thrust relationship,

$$\frac{1}{P_I} = \frac{1}{P_X} + \frac{1}{P_Y} - \frac{1}{P_0} \qquad (1.2.2.1)$$

where P_I = ultimate load subjected to biaxial eccentricities e_x and e_y simultaneously,

P_X = ultimate load subjected to eccentricity e_x only,

P_Y = ultimate load subjected to eccentricity e_y only,

P_0 = axial ultimate load (squash load).

The advantages of the above method is that it is simple in form, all the parameters are determined in a simple manner, and it yields good results for common column shapes.

The second method was called the elliptical moment ratio function,

$$\left(\frac{M_X}{M_{X0}}\right)^{\alpha} + \left(\frac{M_Y}{M_{Y0}}\right)^{\beta} = 1.0 \qquad (1.2.2.2)$$

where M_X, M_Y = design ultimate moments,

M_{X0}, M_{Y0} = ultimate uniaxial bending capacities,

α, β are empirical constants depending on column dimensions, amount and distribution of the steel reinforcement, stress-strain characteristics of steel and concrete, amount of concrete cover, and size of lateral ties or spirals (Bresler reported that the calculated values of to vary from 1.15 to 1.55).

In 1961, Furlong studied the ultimate theoretical capacity for square, tied columns to carry biaxially eccentric compressive loads. Columns with equal amounts of steel reinforcement in each of the four faces were studied, and data were presented for such columns and for square columns with steel reinforcement in opposite faces only. Furlong noted that with a maximum extreme failure strain of 0.003 in compression, and the accepted assumptions that plane sections

before bending remain plane after bending, it is possible for any assumed neutral axis to describe strains at all points of the cross section. Furlong also noted that Whitney's rectangular stress block is probably the most convenient aid in estimating the volume and locating the centroid for a stress "wedge" of concrete at failure conditions. Furlong cited Rusch in stating that the ultimate concrete strain exceeds the 0.003 values in cases where the maximum strains exist only at one point representing the apex of a triangular area, but noted that by using the 0.003 value and a constant maximum stress throughout the triangular area yields reasonable and safe results since the area of application of the stress is smaller than the actual stressed area to be expected at failure. Furlong generated the interaction digrams by calculating the ultimate forces and moments corresponding to several neutral axis positions and inclinations. Upon analyzing the data, Furlong made the following conclusions :

1. The capacity of square reinforced concrete columns to eccentric compression loads is a maximum when the load causes bending about the major axis of the cross section.
2. The capacity of columns to resist moments about any axis is virtually constant for eccentricities less than one-tenth of the thickness of the column.

3. The capacity of square columns with equal amount of steel in each of the four faces to resist eccentric compression loads is smallest when load causes bending about an axis at 45 degrees from the major axis.

4. Design ultimate moment capacity for square columns at a particular load Pu should in no case exceed the limits of an ellipse whose axis are the ultimate moment capacities when the load Pu acts along the principal axes of the column cross section.

$$\left(\frac{m_X}{M_X}\right)^2 + \left(\frac{m_Y}{M_Y}\right)^2 \leq 1.0 \qquad (1.2.2.3)$$

Where m_X, m_Y =the moment components in the direction of the major and minor axes respectively,

M_X , M_Y =the moment capacities when Pu acts along the major and minor axes respectively.

5. Rectangular columns reinforced in only two faces show a higher deviation from the elliptical arc when subjected to biaxial bending. This suggests that even greater reduction in Pu and Mn from an elliptical arc may be neccessary.

In 1963, Pannell suggested that the three dimensional axial load biaxial moment interaction surface could be represented by a uniaxial load moment interaction diagram plus a biaxial interaction diagram. Pannell further assumed that the biaxial moment interaction could be related to the uniaxial behaviour by the deviation between the major axis moment and the moment about the diagonal by a simple trigonometric relationship (Figure 1.2.2.2).

$$M_{fy} = \frac{M_y \sec(\theta)}{1 - N \sin^2(\theta)} \qquad (1.2.2.4)$$

where M_{fy} = ultimate moment about the y-axis,
M_{fx} = ultimate moment about the x-axis,
M_y = design ultimate moment about the y-axis,
M_x = design ultimate moment about the x-axis,

and,

$$\tan(\theta) = \Phi \frac{M_y}{M_x}$$

$$\Phi = \frac{M_{fy}}{M_{fx}}$$

This method of designing columns subjected to biaxial bending, is fundamentally different from the method suggested by Au in that it is completely generalized. However, it is more approximate, since it depends on

the similarity between the interaction surface and the surface of revolution.

In 1966, the Portland Cement Association presented a design aid for the design of short rectangular reinforced concrete columns subjected to biaxial bending. The P.C.A. modified Bresler equation to ;

$$\left(\frac{M_x}{M_{xo}}\right)^{\frac{\log 0.5}{\log \beta}} \left(\frac{M_y}{M_{yo}}\right)^{\frac{\log 0.5}{\log \beta}} = 1.0 \qquad (1.2.2.5)$$

in which β equals the ordinate to the contours at the point where the relative moments are equal, and for design convenience, a plot of the curves generated by nine values of β was given (Figure 1.2.2.3). The P.C.A. reported that the value of β mainly depends on the ratio of Pu/Po. The maximum difference in β amounted to about 5% for values of Pu/Po ranging from 0.1 to 0.9 .

With the increasing use of electronic computers, many researchers began using numerical summation methods to obtain the ultimate strength of reinforced concrete column sections of any shape or reinforcement pattern under biaxially eccentric compression loading. The procedure is based on the usual assumptions of a linear strain distribution and on the equation of static equilibrium. Any desired stress-

strain relationships can be used for the steel and the concrete, and the effect of the tensile strength of the concrete may be included.

Using this numerical summation method, Row and Paulay presented interaction diagrams defining the failure surface of short rectangular reinforced concrete columns, in terms of dimensionless parameters, with respect to a few distinct directions of loading (Figure 1.2.2.4).

As for the L-shaped sections, information for their analysis and design are not generally available to the structural engineers.

In 1959, Muller published an elastic method which can be used to design short L-shaped columns symmetrical about the 45 degree axis, and subjected to small biaxial eccentricities.

As far as is known, the first design charts for the ultimate biaxial bending of L-shaped section were presented by M. K. Tadros in 1976. The charts are entered by the following parameters :

1. The ratio h_1/h_2 .
2. The values of f_y and f_c' .
3. The steel distribution in the section. The total reinforcement area As is divided into three groups As_1, As_2, and As_3 assumed to be arranged as shown in Figure 1.2.2.5 .

The design charts (Figure 1.2.2.6) showed interaction surfaces in a non-dimensional form, with three cartesian axes representing $Nu/f_c' h_1^2$, $Mxu/f_c' h_1^3$, and $Myu/f_c' h_1^3$, where

Nu = the ultimate axial load,

Mxu = the ultimate moment about the x-axis,

Myu = the ultimate moment about the y-axis,

f_c' = the concrete cylinder compressive strength.

In 1979, J. Marin presented a more comprehensive design aid for L-shaped reinforced concrete columns. These charts had the following parameters :

1. The concrete cross-sections were considered symmetrical.
2. Five thickness ratios (the ratio of the largest side to the least dimension of the L-shaped column) of 2, 2.5, 3.33, and 5 were used.
3. One steel distribution was used for each thickness ratio (Figure 1.2.2.7)
4. The remaining parameters can be seen from a typical chart (Figure 1.2.2.8).

At the 1981 American Concrete Institute fall convention, Mr. M. Iqbal presented results for L and chamfered-rectangular column sections subjected to biaxial eccentricity. As explained in the preface, the interaction surfaces had sharp discontinuities.

These results are not in agreement with Marin and would not have been expected from the conclusions of the previous work quoted above.

1.3 EFFECT OF THE CONCRETE STRESS-STRAIN REPRESENTATION ON THE ANALYTIC CALCULATION OF THE ULTIMATE LOADS AND MOMENTS

In 1979, Furlong compared measured forces and moments of several rectangular and rounded-end columns with the analytically calculated values using several stress-strain representations for the concrete (FIGURE 1.2.3.1). All of the stress-strain representations for the concrete under estimated the observed values for the loads and moments (TABLE 1.2.3.1). This is probably due to :-

1. The effective lateral confinement of concrete provided by the spacing of the longitudinal bars and transverse ties increases the concrete strength.
2. Experimental errors mostly from the measurement of the strains across the section.

A very widely used representation of the strength of concrete is the rectangular stress block. In this representation, failure of the section is assumed when the most compressed concrete fibre reaches 0.003 . This method has the advantage of simplicity, but it less accurate than the non-linear stress-strain relationships presented above, especially for cases where low strain gradient exsists over the section.

Chapter II

METHOD

2.1 INTRODUCTION

The purpose of this chapter is to present the method used in approaching the problem of biaxial bending of reinforced concrete column sections. The basic assumptions and the stress-strain characteristics of the concrete and steel are developed.

The results of the calculations of the ultimate bending moments are presented as interaction surfaces and isoload contours. Also the results of the calculations of the ultimate biaxial curvatures are presented in tabular form.

2.2 ASSUMPTIONS

The assumptions used in determining the interaction surfaces of biaxially loaded column sections are those stated in " CSA A23.3M " namely :-

1. Plane sections normal to the neutral axis before bending remain plane after bending.
2. Perfect bond exists between the steel reinforcement and the concrete.
3. The maximum fibre strain in the concrete may not ex-

ceed a specified value[3] (0.0025, 0.0030, 0.0035, 0.0040).

4. The tensile strength of the concrete is neglected. It could, however, easily be taken into account if the appropriate stress-strain curve is given.
5. Elastic-perfectly plastic stress-strain relationship for the reinforcing steel.
6. The strain in the steel and concrete is a linear function of the distance from the neutral axis.

2.3 PROCEDURE

The procedure used in analyzing reinforced concrete column sections subjected to biaxial bending may be outlined as follows:-

1. Divide the concrete section into a number of small elements (the size of the divisions depends on the available computer facilities and the accuracy sought).
2. Determine the coordinates of the plastic centroid with respect to any reference point. The plastic centroid is defined as the centroid of resistance of the section if all the concrete is compressed to the maximum stress(0.85Fc), and all the steel is compressed to the yield stress(Fy), with uniform strain over the section. For any section, the procedure which can

[3] CSA specifies a maximum fibre strain of 0.0030

be used to calculate the plastic centroid by the numerical summation method is as follows:-

a) The neutral axis is located at an infinite distance from the section (this is done to insure that uniform strain will exist throughout the section).

b) The strain of the most compressed concrete fibre is assigned the value of the strain corresponding to the maximum stress in the concrete. This will also insure that the steel is yielding since the strain which corresponds to the maximum stress of the concrete is greater than the yield strain of all commercially available reinforcing steels.

3. Determine the coordinates of the centroids of all the concrete elements and the reinforcing steel bars, taking the plastic centroid as the center of the coordinate system.
4. Assume a neutral axis inclination (FIGUREs 2.3.1, 2.3.2)
5. Assume a neutral axis position.
6. Determine the perpendicular distance from the neutral axis to the centroid of all the concrete elements and steel bars, then assign the maximum allowable concrete strain to the most compressed concrete element.
7. Using the assumption that plane sections normal to the neutral axis before bending remain plane after

bending, and the assumption that the stress over each element and steel bar is constant and equal to the value determined by the strain at it's centroid, determine the strains and stresses at the centroids of all the concrete elements lying on the compression side, and of all the reinforcing steel bars (compressive stresses are taken positive).

8. Determine the ultimate load Pu, and the ultimate moments about the x-axis and the y-axis Mux, Muy respectivly, by summing the incremental forces and moments.
9. If more points are needed to define the interaction curve for this inclination of the neutral axis, then return to STEP (5).
10. If the interaction curve for another inclination of the neutral axis is required, then return to STEP (4).
11. After a sufficient number of interaction curves which can define the interaction surface have been obtained, the isoload contours are plotted.

A FORTRAN program was written to perform all the required steps. The listing of the program is given in appendix B.

2.4 CALCULATION

2.4.1. The Concrete Stress-Strain Relationship

The Hognestad stress-strain relationship for concrete was adopted for the present analysis (FIGURE 2.4.1.1). the stress-strain charactistic of the concrete according to Hognestad is

$$f_C = f''_C \frac{2\varepsilon}{\varepsilon_0} - \left(\frac{\varepsilon}{\varepsilon_U}\right)^2 \quad \ldots\ldots (2.4.1.1)$$

Where f_C = the stress in the concrete corresponding to a given strain (MPa).

f''_C = the maximum compressive strength of concrete
$= 0.85 f_C$ (MPa)

ε = the strain of the concrete.

ε_0 = the strain corresponding to the maximum stress
$= \frac{2f''_C}{E_C}$

ε_U = the maximum allowable concrete strain.

f'_C = the strength of 6 by 12 inch concrete cylinder (MPa).

E_C = the initial modulus of elasticity of concrete
$= 12411 + 460 f_C$ (MPa).

It should be noted that the 0.85 strength coefficient was developed on the basis of numerous tests of concentrically loaded columns having square and circular sections. Although it is well known that the compressive strength of concrete

depends on the specimen size and shape, it is however assumed in this study that the 0.85 factor also applies to columns subjected to biaxial bending and to the " L-SHAPE " section used.

2.4.2 The Steel Stress-Strain Relationship

The stress-strain relationship of the steel has been assumed to be perfectly elastic-plastic ; elastic up to the specified yield strength, Fy, and equal to Fy for greater strains (FIGURE 2.4.2.1). The modulus of elasticity Es, for steel has been taken as 200,000 MPa .

2.4.3 Generation of Results

The "L-SHAPED" section used in this analysis is shown in FIGURE 2.4.3.1 . The concrete section was divided into a grid of 2201 discrete rectangular elements, each with dimensions of 10 by 10 mm . The neutral axis was rotated from 0 to 360 degrees by a 15 degrees interval, and it's position is varied until the biaxial moments corresponding to the desired load levels were obtained for each inclination. A systematic method for the calculation of the ultimate load and biaxial moments was presented in the previous section.

A plot of the biaxial moments for different load levels corresponding to a given neutral axis inclination will be referred to as an interaction curve, and a plot of a series of interaction curves will be referred to as an interaction

surface. Plots showing a plan view of the interaction surface for different values of the maximum allowable concrete strain (0.0025, 0.0030, 0.0035, 0.0040) are presented in FIGURES 2.4.3.2 to 2.4.3.5 . Using these interaction surfaces, the isoload contours can be determined by connecting points of a given axial load. Plots of the isoload contours for the different maximum allowable concrete strain (0.0025, 0.0030, 0.0035, 0.0040) are presented in FIGURES 2.4.3.6a to 2.4.3.9b . Plots showing the isoload contour for a given load level (6500, 6000, 5000, 4000, 3000, 2000, 1000, 0KN) as calculated by using different values of the maximum allowable concrete strain (0.0025, 0.0030, 0.0035, 0.0040) are presented in FIGURES 2.4.3.10 to 2.4.3.17.

The ultimate biaxial curvatures are calculated for several points along the isoload contour (6500, 6000, 5000, 4000, 3000, 2000, 1000, 0KN) for both the 0.0030 and the 0.0040 values of the maximum allowable concrete strain. The results are presented in TABLES 2.4.3.1 to 2.4.3.17 .

Chapter III

ANALYSIS AND DISCUSSION

3.1 INTRODUCTION

This chapter presents the results of the present study in the form of interaction surfaces and isoload contours. The isoload contours are compared with those presented by Mr. Mohammed Iqbal.

Also the changes in behaviour of the interaction surfaces and isoload contours, with different values of the maximum allowable concrete strain are investigated.

Finally the computer model developed allows a parametric investigation of quantities not normally considered in column analysis, namely curvature.

3.2 PROPERTIES OF THE ULTIMATE ISOLOAD CONTOURS

In this section an attempt is made to analyze the ultimate isoload contours determined for the "L-shape" section used.

The ultimate isoload contours show that that only two quadrants (any two quadrants between the 45 and the 225) need to be plotted since the interaction surface is symmetrical about the axis of symmetry of the section.

It is also observed that for some cases, the ultimate isoload contours of different load levels, intersect at one

or more points (FIGURES 2.4.3.6b, 2.4.3.7b, 2.4.3.8b). This is explained by the fact that the balanced axial load for different inclinations of the neutral axis may not be the same.

The ultimate isoload contours also show that the deviation from the general shape of the isoload curve seems to appear only in cases where the neutral axis is parallel to the dimension of the section. This seems to be more magnified as the allowable concrete strain is increased and as the section is subjected to more compression.

It is also observed that the general shape of the ultimate isoload contour seems to follow the same pattern for load cases above the balanced load, and a different and less uniform pattern for load cases below the balanced load. This can be better seen from the plots of the plan view of the interaction curve (FIGURES 2.4.3.2 to 2.4.3.5). It is seen that each interaction curve follows almost a linear pattern up to the balanced load and then warps (except for the interaction curves at the axis of symmetry).

3.3 COMPARISSION OF THE ULTIMATE ISOLOAD CONTOURS WITH THOSE OBTAINED BY MR. MOHAMMED IQBAL

The ultimate load contours presented by Mr. Mohammed Iqbal show " re-entrant " corners at the axis of symmetry. The explanation of this was given by :-

1. When the neutral axis inclination corresponds with that of the axis of symmetry, the column capacity is

lower when the column toe is in compression than the case when the column heel is in tension.

2. In the compression zone, the column section with it's toe in compression and heel in tension has lower capacity than the same column with it's heel in compression and toe in tension.
3. In the tension zone, the situation reverses as the effect of other corners enter into the picture.

It should be noted that all the points cited above were also observed in this study, but there were no "re-entrant" corners in the isoload contours at the axis of symmetry.

Figure 3.3.1 shows the isoload contours from Mr. M. Iqbal's work and the equivalent isoload contour obtained by the present study. The angular interval used to generate the isoload curves was only 5 degrees compared to the 15 degrees interval used by Mr. M. Iqbal. It is evident that the sharp discontinuities in the isoload contours presented by Mr. M. Iqbal were not found in this study.

As was stated in the preface, the sharp changes in the moment capacity in the isoload contours with small changes in the inclination of the neutral axis, would seem to be unreasonable. The intuition is supported by the present work and it must be concluded that the work presented by Mr. M. Iqbal is in error.

3.4 THE EFFECT OF THE MAXIMUM ALLOWABLE CONCRETE STRAIN ON THE ULTIMATE BENDING MOMENTS

The investigation of the effect of varying the maximum concrete strain from 0.0030 to 0.0040 on the ultimate biaxial bending moments showed that :-

1. At the 6500 KN load level, the ultimate bending moments decrease by an average of 30% (FIGURE 2.4.3.10).
2. At the 6000 KN load level, the ultimate bending moments decrease by an average of 6.5% (FIGURE 2.4.3.4).
3. At the 5000 KN load level, the ultimate bending moments increase by an average of 5.5% (FIGURE 2.4.3.2)
4. At the 4000 KN, 3000 KN, and the 2000 KN load levels, the ultimate bending moments increase by an average of 6% (FIGURES 2.4.3.13, 2.4.3.14, 2.4.3.15).
5. At the 1000 KN load level, the ultimate bending moments increase by an average of 3.5% (FIGURE 2.4.3.16).
6. At the 0 KN load level, the ultimate bending moments increase by an average of 2% (FIGURE 2.4.3.17).

As can be seen from the above, the change in the ultimate bending moments also shows a dependence on the load level. Investigation of the strain distribution across the section showed that :-

1. If the neutral axis lies outside the section, the ultimate bending moments decrease as the maximum allo-

wable concrete strain is increased from 0.003 to 0.004, as was the case for the 6500,and the 6000 KN load levels. This decrease in the ultimate bending moments seems to decrease substantially as the neutral axis moves towards the section.

2. If the neutral axis lies within the section and is below the plastic centroid, the ultimate bending moments increase by about 6% as the maximum allowable concrete strain is increased from 0.003 to 0.004, as was the case for the 5000, 4000, 3000, and the 2000 KN load levels.
3. If the neutral axis lies within the section and is above the plastic centroid, the ultimate bending moments increase by about 3% as the maximum allowable concrete strain is increased from 0.003 to 0.004, as was the case for the 1000, and the 0 KN load levels.

3.5 THE EFFECT OF THE MAXIMUM ALLOWABLE CONCRETE STRAIN ON THE ULTIMATE BIAXIAL CURVATURES

The investigation of the effect of increasing the maximum concrete strain from 0.003 to 0.004 on the ultimate biaxial curvature are summarized in TABLE 3.5.1 . It is seen that the curvatures increase by about 35 to 48 percent depending on the load level. Generally, it seems that as the load level decreases, the change in the ultimate bending curvature decreases. Also the increase in the ultimate bending curvatures between any two successive load levels for the 0.003

value of the maximum allowable concrete strain case is generally slightly higher than for the 0.004 value of the maximum concrete strain case (TABLE 3.5.2).

Chapter IV

CONCLUSIONS

The theoretical analysis of the problem of biaxial bending of L shaped column sections leads to the following conclusions :-

1. The ultimate isoload contours show that the deviation from the general shape of the isoload curve semms to appear only in cases were the neutral axis is parallel to the dimension of the section. This seems to be more magnified as the allowable concrete strain is increased and as the section is subjected to more compression.
2. The general shape of the ultimate isoload contour seems to follow the same pattern for load levels above the balanced load, and a different and less uniform pattern for load cases below the balanced load.
3. The effect of the maximum allowable concrete strain on the ultimate bending moments is as follows :-
   a) For high load levels (the neutral axis lies outside the section), the ultimate bending moments decrease as the maximum allowable concrete strain is increased from 0.003 to 0.004 . This decrease

(between 6.5 and 30%) in the ultimate bending moments seems to decrease substantially as the neutral axis moves towards the section.

b) For moderate load levels (the neutral axis lies within the section and is below the plastic centroid), the ultimate bending moments increase by about 6% as the maximum allowable concrete strain is increased from 0.003 to 0.004 .

c) For low load levels (the neutral axis lies within the section and is above the plastic centroid), the ultimate bending moments increase by about 3% as the maximum allowable concrete strain is increased from 0.003 to 0.004 .

4. The ultimate biaxial curvatures increase by about 35 to 48 percent as the maximum allowable concrete strain is increased from 0.003 to 0.004 . Generally, it seems that as the load level decreases, the effect of increasing the maximum allowable concrete strain on the ultimate biaxial curvature decreases.

5. The method used for the analysis of biaxial bending of column sections (element summation method) is ideal for the use of electronic computers. It is based on the usual assumptions of a linear strain distribution and on the equations of static equlibrium. It can be used to analyze any desired cross-section, and any desired stress-strain relationships for the steel and the concrete can be used.

BIBLIOGRAPHY

ACI-ASCE Committee 327, "Ultimate Strength Design", ACI Journal, Proceedings v. 52, Jan. 1956, pp. 505-524.

Craemer, Herman, "Skew Bending in Reinforced Concrete Computed by Plasticity", ACI Journal, Proceedings V. 48, February 1952, pp. 516-519.

Au, Tung, "Ultimate Strength Design of Rectangular Members Subjected to Unsymmetrical Bending", ACI Journal, Proceedings V. 54, Feb. 1958, pp. 657-674.

Whitney, Charles S., and Cohen, Edward, "Guide for Ultimate Strength Design of Reinforced Concrete", ACI Journal, Proceedings V. 53, Nov. 1958, pp. 455-490.

Bresler, Boris, "Design Criteria for Reinforced Columns Under Axial Load and Biaxial Bending", ACI Journal, Proceedings V. 57, Nov. 1960, pp. 481-490.

Pannell, F. N., "Biaxially Loaded Reinforced Concrete Columns", J. Struc. Div., Am. Soc. C. E., V. 85, ST6, June 1959, pp. 47-54.

Pannell, F. N.,"The Design of Biaxially Loaded Columns by Ultimate Load Methods", Magazine of Concrete Research, V. 12, No. 35, July 1960, pp. 99-108.

Brettle, H. J., and Warner, R. F., "Ultimate Strength Design of Rectangular Reinforced Concrete Sections in Compression and Biaxial Bending", The Institution of Engineers - Australia, Civil Engineering Transactions, April 1968, pp. 101-110.

Paulay, T., and Row, D. G., "Biaxial Flexure and Axial Load Interaction in Short Rectangular Reinforced Concrete Columns", Bulletin of the N. Z. Soc. for Earthquake Engineering, V. 6, No. 3, September 1973, pp. 110-121.

Warner, R. F., "Biaxial Moment Thrust Curvature Relations", J. Struc. Div., Am. Soc. C. E., V. 95, ST5, May 1969, pp. 923-940.

Portland Cement Association, "Capacity of Reinforced Rectangular Columns Subjected to Biaxial Bending", Advanced Engineering Bulletin No. 18, 1966.

Farah, A., "Analysis of Reinforced Concrete Columns Subjected to Longitudinal Load and Biaxial Bending", ACI Journal, Proceedings V. 66, No. 7, July 1969, pp. 569-575.

Lachance, L., "Stress Distribution in Reinforced Concrete Sections Subjected to Biaxial Loading", ACI Journal, March-April 1980, pp. 116-123.

Furlong, R. W., "Ultimate Strength of Square Columns Under Biaxialy Eccentric Loads", ACI Journal, Proceedings V. 57, No. 9, March 1961, pp. 1129-1140.

Rusch, Hubert, "Researchs Towards a General Flexural Theory for Structural Concrete", ACI Journal, Proceedings V. 57, No. 1, July 1960, pp. 1-28.

Sargin, M., "Stress-Strain Relationships for Concrete and the Analysis of Structural Concrete Sections", Solid Mechanics Division, University of Waterloo, Study No. 4, 1972, 167 pp.

Parme, Alfred; Nieves, Jose M.; and Gouwens, Albert, "Capacity of Reinforced Rectangular Columns Subjected to Biaxial Bending", ACI Journal, Proceedings V. 63, No. 9, Sept. 1966, pp. 911-923.

Furlong, R. W., "Concrete Columns Under Biaxially Eccentric Thrust", ACI Journal, Proceedings V. 76, No. 10, October 1979, pp. 1093-1118.

Marin, J., "Design Aids for L-Shaped Reinforced Concrete Columns", ACI Journal, Proceedings V. 76, No. 11, Nov. 1979, pp. 1197-1216.

Tadros, Maher K., "Design Charts for Reinforced Concrete L-Sections", Canadian Journal of Civil Engineering, V. 3, No. 4, Dec. 1976, pp. 479-483.

Hognestad, Eivind, "Inelastic Behavior in Tests of Eccentrically Loaded Short Reinforced Concrete Columns", ACI Journal, Proceedings V. 24, No. 2, October 1952, pp. 117-139.

Park, R., and Paulay, T., "Reinforced Concrete Structures", A Wiley-Interscience Publication, John Wiley and Sons, 1975, 769 pp.

Appendix A

NON-RECTANGULAR COLUMN AND SHEARWALL SECTIONS WITH BIAXIAL BENDING

A paper presented by Mr. Mohammed Iqbal

at the 1981 American Concrete Institute fall convention

NON-RECTANGULAR COLUMN AND SHEARWALL SECTIONS WITH BIAXIAL BENDING

Mohammad Iqbal
Project Engineer

Skidmore, Owings & Merrill
Chicago, Illinois

INTRODUCTION

The analysis of reinforced concrete sections subjected to axial load combined with biaxial bending has been the subject of serious discussions among researchers for the last twenty years. Although several noteworthy articles[1-22] on biaxial bending contributing to the understanding of this subject have appeared, significant gaps still exist in the area of design for biaxial bending. The primary difficulty associated with determining ultimate capacity of such sections has been the complexity of the problem itself, which requires lengthy and tedious arithmatical calculations. This limited most researchers to consider rather straightforward cases such as square columns with symmetric reinforcement. To reduce the labor required to predict the behavior of columns with biaxial bending, approximate formulae have been developed which simplify a biaxial bending case to a combination of two uniaxial bending cases. Design aids based on the approximate formulae are available for some square and rectangular columns with symmetric reinforcement patterns. Marin[20] published design charts for L-shaped columns with equal legs and a symmetric reinforcement pattern. Such charts have limited application in design of modern tall reinforced concrete buildings wherein a variety of shapes and reinforcement patterns are used.

Consider, for example, the plan of a 53-story building shown in Fig. 1. The scheme using two partial exterior tubes linked with the interior core tube through composite floor framing was recently studied for system evaluation. As Fig. 1 shows, the exterior framed tubes contain closely spaced columns, each being non-rectangular in shape. And, the shear core is comprised of complicated intersecting shearwalls that house vertical services. The portions of the central core are dropped off at various levels along the building height, creating further asymmetry. Since lateral loads are resisted by the entire three-dimensional form of this tube-in-tube system, axial force and biaxial moments are induced in the columns and shearwalls.

Fig. 2 shows column sections that have been used in some tubular buildings recently constructed or currently under construction. The most sections shown in Fig. 2 are part of the exterior tube and resist lateral force. The column sections require biaxial bending consideration; however, no data aids are available.

This indicates the need for a design procedure by which column and shearwall sections of various shapes could be sized with any desired accuracy. To meet this need, a general method of analysis and design for columns and shearwalls under axial compression and biaxial bending is presented in this paper. The method uses the finite approach and is applicable to columns and shearwalls of arbitrary shapes. A step-by-step algorithm is described next. Then, analyses of four different column and shearwall sections are presented. Design guidelines are given at the end.

NATURE OF BIAXIAL BENDING PROBLEM

A rational method for calculating the ultimate load capacity of a biaxially loaded column was given by Whitney[1] and later expanded by Mattock, Kriz and Hognestad.[2] It is well accepted now that the ultimate strength of an eccentrically loaded column is governed by the crushing resistance of concrete, assuming that reinforcing bars are ductile enough to deform at a constant yield stress with concrete crushing in compression. ACI Code[23] recommends a maximum strain of 0.003 at which concrete may be depended on to resist crushing. With a maximum extreme fiber strain of 0.003 in compression, and the accepted assumption that plane sections remain plane after bending, strain distribution at all points of a cross-section can be described for an assumed strain distribution. For a polygonal shaped column section, the strain, stress and force distributions are shown in Fig. 3. A three-dimensional strain distribution is illustrated in Fig. 4. The corresponding 3-D stress distribution can be plotted in a similar way.

In design, the problem is to determine the neutral axis position given ultimate load and associated biaxial moments. For symmetric sections, the neutral axis is perpendicular to the resultant eccentricity and, thus, determination of the neutral axis is relatively straightforward. For asymmetric sections, however, the neutral axis is not perpendicular to the resultant eccentricity. The determination of neutral axis is, therefore, not a straightforward task and requires trial and adjustments. Some numerical procedure has been suggested to compute the exact neutral axis using the Newton-Ralphson procedure. This procedure may work very well for very simple cases, however, convergence may be difficult to achieve for most sections with several sharp corners. The second approach to design columns with biaxial eccentricities is more traditional wherein the problem is reversed. First a neutral axis position is selected and corresponding axial load and bending moment capacities are determined. By translating the neutral axis at the selected inclination, an interaction curve can be obtained. And, by varying the inclination of the neutral axis, it is possible to obtain a series of interaction curves at various angles to the major axes of the section. A complete set of interaction curves for a given section describes the interaction surface (or failure surface), as illustrated in Fig. 5a. Each point on this surface represents one particular set of axial load P_u and moments about major axes M_{nx} and M_{ny}, which together produce failure of the section. This is an indirect, yet an optimum, approach to determine column capacity. The procedure requires considerably more calculations; however, no convergence problem is encountered.

If a horizontal section is taken through the interaction surface, the interaction line obtained give the possible combinations of M_{nx} and M_{ny} that would cause failure at a given axial load P_u. Such lines (Fig. 5a) are essentially load contours of the interaction surface and can be used in determining the capacity of a biaxially loaded column section. This approach is developed to analyze column and shearwall sections

of various shapes.

METHOD OF ANALYSIS AND DESIGN

Consider a column section (Fig. 3) subject to biaxial bending. Area of stress block can be conveniently calculated using a finite method wherein the concrete area is divided into several small discrete elements. Summation of elemental forces acting on the elemental areas thus allows axial forces to be determined, while summation of moments of the elemental forces is used to determine biaxial moments. Although such calculations are necessarily approximate, any desired accuracy can be obtained by increasing the grid fineness used to partition the cross-section into elemental areas. The finite approach used in this study has been discussed in literature. Here, its use is extended to columns and shearwalls of various shapes.

Several advantages exist in this finite method over a closed-form solution. The stress-strain relations for concrete and steel of almost any desired form can be used, without appreciably increasing complexity of the method or computer time. The finite method is, therefore, not limited to the assumption of a highly idealized concrete stress block. In fact, effects such as strain hardening, limit strain of steel, concrete tensile strength, unloading of concrete in post crushing range, all become amenable to the detailed analysis. Irregularity in shapes of the cross-section and in placement of steel reinforcement can both be taken into account.

A step-by-step algorithm to design a column or a shearwall section subjected axial compression and biaxial bending moments is given below. The assumptions used here in determining an interaction surface of a biaxially loaded section are consistent with the provisions of ACI 1977 code[23]. These are:

1. Plane sections remain plane after bending.

2. Perfect bond exists between steel reinforcement and concrete.

3. Concrete stress block of uniform intensity equal to $0.85f'_c$ and depth $a = k_1 c$, where c is the normal distance from the neutral axis to extreme fiber in compression and $k_1 = 0.85$ for concrete strengths less than or equal to 4000 psi and is reduced continuously at the rate of 0.05 for each 1000 psi in excess of 4000 psi, but not to any value less than 0.65.

4. Maximum concrete strain at ultimate load equals 0.003.

5. Concrete has no strength in tension.

6. Elastic-perfectly plastic stress-strain relationship for reinforcing steel.

7. Effective steel stress equal to $f_s - 0.85f'_c$ to account for the area of concrete displaced by steel (for bars inside the compression block only).

STEP-BY-STEP ALGORITHM

1. Divide the concrete section into several small discrete areas.

2. Determine plastic centroid of the section. (The plastic centroid can be defined as the point of application of force P_u, such that no strain gradient exists over the section).

3. Assume an angle of inclination of the neutral axis. A good initial approximation is obtained by positioning the neutral axis perpendicular to the moment arm of the applied force. For an unsymmetrical section, the neutral axis is not perpendicular to the resultant eccentricity, and therefore, estimation becomes difficult.

4. Assume a neutral axis position by fixing the shortest distance between the neutral axis and one of the axes passing through the plastic centroid.

5. Establish the farthermost point from the neutral axis in compression region of concrete and assume that its strain is the specified limit of 0.003.

6. Determine the strains at the centroid of each concrete and steel elemental area from the assumed planar strain distribution. The defines the ultimate strain plane (Fig. 4).

7. Determine the equivalent force in the concrete compression zone and the moment of this force about the plastic centroidal axes, X and Y, of the cross-section. Since the section has been divided into small discrete elements, both forces, and moments are computed using the following numerical integration procedure. In other words, the resultant force is the algebric sum of forces on the small elements. And, the resultant moment about an axis is the sum of all the moments about the axis.

8. Translate the neutral axis by a small distance, keeping it parallel to its old position. Return to step 5 and repeat the procedure until the required range of eccentricities is covered. Thus, an interaction curve can be obtained.

9. Rotate the neutral axis by a small angle and return to step 4. By repeating the process several times, a full interaction surface can be determined and then plotted.

10. Cut sections in the interaction surface such that column load is constant. A set of such isoload contours provides a convenient way to evaluate design feasibility of a column section subjected to a given set of an axial thrust and biaxial moments.

11. If needed, change column geometry, reinforcement ratio, bar locations, or concrete strength and repeat the procedure above. Thus, new interaction surface and a new set of isoload contours can be plotted.

SOLVED EXAMPLES

The procedure provides an optimum way to determine the exact column capacity. It can be readily programmed into a desk computer. Here are few examples using the algorithm.

Example 1: Square column with four corner bars.

Consider a 20 in. square column with 4#9 corner bars, f'_c = 4 ksi and f_y = 60 ksi. The column has four axes of symmetry: two major axes and two diagonal axes. For the purpose of computer analysis, the column section was divided into 100 small square elements and the neutral axis was rotated from 0 to 360 degrees with 15 degrees increments. The 3-D interaction surface is shown in Fig. 5a. A plan view of the interaction surface (Fig. 5b) indicates that most interaction curves generated by rotating the neutral axis are warped. It implies that ratio of resultant moments M_{nx} and M_{ny} is not constant and that resultant eccentricity is not perpendicular to the neutral axis. Fig. 5b also shows that interaction curves are planar when the section is rotated about the axes of symmetry. The isoload contours for compression and tension failure zones are shown in Fig. 6a and 6b, respectively. The ultimate moments M_{nx} and M_{ny} are used as basis vectors. The right-hand rule is used in

plotting. The shape of load contour under heavy axial load of 1400 kips is almost a circle. In this zone, Bresler's inverse load formula[3] works very well. Near the balanced load, the load contour is no longer a circle, but it has a rossette shape. In tension zone (Fig. 6b), the contour shape changes further as the load is reduced and failure mode becomes predominantly flexural. It is also pointed out that the column load at balanced condition is not constant for the entire interaction surface but varies as the neutral axis is rotated about the major axes.

Example 2: L-shaped column

The L-shaped column section and its interaction surface is shown in Fig. 7a. For purpose of analysis, the section was divided into 256 square elements and the neutral axis was rotated from 0 to 360 degrees with 15 degrees increments. The plan view of the 3-D interaction surfaces (Fig. 7b) shows that only two interaction curves (marked A and B) are planar; the remaining curves are warped due to asymmetry of the L-shaped section. The neutral axis inclined at 135 degrees, with respect to x-axis, correspond to interaction curves A and B. When the compression is on the toe (marked A on the section) with neutral axis inclined at 135°, the interaction curve A is obtained. And, when the compression is on the heel side (marked B on the section), the interation curve B is obtained. The column capacity differs in each case: When column toe is in compression, capacity is lower. That is one reason why load contours (Figs. 8a and b) show re-entrant corners at the axis of symmetry.

In compression zone, the column section with its toe in compression and heel in tension has lower capacity than the same column with its heel in compression and toe in tension. In tension zone, the situation reverses as the effects of other corners (marked C and D) enter into the picture. The re-entrant corners (Figs. 8a and 8b) show this effect. Another interesting aspect of the load contours is their intersecting characteristic near balanced condition. This is because the balanced point is

not an invarient. In fact, the magnitude axial force P_u at balanced condition may be different for each inclination of the neutral axis. And, this effect combined with the usual curvature change (from concave to convex) at balanced point along an interaction curve causes intersection of closely-spaced load contours. Similar observations can also be made from the load contours shown in Ref. 20.

Example 3: Chamfered column

A typical column from the 53-story tower (Fig. 1) is analyzed next. The column dimensions and reinforcement pattern is shown in Fig. 9a. The computer model consisted of 242 square and triangular elements. The neutral axis was rotated from 0 to 360 degrees with a 15 degree increment. The 3-D interaction surface and plan view of the interaction curves are shown in Figs. 9a and 9b, respectively. Only two of twenty-five interaction curves shown in Fig. 9b are planar; the remaining curves are warped. The planar curves correspond to the case when the neutral axis coincides with or is parallel to the x-axis. Two situations can arise: moment may cause short face (marked A) to be in compression or it may cause long face (marked B) to be in compression. Column capacity is slightly different for each situation, as shown in Fig. 10a. A slight inclination of the neutral axis from x-axis enhances column moment capacity (at a given P_u) due to an increase in effective lever arm. However, the manner by which moment capacity increases is of interest. In compression zone, the moment increase is smooth when compression block is on face B. On the other hand, when compression block is on face A, the moment increase shows joggedness. The situation reverses in tension zone, as shown in Fig. 10b. In order to study the effect of finite mesh on the result, another model consisting of 968 elements was analyzed. For a 400% increase in grid fineness, the increase in accuracy was only 4%. The load contour configuration remained unchanged. The joggedness observed in the results is due to sharp corners encountered when the neutral axis is rotated from 0 to 30 degrees. Beyond this range, the variations are

quite gradual. It is expected that smaller increments in neutral axis inclination, say 1 or 2 degrees at a time, would improve result accuracy.

Example 4: C-shaped wall section

Fig. 11a shows a C-shaped wall section which was analyzed using the finite method. The wall section is asymmetrical in shape with four boundary elements. For convenience, the temperture steel usually provided in shearwalls was neglected in analysis. The concrete section was divided into about 500 elements and neutral axis was rotated for 0 to 36° with a 15 degree increment. The compression zone load contours are shown in Fig. 11b. As expected, no symmetry is noted in the contour plot. The ridges and valleys noted in Fig. 11b are characteristics of such an asymmetrical section. Plotting of such a load contour is best done by using a computer and a plotter.

OTHER APPLICATIONS

The use of the finite approach can be extended to composite columns under biaxial bending. Composite columns are reinforced concrete columns with structural steel embedments (Fig. 2F). Recent SSRC recommendations[24] stipulate that for a column to be considered as a composite column, it should have at least 4% steel area as embedment. Special provisions are necessary to develop bond. Assuming full bond between the steel embedments and concrete, the assumption that strain distribution is linear within the section is valid. Consequently, the steel embedment can be divided into several small elements. Two types of steel are involved in a composite column. Usually, reinforcing bars have a yield strength of 60 ksi, whereas steel embedment can be of A36 or A50 structural steel. Thus, care is necessary in assigning material properties to steel elements.

The method can also be extended to columns and wall sections with axial tension and biaxial bending. However, new plastic centroid needs to be computed in determining sectional capacity.

CONCLUSIONS

The literature review shows that current design methods for columns and shearwall sections under biaxial bending have been limited to some simple column shapes such as rectangular columns with a symmetrical reinforcement pattern. Consequently, when designing a column or shearwall having a complex shape, biaxial bending has been treated inadequately or ignored in practice. Due to advent of computer applications in structural analysis, 3-D analyses are becoming the essential part of the modern structural design. Thus, biaxial bending needs to be considered if the assumptions made are to be consistent throughout the analysis and design phases. This paper proposes a design procedure wherein a section is divided into several finite elements and then analyzed using force equilibrium, strain compatibility and stress-strain properties of concrete and steel. A step-by-step algorithm is given to use the finite approach. Several solved examples demonstrate analysis procedure. Considerable experimental and analytical research is needed to expand current design procedure for columns and shearwalls under biaxial bending.

REFERENCES

1. Whitney, C.S., and Cohen, E., "Guide for Ultimate Strength Design of Reinforced Concrete," ACI Journal, Proceedings V. 53, No. 5, Nov. 1956, pp. 455-490.

2. Mattock, A.H., Kriz, L.B., and Hognestad, E., "Rectangular Concrete Stress Distribution in Ultimate Strength Design," ACI Journal, Proceedings V. 57, No. 8, Feb. 1961, pp. 875-928.

3. Bresler, B., "Design Criteria for Reinforced Concrete Columns Under Axial Load and Biaxial Bending," ACI Journal, Proceedings V. 57, Nov. 1960, pp. 481-490.

4. Pannell, F.N., "Failure Surfaces for Members in Compression and Biaxial Bending," ACI Journal, Proceedings V. 60, Jan. 1963, pp. 129-140.

5. Furlong, R.M., "Ultimate Strength of Square Columns Under Biaxially Eccentric Loads," ACI Journal, Proceedings V. 57, March 1961, pp. 1129-1140.

6. Fleming, J.F., and Werner, S.D., "Design of columns Subjected to Biaxial Bending," ACI Journal, Proceedings V. 62, March 1965, pp. 327-342.

7. Parme, A.L., Nieves J.M., and Gouwens, A.J., "Capacity of Reinforced Rectangular Columns Subject to Biaxial Bending," ACI Journal, Proceedings V. 63, Sept. 1966, pp. 911-923.

8. Aas-Jakobsen, A., "Biaxial Eccentricities in Ultimate Load Design," ACI Journal, Proceedings V. 61, March 1964, pp. 293-315.

9. Weber, D.C., "Ultimate Strength Design Charts for Columns with Biaxial Bending," ACI Journal, Proceedings V. 63, Nov. 1966, pp. 1205-1230.

10. Meek, J.L., "Ultimate Strength of Columns with Biaxially Eccentric Loads," ACI Journal Proceedings V. 63, Sept 1966, pp. 911-923.

11. Abolitz, A.L., "Short and Long Columns Under Uniaxial and Biaxial Flexure," ACI Journal, Proceedings, V. 65, June 1968, pp. 462-469.

12. Huggins, M.W., and Farah, A., "Analysis of Reinforced Concrete Columns Subjected to Longitudinal Load and Biaxial Bending," ACI Journal, Proceedings V. 66, July 1969, pp. 569-575.

13. "Biaxial and Uniaxial Capacity of Rectangular Columns," Advanced Engineering Bulletin 20, Portland Cement Association, Skokie, IL, 1967, 22 pp.

14. Gouwens, A.J., "Biaxial Bending Simplified," Publication SP-50, American Concrete Institute, Detroit, Michigan, 1975.

15. Heindahl, P.D., and Bianchini, A.C., "Ultimate Strength of Biaxially Eccentrically Loaded Concrete Columns Reinforced with High Strength Steel," Publication SP-50, American concrete Institute, Detroit, Michigan, 1975.

16. Abdel-Sayed, S.I., and Gardner, N.J., "Design of Symmetric Square Slender Reinforced Concrete Columns Under Biaxially Eccentric Loads," Publication SP-50, Americian Concrete Institute, Detroit, Michigan, 1975.

17. Shah, M.J. and Gesund, H., "The Analysis of Nonlinear Three-Dimensional Frames," Computers and Structures, Vol. 2, 1972, pp. 943-954.

18. Gesund, H., and Vandevelde, C.E., "Stiffness of Reinforced Concrete Columns in Biaxial bending," Planning and Design of Tall Buildings, Proceedings of ASCE-IABSE International Conference, Vol. III, No. 22-D1, ASCE, New York.

19. Magalhaes, M.P., "Biaxially Loaded Concrete Sections," Journal of Structural Division, Proceedings, ASCE, Vol. 105, ST12, December, 1979, pp. 2639-2656.

20. Marin, J., "Design Aids for L-Shaped Reinforced Concrete Columns," ACI Journal, Proceedings, V. 76, November 1979, pp. 1197-1216.

21. Furlong, R.W., "Concrete Columns under Biaxially Eccentric Thrust," ACI Journal, Proceedings, V. 76, October 1979, pp. 1093-1117.

22. Marin, J., "Computing Undimensional Normal Stress Resultants," Journal of Structural Division, Proceedings, ASCE, Vol. 106, ST1, January 1980.

23. ACI Committee 318, "Building Code Requirements for Reinforced Concrete (ACI 318-77)," American Concrete Institute, Detroit, Michigan, 1977, 102 pp.

24. Task Group 20, Structural Stability Research Council (H. Iyengar, Chairman), "A Specification for the Design of Steel Concrete Composite Columns," Engineering Journal, American Institute of Steel Construction, Fourth Quarter, 1979.

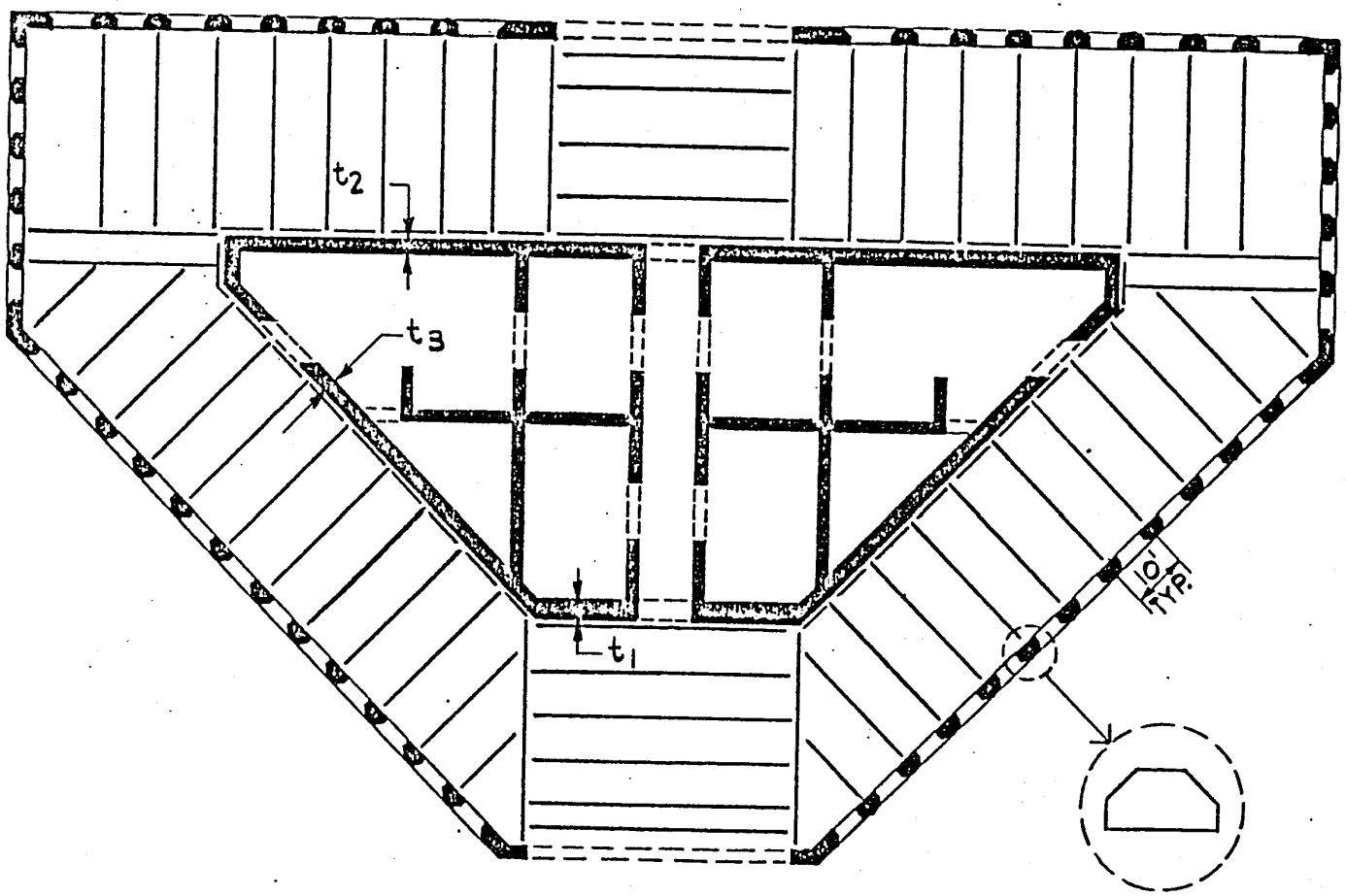

Fig. 1 Floor Plan of a 52 - Story Tower

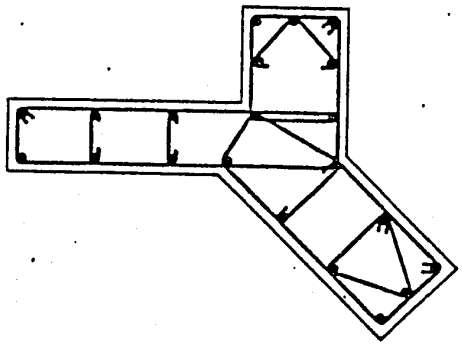

(A)

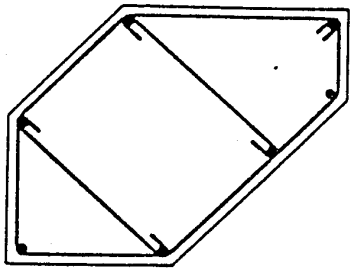

(B)

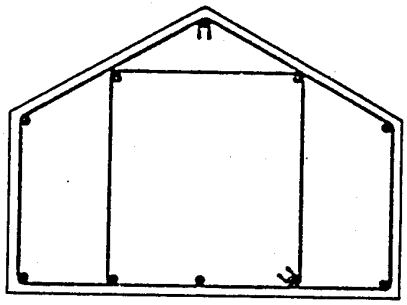

(C)

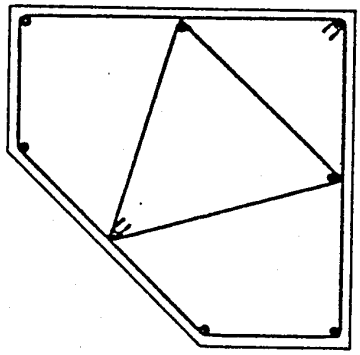

(D)

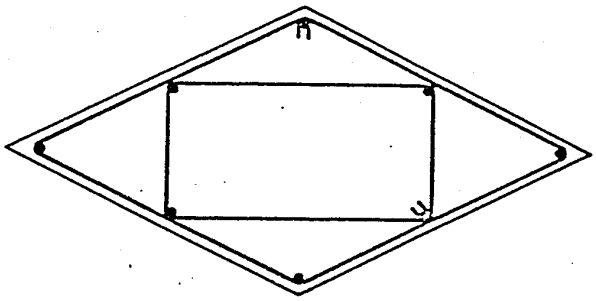

(E)

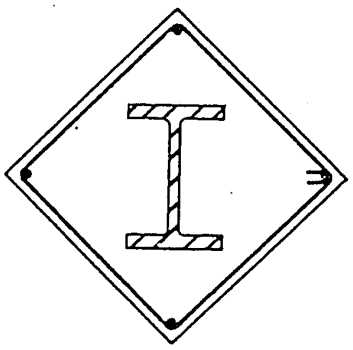

(F)

Fig. 2 Various Column Shapes Used in Modern Buildings

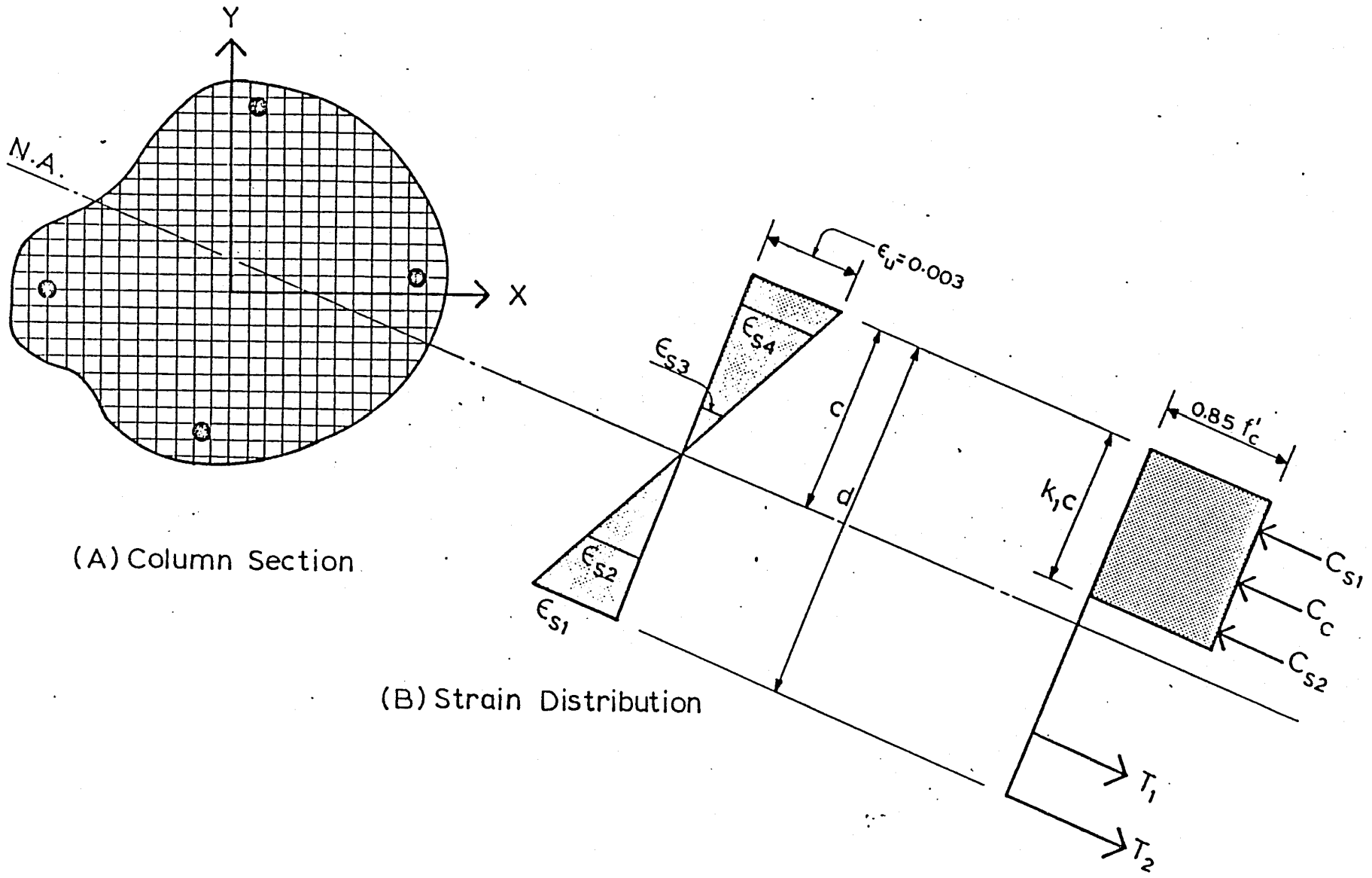

Fig. 3 Column Section Subjected to Biaxial Bending

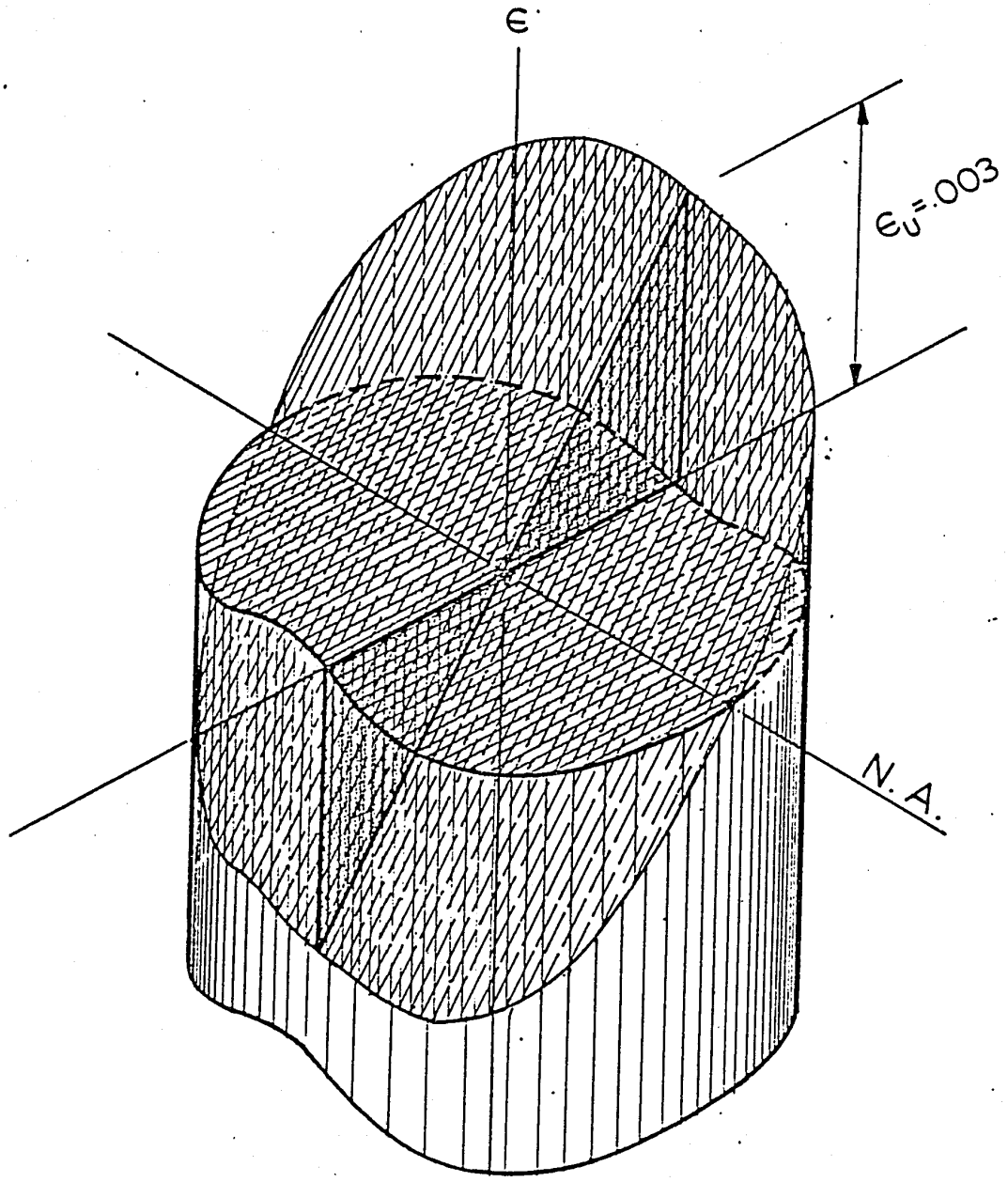

Fig. 4 THREE - DIMENSIONAL STRAIN DISTRIBUTION IN A COLUMN

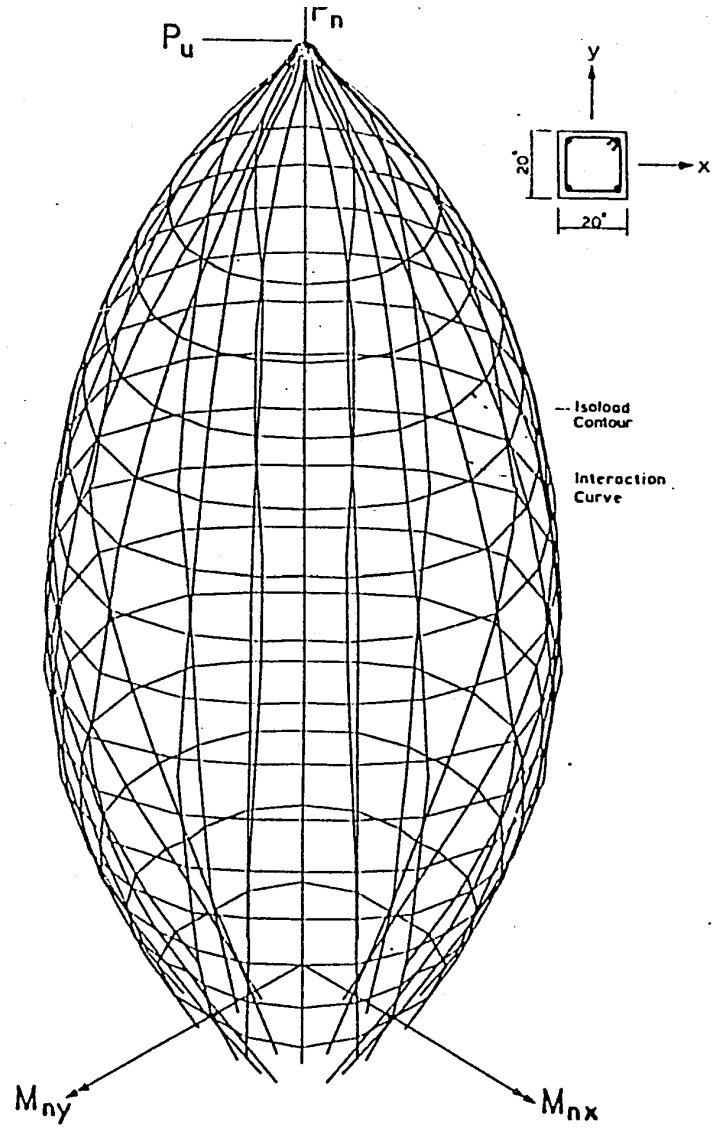

(A) INTERACTION SURFACE

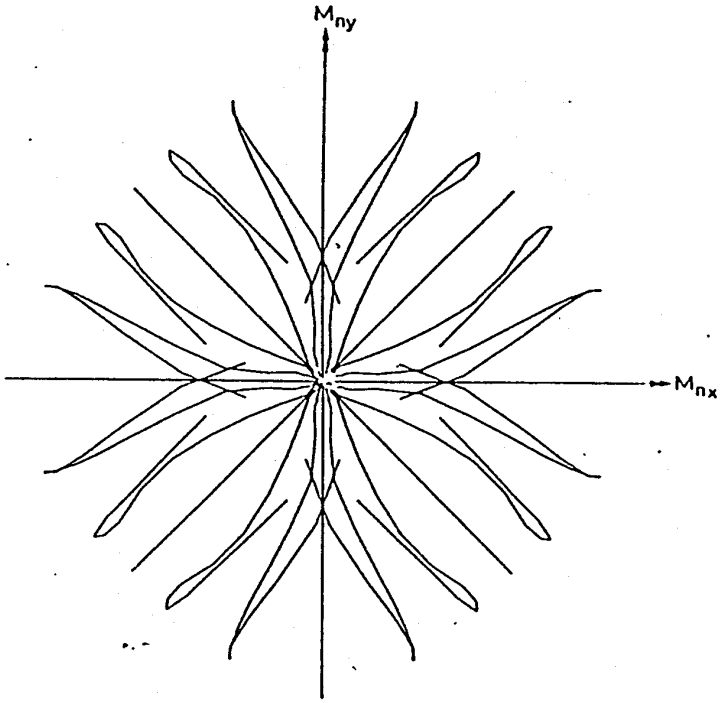

(B) PLAN VIEW OF INTERACTION CURVES

Fig. 5 INTERACTION SURFACE OF A SQUARE COLUMN SECTION

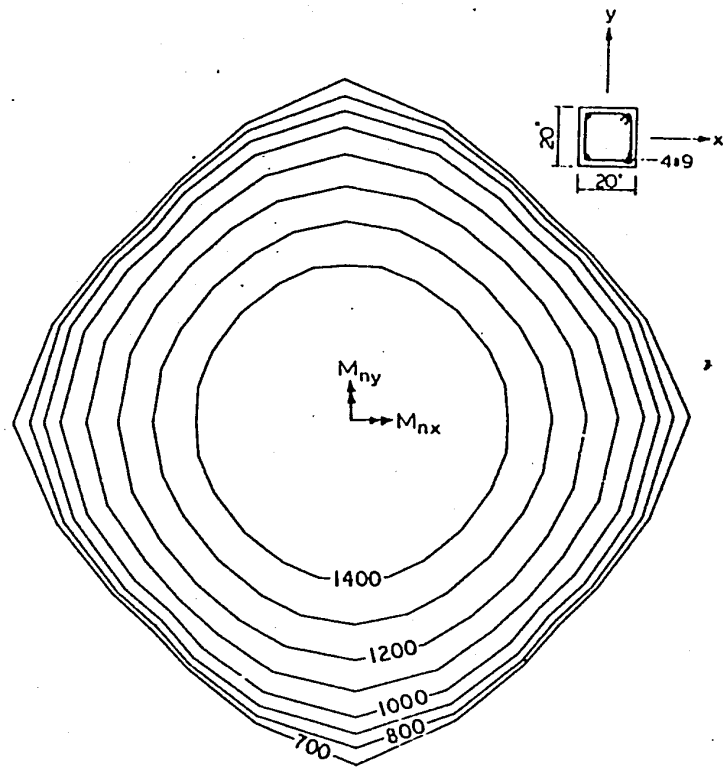

(A) COMPRESSION ZONE

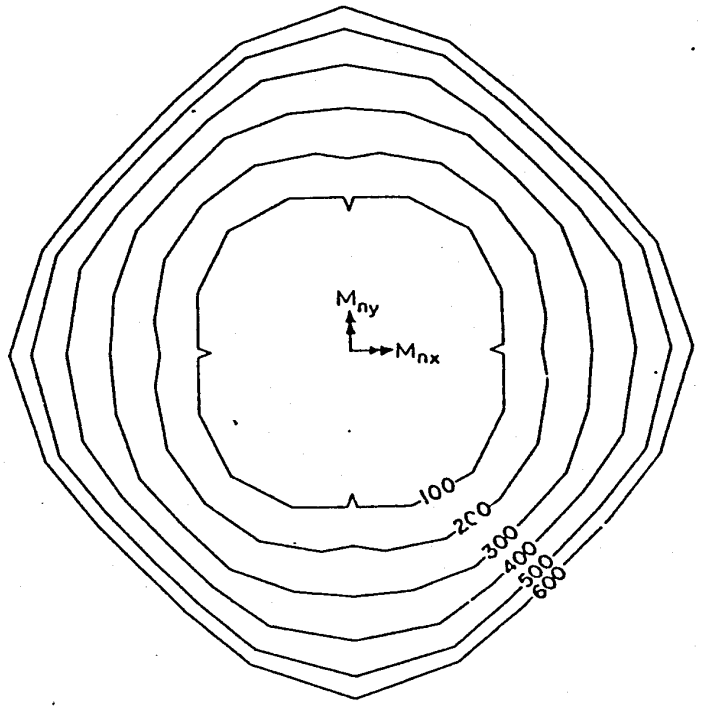

(B) TENSION ZONE

Fig. 6 ULTIMATE LOAD CONTOURS OF A SQUARE COLUMN SECTION

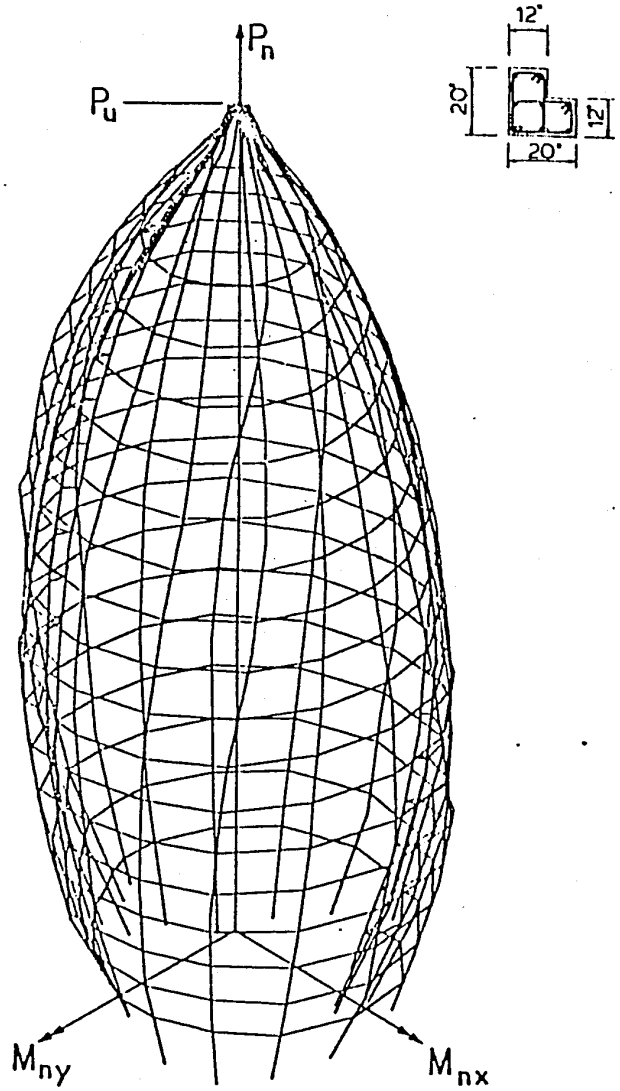

(A) INTERACTION SURFACE

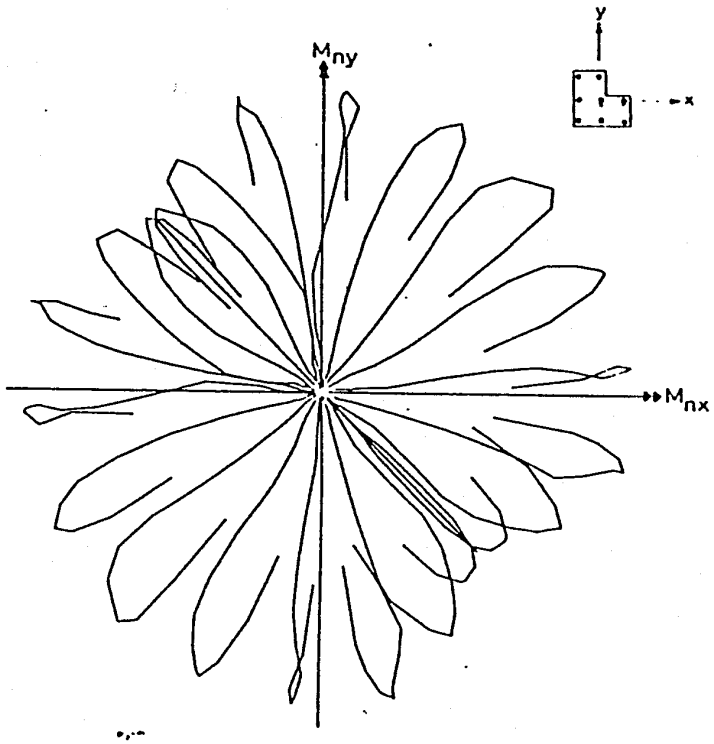

(B) PLAN VIEW OF INTERACTION CURVES

Fig. 7 INTERACTION SURFACE OF AN L-SHAPED COLUMN SECTION

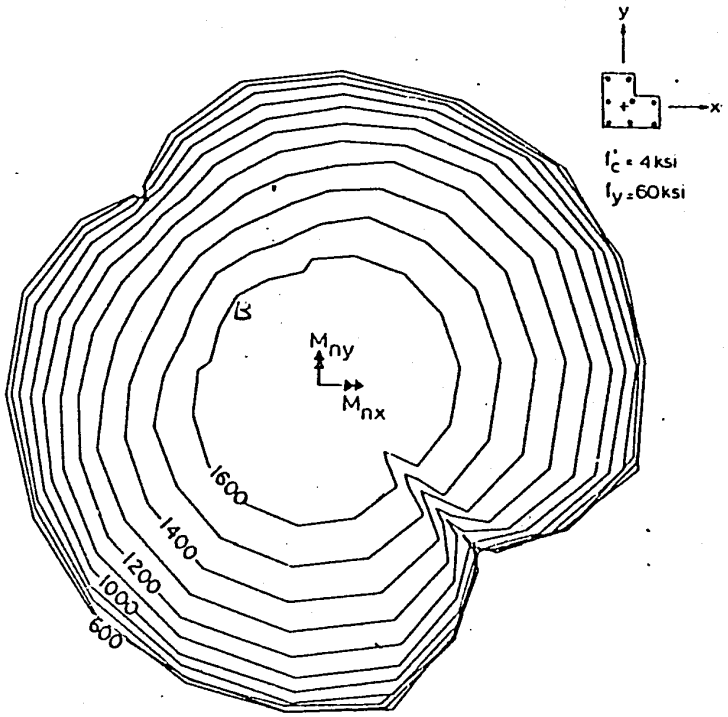

(A) COMPRESSION ZONE

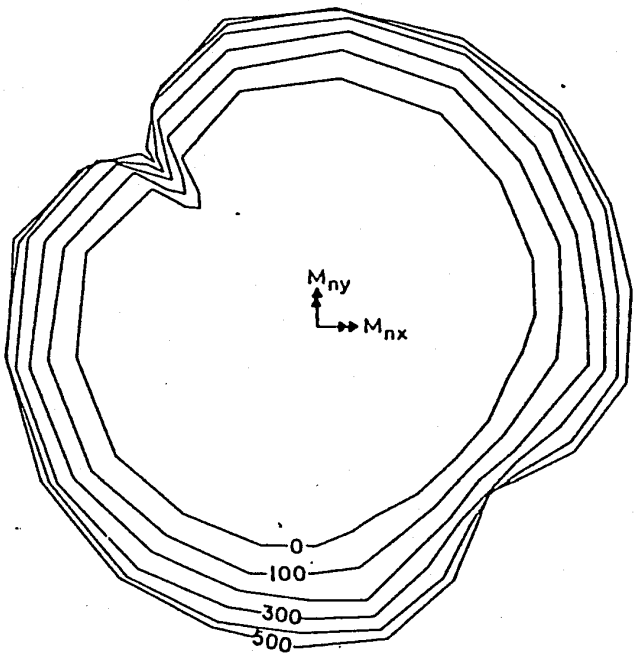

(B) TENSION ZONE

Fig. 8 ULTIMATE LOAD CONTOURS OF AN L-SHAPED COLUMN SECTION

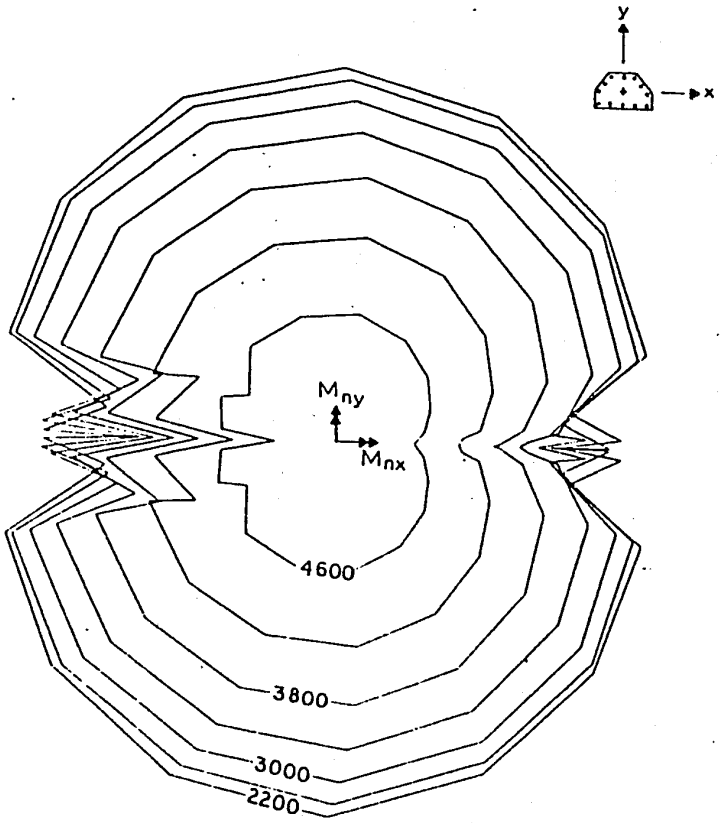

(A) COMPRESSION ZONE

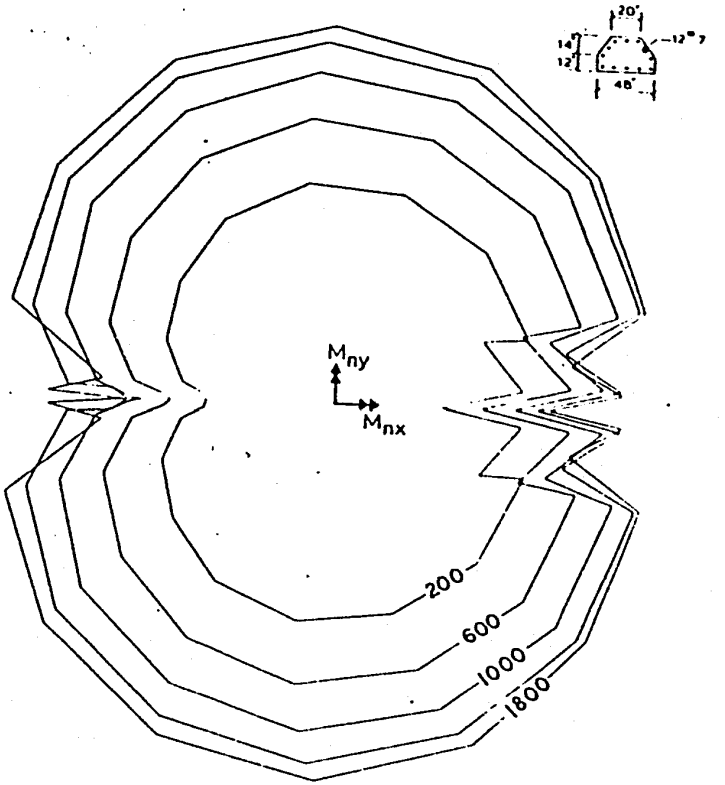

(B) TENSION ZONE

Fig. 10 ULTIMATE LOAD CONTOURS OF A CHAMFERED RECTANGULAR COLUMN SECTION

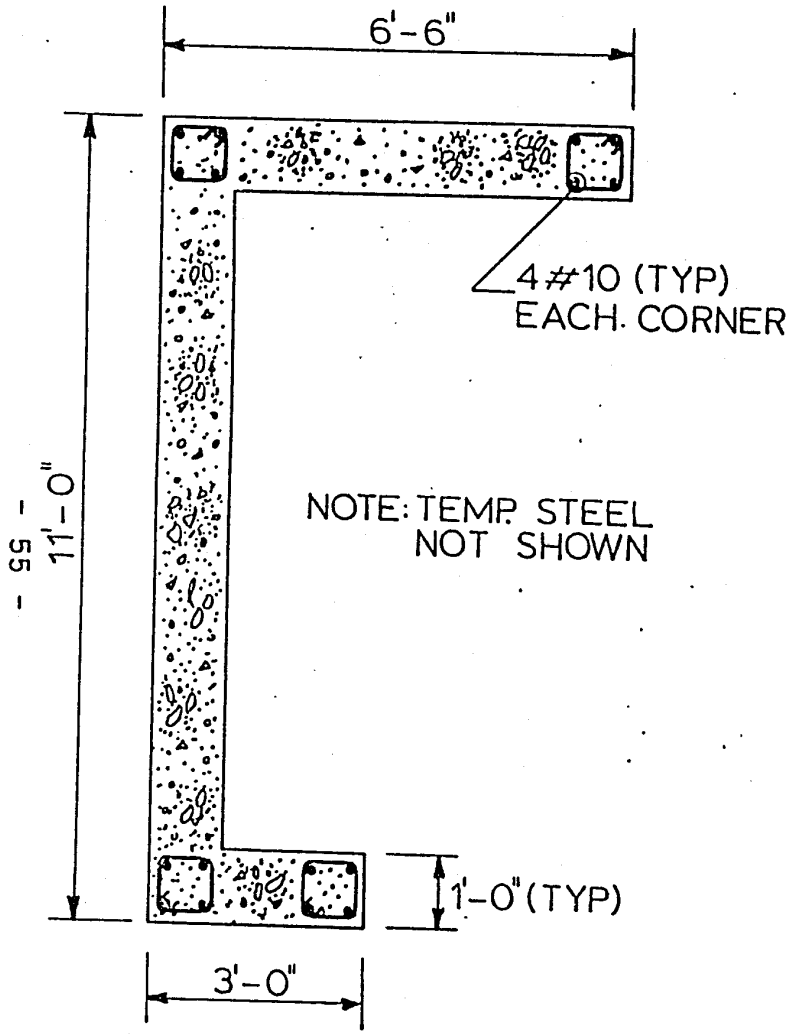

(A) SECTION

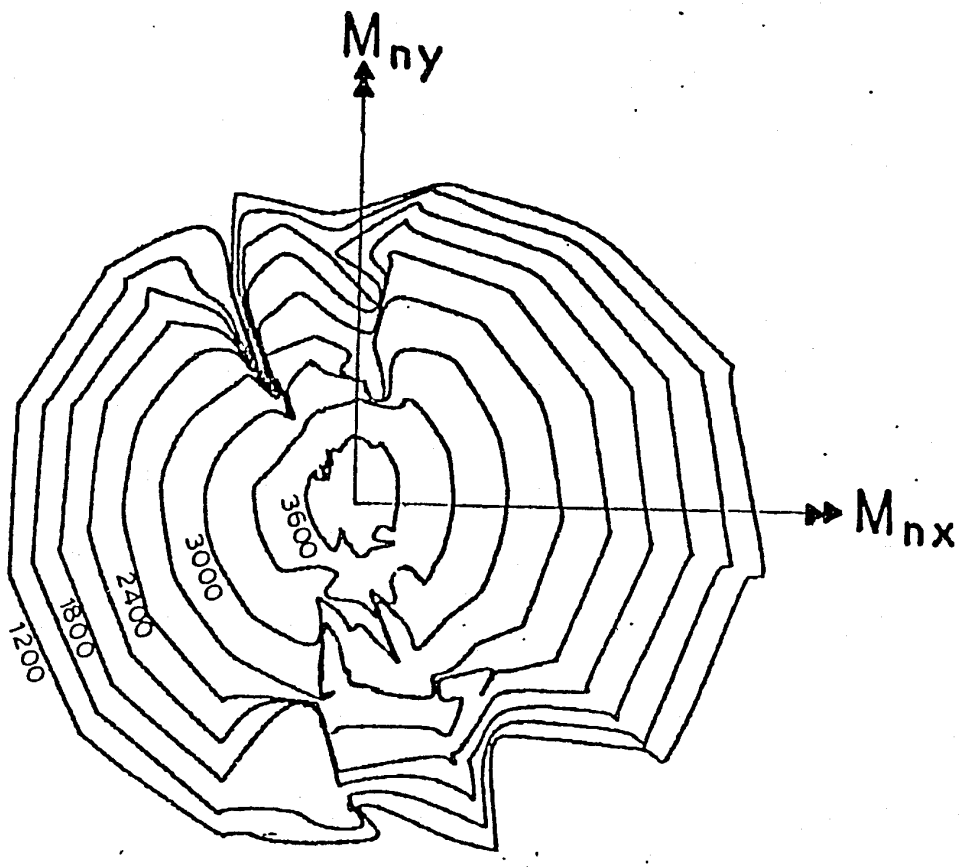

(B) LOAD CONTOURS IN COMPRESSION ZONE

Fig. 11 C – SHAPED WALL IN BIAXIAL BENDING

Appendix B

THE COMPUTER PROGRAM

```
C
C     BIAXIAL BENDING OF UNSYMMETRICAL REINFORCED CONCRETE COLOUMNS .
C
C      TEST SECTION 'L' SHAPE
C
C     VERSION= LATEST (1982.08.12)
C
C
      IMPLICIT REAL*8(A-H,O-Z)
      DIMENSION SX(20),SY(20),CX(2500),CY(2500),NA(2500),K(20),
     *PDC(2500),AS(20),PDS(20),STC(2500),STS(20),FCC(2500),FSS(20)
      REAL*8 N,M,IP1,IP2,MX,MY,MSTY,MSTX,MSTX1,MSTY1
C
C
C     READING THE GEOMETRICAL PROPERTIES OF THE SECTION .
C
      READ(5,1) N,M,IP1,IP2
 1    FORMAT(4F5.1)
C
C
C     READING THE DIMENSIONS OF THE BLOCKS TON BE USED .
C
      READ(5,2) DELX,DELY
 2    FORMAT(2F6.2)
C
C
C     READING THE COCRETE CYLINDER COMPRESSIVE STRENGTH .
```

```
      READ(5,3) FC
    3 FORMAT(F5.2)
C
C
C
C
C     READING THE COORDINATES OF THE STEEL BARS .
C
C
C     SX=X-COORDINATE OF A BAR CENTROID .
C     SY=Y-COORDINATE OF A BAR CENTROID .
C     NSB=NUMBER OF STEEL BARS .
C     SIGMAY=THE YEILD STRESS OF THE STEEL BARS .
C
C
      READ(5,200) NSB,SIGMAY
  200 FORMAT(I2,F6.1)
      DO 201 I=1,NSB
      READ(5,202) SX(I),SY(I),AS(I)
  202 FORMAT(3F8.3)
  201 CONTINUE
C
C
C
C     PROPERTIES OF THE SECTION OUTPUT :
C
C
```

```
      WRITE(6,6001)
 6001 FORMAT('1',40X,'THE SECTION PROPERTIES ARE :')
      WRITE(6,6002) N,M,IP1,IP2
 6002 FORMAT('0',15X,'N=',F6.1,15X,'M=',F6.1,15X,'IP1=',F6.1,15X,'IP2='
     *,F6.1)
      WRITE(6,6003) DELX,DELY
 6003 FORMAT('0',20X,'DELX=',F6.1,20X,'DELY=',F6.1)
      WRITE(6,6004) FC
 6004 FORMAT('0',25X,'THE CYLINDER COMPRESSIVE STRENGTH OF CONCRETE =',
     *F8.3)
      WRITE(6,6005) SIGMAY
 6005 FORMAT('0',25X,'THE STEEL YEILD STRENGTH =',F8.3)
C
C
      WRITE(6,9147)
 9147 FORMAT('1',50X,'T H E   A R E A S   O F   T H E   S T E E L   B A
     *R S   A R E')
      DO 9145 IT=1,NSB
      WRITE(6,9146) IT,AS(IT)
 9146 FORMAT('0',10X,'THE AREA OF BAR NUMBER',I2,'=',F8.2)
 9145 CONTINUE
C
C
C
C     CX=X-COORDINATE OF A BLOCK
C
C     CY=Y-COORDINATE OF A BLOCK
```

```
C
C
      NM=0
      ZNB1=N/DELX
      ZNB2=IP1/DELY
      ZNB3=M/DELX
      ZNB4=IP2/DELY
      NB1=ZNB1
      NB2=ZNB2
      NB3=ZNB3
      NB4=ZNB4
      Y=-DELY/2.D0
      DO 1000 I=1,NB2
      X=-DELX/2.D0
      Y=Y+DELY
      DO 2000 J=1,NB1
      X=X+DELX
      NM=NM+1
      CX(NM)=X
      CY(NM)=Y
 2000 CONTINUE
 1000 CONTINUE
      IF(NB3 .EQ. 0.D0) GO TO 1819
      DO 3000 I=1,NB4
      X=-DELX/2.D0
      Y=Y+DELY
      DO 4000 J=1,NB3
```

```
      X=X+DELX
      NM=NM+1
      CX(NM)=X
      CY(NM)=Y
 4000 CONTINUE
 3000 CONTINUE
C
 1819 WRITE(6,1932) NM,NSB
 1932 FORMAT('1',10X,'THENUMBER OF CONCRETE BLOCKS =',I5,20X,'THE NUMBER
     * OF STEEL BARS =',I3)
C
C     CALCULATION OF THE PLASTIC CENTROID .
C
C
C     NSB=NUMBER OF STEEL BARS .
C     SIGMAY=THE STEEL YIELD STRESS .
C     AS(I)=AREA OF THE ITH STEEL BAR .
C     FC=THE CONCRETE CYLINDER STRENGTH .
C
C
      MSTX=0.D0
      MSTY=0.D0
      FSTX=0.D0
      FSTY=0.D0
      FCONC=85.D-2*FC*((N*IP1)+(M*IP2))
      XXC=(((M**2/2.D0)*IP2)+((N**2/2.D0)*IP1))/(N*IP1+M*IP2)
      YYC=(((IP1**2/2.D0)*N)+(M*IP2)*(IP1+(IP2/2.D0)))/(N*IP1+M*IP2)
```

```
      MCONCX=FCONC*XXC
      MCONCY=FCONC*YYC
      DO 100 I=1,NSB
      FSX1=AS(I)*(SIGMAY-(85.D-2*FC))
      FSY1=AS(I)*(SIGMAY-(85.D-2*FC))
      FSTX=FSTX+FSX1
      FSTY=FSTY+FSY1
      MSTX1=FSX1*SX(I)
      MSTY1=FSY1*SY(I)
      MSTX=MSTX+MSTX1
      MSTY=MSTY+MSTY1
  100 CONTINUE
      XPC=(MSTX+MCONCX)/(FSTX+FCONC)
      YPC=(MSTY+MCONCY)/(FSTY+FCONC)
C
      WRITE(6,1357)  XPC,YPC
 1357 FORMAT('1',20X,'XPC=',F10.4,20X,'YPC=',F10.4)
C
C
      CALL CENTPC(CX,CY,NM,XPC,YPC)
      CALL CENTPC(SX,SY,NSB,XPC,YPC)
      ICOUNT=2
      YINT=1205.D0
      DELTA=5.D0
      THETA=0.D0
      DO 5195 IJCM=1,1
      IF(THETA .LT. 180.D0) BN=-YINT
```

```
      IF(THETA .GE. 180.D0) BN=YINT
      IF(THETA .EQ. 90.D0) X0=-YINT
      IF(THETA .EQ. 270.D0) X0=YINT
 9192 STRN=19.D-04
      WRITE(6,444)
 444  FORMAT('1')
      THETAR=THETA*1745.D-5
      CALL COMP (CX,CY,THETA,THETAR,NA,NM,DELX,DELY,BN,X0)
      CALL COMPS (SX,SY,THETA,THETAR,K,NSB,BN,X0,AS)
      CALL PERPED (CX,CY,NM,THETA,BN,PDC,THETAR,X0)
      CALL PERPED (SX,SY,NSB,THETA,BN,PDS,THETAR,X0)
 6918 IF(ICOUNT .EQ. 2) STRN =STRN + 1.D-04
      CALL STRAIN (NM,NSB,PDC,PDS,NA,K,STC,STS,SIGMAY,ZMAX,STRN)
      IF(ZMAX .EQ. 0.D0) GO TO 222
      CALL STRESS (NM,NSB,STC,STS,FCC,FSS,FC,NA,K,SIGMAY)
C
C
C
C
C
C
C
C     CALCULATION OF ULTIMATE LOADS & MOMENTS
C
      A=DELX*DELY
      PU=0.D0
      MX=0.D0
```

```
      MY=0.D0
      PU1=0.D0
      PU2=0.D0
      ZMX1=0.D0
      ZMX2=0.D0
      ZMY1=0.D0
      ZMY2=0.D0
      PU11=0.D0
      PU22=0.D0
      ZMX11=0.D0
      ZMX22=0.D0
      ZMY11=0.D0
      ZMY22=0.D0
      IF(ICOUNT .EQ. 1) WRITE(6,5353)
 5353 FORMAT('1','BLOCK   X-COORD.    Y-COORD.   NA        STRAIN
     *   STRESS             LOAD            X-MOMENT          Y-MOMENT')
      DO 5101 I=1,NM
      IF(NA(I) .EQ. 1) PU11=A*FCC(I)
      IF(NA(I) .EQ. 0) PU11=0.D0
      ZMX11=PU11*(CY(I))
      ZMY11=PU11*(CX(I))
      IF(ICOUNT .EQ. 1) WRITE(6,5252) I,CX(I),CY(I),NA(I),STC(I),FCC(I),
     *PU11,ZMX11,ZMY11
 5252 FORMAT(' ',I5,2X,F10.2,2X,F10.2,2X,I2,2X,G15.7,2X,G15.7,2X,G15.7,
     * 2X,G15.7,2X,G15.7)
      PU1=PU1+PU11
      ZMX1=ZMX1+ZMX11
```

```
      ZMY1=ZMY1+ZMY11
 5101 CONTINUE
      IF(ICOUNT .EQ. 1) WRITE(6,5454) PU1,ZMX1,ZMY1
 5454 FORMAT('1',10X,'PU1=',G15.7,10X,'ZMX1=',G15.7,'ZMY1=',G15.7)
      IF(ICOUNT .EQ. 1) WRITE(6,7171)
 7171 FORMAT('1',' BAR    X-COORD.    Y-COORD.    K       STRAIN
     *   STRESS              LOAD            X-MOMENT          Y-MOMENT')
      DO 5102 I=1,NSB
      PU22=AS(I)*FSS(I)
      ZMX22=PU22*(SY(I))
      ZMY22=PU22*(SX(I))
      IF(ICOUNT .EQ. 1) WRITE(6,7272) I,SX(I),SY(I),K(I),STS(I),FSS(I),
     *PU22,ZMX22,ZMY22
 7272 FORMAT(' ',I5,2X,F10.2,2X,F10.2,2X,I2,2X,G15.7,2X,G15.7,2X,G15.7,
     * 2X,G15.7,2X,G15.7)
      PU2=PU2+PU22
      ZMX2=ZMX2+ZMX22
      ZMY2=ZMY2+ZMY22
 5102 CONTINUE
      IF(ICOUNT .EQ. 1) WRITE(6,7474) PU2,ZMX2,ZMY2
 7474 FORMAT('1',10X,'PU2=',G15.7,10X,'ZMX2=',G15.7,'ZMY2=',G15.7)
      PU=(PU1+PU2)/1000.D0
      MX=(ZMX1+ZMX2)/1000000.D0
      MY=(ZMY1+ZMY2)/1000000.D0
  222 IF((THETA .EQ. 90.D0).OR.(THETA .EQ. 270.D0)) GOTO 5917
      WRITE(6,9988) THETA,BN,ZMAX,STRN
 9988 FORMAT('0',5X,'THETA=',F5.1,5X,'N.A. INTERCEPT=',G25.16,5X
```

```
     *,'ZMAX=',G25.16,5X,'STRAIN=',G15.7)
       GO TO 9381
 5917 WRITE(6,9988) THETA,X0,ZMAX,STRN
 9381 IF((ZMAX .EQ. 0.D0).AND.(ICOUNT .EQ. 1)) GO TO 666
      IF(ZMAX .EQ. 0.D0) GO TO 7195
      WRITE(6,8899) PU,MX,MY
 8899 FORMAT('0',20X,'PU=',G15.7,20X,'MX=',G15.7,20X,'MY=',G15.7)
      WRITE(6,4455)
 4455 FORMAT(132('*'))
      IF(ICOUNT .EQ. 1) GO TO 666
C     ****************************************************************
      IF(ZMAX .LT. 725.D0) GO TO 666
C     ****************************************************************
      IF((ICOUNT .EQ. 2) .AND. (STRN .GE. 3.D-03)) GO TO 6195
      IF(ICOUNT .EQ. 2)GO TO 6918
 6195 IF(THETA .LT. 180.D0) BN=BN+DELTA
      IF(THETA .GE. 180.D0) BN=BN-DELTA
      IF(THETA .EQ. 90.D0) X0=X0+DELTA
      IF(THETA .EQ. 270.D0) X0=X0-DELTA
      GO TO 9192
 7195 THETA = THETA+15.D0
 5195 CONTINUE
C
  666 STOP
      END
      SUBROUTINE CENTPC (X,Y,N,X0,Y0)
      IMPLICIT REAL*8(A-H,O-Z)
```

```
C
C
      DIMENSION X(N),Y(N)
C
C
C     THIS SUBROUTINE FINDS THE COORDINATES OF THE CENTROID OF EACH
C     BLOCK OR BAR WITH RESPECT TO THE PLASTIC CENTROIDAL AXIS .
C
C
C     X=X-COORDINATE OF A BLOCK OR A BAR .
C     Y=Y-COORDINATE OF A BLOCK OR A BAR .
C     N=NO. OF B;OCKS OR BARS .
C     X0=X-COORDINATE OF THE PLASTIC CENTROID .
C     Y0=Y-COORDINATE OF THE PLASTIC CENTROID .
C
C
      DO 1 I=1,N
      X(I)=X(I)-X0
      Y(I)=Y(I)-Y0
 1    CONTINUE
      RETURN
      END
C
C
C
      SUBROUTINE COMP(X,Y,THETA,THETAR,NN,II,DELX,DELY,BN,X0)
      IMPLICIT REAL*8(A-H,O-Z)
```

```
C
C
C
      DIMENSION X(II),Y(II),NN(II)
C
C
C
C     THIS SUBROUTINE FINDS WHEATHER THE BLOCK LIE ON THE
C     TENSION OR COMPRESSION SIDE .
C
C
C     X=X-COORDINATE OF A BLOCK .
C     Y=Y-COORDINATE OF A BLOCK .
C     THETA=THE SLOPE OF THE NEUTRAL AXIS (DEGREES) .
C     THETAR=THE SLOPE OF THE NEUTRAL AXIS (RADIANS) .
C     NN=A VARIABLE WHICH IDENTIFIES IF THE BLOCK LIES
C        ON THE COMPRESSION SIDE OR ON THE TENSION SIDE .
C          NN=0 ....> THE BLOCK LIES ON TENSION SIDE .
C          NN=1 ....> THE BLOCK LIES ON COMPRESSION SIDE .
C     II=NUMBERS OF BLOCKS .
C     DELX=DIMENSION OF EACH BLOCK IN THE X-DIRECTION .
C     DELY=DIMENSION OF EACH BLOCK IN THE Y-DIRECTION .
C     BN=INTERCEPT OF THE NEUTRAL AXIS WITH THE Y CENTROIDAL AXIS .
C     X0=X-INTERCEPT OF A VERTICAL NEUTRAL AXIS .
C
C
      IF(THETA .EQ. 0.D0 .OR. THETA .EQ. 360.D0) GO TO 1
```

```
      IF(THETA .LT. 90.D0) GO TO 2
      IF(THETA .EQ. 90.D0) GO TO 3
      IF(THETA .LT. 180.D0) GO TO 4
      IF(THETA .EQ. 180.D0) GO TO 5
      IF(THETA .LT. 270.D0) GO TO 6
      IF(THETA .EQ. 270.D0) GO TO 7
C
C
      SL=DTAN(THETAR)
      DO 8 I=1,II
      A=X(I)+(DELX/2.D0)
      B=Y(I)+(DELY/2.D0)
      C=((B-BN)/SL)
      IF(C .GE. A) NN(I)=1
      IF(C .LT. A) NN(I)=0
    8 CONTINUE
      GO TO 16
C
C
    1 DO 9 I=1,II
      D=Y(I)-(DELY/2.D0)
      IF(D .GE. BN) NN(I)=1
      IF(D .LT. BN) NN(I)=0
    9 CONTINUE
      GO TO 16
C
C
```

```
   2    SL=DTAN(THETAR)
        DO 10 I=1,II
        E=X(I)+(DELX/2.D0)
        F=Y(I)-(DELY/2.D0)
        G=((F-BN)/SL)
        IF(G .GE. E) NN(I)=1
        IF(G .LT. E) NN(I)=0
  10    CONTINUE
        GO TO 16
C
C
   3    DO 11 I=1,II
        H=X(I)-(DELX/2.D0)
        IF(H .GE. X0) NN(I)=1
        IF(H .LT. X0) NN(I)=0
  11    CONTINUE
        GO TO 16
C
C
   4    SL=DTAN(THETAR)
        DO 12 I=1,II
        AA=X(I)-(DELX/2.D0)
        BB=Y(I)-(DELY/2.D0)
        CC=((BB-BN)/SL)
        IF(AA .GE. CC) NN(I)=1
        IF(AA .LT. CC) NN(I)=0
  12    CONTINUE
```

```
      GO TO 16
C
C
  5   DO 13 I=1,II
      DD=Y(I)+(DELY/2.D0)
      IF(DD .LE. BN) NN(I)=1
      IF(DD .GT. BN) NN(I)=0
  13  CONTINUE
      GO TO 16
C
C
  6   SL=DTAN(THETAR)
      DO 14 I=1,II
      EE=X(I)-(DELX/2.D0)
      FF=Y(I)+(DELY/2.D0)
      GG=((FF-BN)/SL)
      IF(EE .GE. GG) NN(I)=1
      IF(EE .LT. GG) NN(I)=0
  14  CONTINUE
      GO TO 16
C
C
  7   DO 15 I=1,II
      HH=X(I)+(DELX/2.D0)
      IF(HH .LE. X0) NN(I)=1
      IF(HH .GT. X0) NN(I)=0
  15  CONTINUE
```

```
   16  RETURN
       END
C
C
      SUBROUTINE COMPS(X,Y,THETA,THETAR,NN,II,BN,X0,AS)
      IMPLICIT REAL*8(A-H,O-Z)
C
C
C
C
      DIMENSION X(II),Y(II),NN(II),AS(II),R(20)
C
C
C     THIS SUBROUTINE FINDS WHEATHER THE  BAR LIE ON THE
C     TENSION OR COMPRESSION SIDE .
C
C
C     X=X-COORDINATE OF  A BAR .
C     Y=Y-COORDINATE OF  A BAR .
C     THETA=THE SLOPE OF THE NEUTRAL AXIS (DEGREES) .
C     THETAR=THE SLOPE OF THE NEUTRAL AXIS (RADIANS) .
C     NN=A VARIABLE WHICH IDENTIFIES IF  THE BAR LIES
C        ON THE COMPRESSION SIDE OR ON THE TENSION SIDE .
C          NN=0 ....> THE  BAR LIES ON TENSION SIDE .
C          NN=1 ....> THE  BAR LIES ON COMPRESSION SIDE .
C     II=NUMBERS OF  BARS .
C     BN=INTERCEPT OF THE NEUTRAL AXIS WITH THE Y CENTROIDAL AXIS .
```

```
C      X0=THE X-COORDINATE OF THE PLASTIC CENTROID .
C      AS=THE AREA OF EACH STEEL BAR .
C
C
C
C
      DO 20 IL=1,II
      R(IL)=DSQRT(AS(IL)/3141592654.D-9)
      R(IL)=2.D0*R(IL)
   20 CONTINUE
C
      IF(THETA .EQ. 0.D0 .OR. THETA .EQ. 360.D0) GO TO 1
      IF(THETA .LT. 90.D0) GO TO 2
      IF(THETA .EQ. 90.D0) GO TO 3
      IF(THETA .LT. 180.D0) GO TO 4
      IF(THETA .EQ. 180.D0) GO TO 5
      IF(THETA .LT. 270.D0) GO TO 6
      IF(THETA .EQ. 270.D0) GO TO 7
C
C
      SL=DTAN(THETAR)
      DO 8 I=1,II
      A=X(I)+(R(I)/2.D0)
      B=Y(I)+(R(I)/2.D0)
      C=((B-BN)/SL)
      IF(C .GE. A) NN(I)=1
      IF(C .LT. A) NN(I)=0
```

```
    8   CONTINUE
        GO TO 16
C
C
    1   DO 9 I=1,II
        D=Y(I)-(R(I)/2.D0)
        IF(D .GE. BN) NN(I)=1
        IF(D .LT. BN) NN(I)=0
    9   CONTINUE
        GO TO 16
C
C
    2   SL=DTAN(THETAR)
        DO 10 I=1,II
        E=X(I)+(R(I)/2.D0)
        F=Y(I)-(R(I)/2.D0)
        G=((F-BN)/SL)
        IF(G .GE. E) NN(I)=1
        IF(G .LT. E) NN(I)=0
   10   CONTINUE
        GO TO 16
C
C
    3   DO 11 I=1,II
        H=X(I)-(R(I)/2.D0)
        IF(H .GE. X0) NN(I)=1
        IF(H .LT. X0) NN(I)=0
```

```
  11  CONTINUE
      GO TO 16
C
C
   4  SL=DTAN(THETAR)
      DO 12 I=1,II
      AA=X(I)-(R(I)/2.D0)
      BB=Y(I)-(R(I)/2.D0)
      CC=((BB-BN)/SL)
      IF(AA .GE. CC) NN(I)=1
      IF(AA .LT. CC) NN(I)=0
  12  CONTINUE
      GO TO 16
C
C
   5  DO 13 I=1,II
      DD=Y(I)+(R(I)/2.D0)
      IF(DD .LE. BN) NN(I)=1
      IF(DD .GT. BN) NN(I)=0
  13  CONTINUE
      GO TO 16
C
C
   6  SL=DTAN(THETAR)
      DO 14 I=1,II
      EE=X(I)-(R(I)/2.D0)
      FF=Y(I)+(R(I)/2.D0)
```

```
      GG=((FF-BN)/SL)
      IF(EE .GE. GG) NN(I)=1
      IF(EE .LT. GG) NN(I)=0
   14 CONTINUE
      GO TO 16
C
C
    7 DO 15 I=1,II
      HH=X(I)+(R(I)/2.D0)
      IF(HH .LE. X0) NN(I)=1
      IF(HH .GT. X0) NN(I)=0
   15 CONTINUE
   16 RETURN
      END
C
C
      SUBROUTINE PERPED (X,Y,N,SLOPE,ZINT,PD,SA,X0)
      IMPLICIT REAL*8(A-H,O-Z)
C
C
      DIMENSION X(N),Y(N),PD(N)
C
C
C     THIS SUBROUTINE FINDS THE PERPENDICULAR DISDTANCE FROM THE
C     CENTROID OF EACH BLOCK OR BAR TO THE NEUTRAL AXIS .
C
C
```

```
C     X=X-COORDINATE OF A BLOCK OR A BAR .
C     Y=Y-COORDINATE OF A BLOCK OR A BAR
C     N=THE NUMBER OF BLOCKS OR BARS .
C     SLOPE=SLOPE OF THE NEUTRAL AXIS (DEGREES) .
C     ZINT=INTERCEPT OF THE NEUTRAL AXIS WITH THE Y CENTROIDAL AXIS .
C     PD=PERPENDICULAR DISDTANCE FROM A BLOCK OR A BAR TO THE NEUTRAL
C        AXIS .
C     SA=SLOPE OF THE NEUTRAL AXIS (RADIANS) .
C
C
      IF((SLOPE .EQ. 90.D0).OR.(SLOPE .EQ. 270.D0))GO TO 1
      IF((SLOPE .EQ. 0.D0).OR.(SLOPE .EQ. 180.D0).OR.(SLOPE .EQ.360.D0))
     *GOTO 8
C
      SS=DTAN(SA)
      DO 2 I=1,N
      XP=((SS*Y(I)+X(I)-SS*ZINT)/(1+(SS**2)))
      YP=ZINT+SS*XP
      PD(I)=DSQRT(((XP-X(I))**2)+((YP-Y(I))**2))
    2 CONTINUE
      GO TO 3
    1 DO 4 I=1,N
      PD(I)=DABS(X0-X(I))
    4 CONTINUE
      GO TO 3
    8 DO 9 I=1,N
      IF(ZINT .EQ. 0.D0) PD(I)=DABS(Y(I))
```

```
      IF((ZINT .LT. 0.D0).AND.(Y(I) .LE. 0.D0)) PD(I)=DABS(DABS(Y(I))-
     *DABS(ZINT))
      IF((ZINT .LT. 0.D0).AND.(Y(I) .GE. 0.D0)) PD(I)=Y(I)+DABS(ZINT)
      IF((ZINT .GT. 0.D0).AND.(Y(I) .LE. 0.D0)) PD(I)=ZINT+DABS(Y(I))
      IF((ZINT .GT. 0.D0).AND.(Y(I) .GE. 0.D0)) PD(I)=DABS(ZINT-Y(I))
 9    CONTINUE
 3    RETURN
      END
      SUBROUTINE STRAIN (N,M,Z,G,IC,IS,STC,STS,SIGMAY,ZMAX,STRN)
      IMPLICIT REAL*8(A-H,O-Z)
      DIMENSION Z(N),G(M),IC(N),IS(M),STC(N),STS(M)
C
C
C     THIS SUBROUTINE FINDS THE STRAIN IN THE COMPRESSED CONCRETE BLOCKS
C    ,  AND THE STRAIN IN THE STEEL BARS .
C
C
C     N=THE NUMBER OF BLOCKS .
C     M=THE NUMBER OF BARS .
C     Z=THE PERPENDICULAR DISDTANCE FROM THE CENTROID OF A BLOCK TO THE
C       NEUTRAL AXIS .
C     G= THE PERPENDICULAR DISDTANCE FROM THE CENTROID OF A BLOCK TO THE
C        NEUTRAL AXIS .
C     IC=IDENTIFIES IF THE BLOCK LIES ON THE COMPRESSION SIDE OF THE
C        NEUTRAL AXIS .
C     IS=IDENTIFIES IF THE BAR LIES UN THE TENSION OR COMPRESSION SIDE
C        OF THE NEUTRAL AXIS .
```

```
C     STC=STRAIN AT THE CENTRE OF THE CONCRETE BLOCK .
C     STS=STRAIN IN THE CENTRE OF THE STEEL BAR .
C
C
C     CALCULATION OF THE PERPENDICULAR DISDTANCE FROM THE NEUTRAL AXIS
C     TO THE MOST COMPRESSED CONCRETE BLOCK .
C
      ZMAX=0.D0
      DO 1 I=1,N
      IF(IC(I) .EQ. 0) GO TO 1
      IF(Z(I) .GT. ZMAX) ZMAX=Z(I)
 1    CONTINUE
C
C
      IF(ZMAX .EQ. 0.D0) GO TO 88
C
C
      DO 6 I=1,N
      IF(IC(I) .EQ. 0) STC(I)=0.D0
      IF(IC(I) .EQ. 1) STC(I)=((Z(I)/ZMAX)*STRN)
 6    CONTINUE
      DO 7 I=1,M
      STS(I)=(G(I)/ZMAX)*STRN
 7    CONTINUE
   88 RETURN
      END
      SUBROUTINE STRESS (N,M,STC,STS,FCC,FSS,FC1,NA,K,SIGMAY)
```

```
      IMPLICIT REAL*8(A-H,O-Z)
C
C
      DIMENSION STC(N),STS(M),NA(N),K(M),FCC(N),FSS(M),FSSC(20)
C
C
C     THIS SUBROUTINE FINDS THE STRESSES AT THE CONCRETE BLOCKS UNDER
C     COMPRESSION      ,AND AT THE STEEL BARS (COMPRESSIVE STRESS IS
C     POSITIVE) .
C
C
C     N=THE NUMBER OF CONCRETE BLOCKS .
C     M=THE NUMBER OF STEEL BARS .
C     STC=THE STRAIN IN CONCRETE BLOCKS .
C     STS=THE STRAIN IN THE STEEL BARS .
C     FCC=THE STRESS IN THE COMPRESSED CONCRETE BLOCKS .
C                          > A STRESS OF ZERO WILL BE ASSIGNED TO THE
C                            CONCRETE BLOCKS WHICH ARE IN TENSION .
C     FSS=THE STRESS IN THE STEEL BARS .
C     FC=THE CYLINDER COMPRESSIVE STRENGTH OF CONCRETE (MPA.) .
C     NA=IDENTIFIES IF THE BLOCK LIES IN THE COMPRESSION ZONE .
C     IDENTIFIES IF THE BAR LIES IN THE TENSION OR THE COMPRESSION ZONE.
C
C
C
C     CALCULATION OF THE STRESSES IN THE COMPRESSED CONCRETE BLOCKS .
C
```

```
      FC=FC1
      FC=85.D-2*FC
      EC=1800000.D0+460.D0*FC*1450326.D-4
      E0=2.D0*FC/EC
      DO 1 I=1,N
      IF(NA(I) .EQ. 0) FCC(I)=0.D0
      IF(NA(I) .EQ. 0) GO TO 1
      FCCM=FC*1450326.D-4
      FCC(I)=((4.D0*STC(I)*EC*(FCCM**2))/(4.D0*(FCCM**2)+((STC(I)**2)*(E
     *C**2))))*6895.D-6
 1    CONTINUE
C
C
C     TO ACCOUNT FOR THE DISPLACED VOLUME OF THE CONCRETE IN THE
C     COMPRESSION ZONE .
C
      EC=1800000.D0+460.D0*FC*1450326.D-4
      E0=2.D0*FC/EC
      DO 1234 I=1,M
      IF(K(I) .EQ. 0) FSSC(I)=0.D0
      IF(K(I) .EQ. 0) GO TO 1234
      FCCM=FC*1450326.D-4
      FSSC(I)=((4.D0*STS(I)*EC*(FCCM**2))/(4.D0*(FCCM**2)+((STS(I)**2)*(
     *EC**2))))*6895.D-6
1234 CONTINUE
C
C     CALCULATION OF THE STRESSES IN THE STEEL BARS .
```

```
C
      DO 2 I=1,M
      SS=SIGMAY/200000.D0
      IF(STS(I) .LT. SS) FSS(I)=200000.D0*STS(I)
      IF(STS(I) .GE. SS) FSS(I)=SIGMAY
      IF(K(I) .EQ. 1) FSS(I)=FSS(I)-FSSC(I)
      IF(K(I) .EQ. 0) FSS(I)=-FSS(I)
 2    CONTINUE
      RETURN
      END
//GO.SYSIN DD *
510.0310.0310.0200.0
010.00010.00
27.58
080413.7
0050.8000050.8000645.000
0259.2000050.8000645.000
0459.2000050.8000645.000
0050.8000259.2000645.000
0259.2000259.2000645.000
0459.2000259.2000645.000
0050.8000459.2000645.000
0259.2000459.2000645.000
/*
```

Appendix C

TABLES

TABLE B Observed Loads and Loads Computed from Strains

Specimen	Observed Forces			Ratio = Computed Value / Observed Value											
				Parabola-Rect.			Mod. Hognestad			Chang			Kent & Park		
	P_u K.	M_x K-ft	M_y K-ft	P_u	M_x	M_y	P_u	M_x	M_y	P_u	M_x	M_y	P_u	M_x	M_y
R1	119	60.6	184	.907	.981	.842	.908	.946	.834	.841	.971	.809	.884	.877	.809
R2	120	124	154.1	.876	.924	.938	.872	.890	.922	.811	.904	.898	.838	.821	.878
R3	129	229	127.4	.769	.894	.921	.755	.869	.895	.700	.854	.876	.725	.814	.840
R4	87.1	40.3	160.8	.799	.860	.970	.799	.838	.968	.724	.856	.917	.786	.796	.953
R5	94.3	128.2	150.4	1.002	.940	.986	.991	.918	.972	.905	.914	.927	.971	.871	.946
R6	85.8	2.18	102.0	.894	.959	.949	.887	.869	.922	.828	.918	.910	.833	.877	.824
R7	53.9	52.2	145.9	.709	.724	.833	.732	.710	.844	.650	.716	.798	.698	.691	.845
R8	40.4	86.6	121.3	.750	.958	.875	.768	.942	.880	.688	.933	.841	.710	.897	.812
R9	40.4	190.4	86.4	.741	.825	.860	.756	.872	.861	.674	.792	.826	.716	.794	.856
B1	136.	0	154.1	.877	-	.972	.898	-	.977	.822	-	.940	.872	-	.962
B2	138.	57.1	188.	.906	1.182	.815	.913	1.147	.826	.860	1.157	.823	.873	1.076	.792
B3	140.	165.1	161.6	.954	.833	.879	.961	.806	.858	.906	.815	.860	.916	.755	.771
B4	153.	268.	147.7	.991	.924	.852	.979	.915	.843	.885	.878	.806	.979	.901	.830
B5	156.	424.	0	.924	.879	-	.917	.856	-	.869	.860	-	.880	.809	-
B6	109.	0	194.2	.851	-	1.004	.833	-	.989	.765	-	.953	.819	-	.965
B7	96.2	67.8	179.1	.917	.880	.912	.930	.867	.911	.859	.860	.882	.896	.835	.887
B8	92.2	171.3	147.1	.996	.883	.923	1.022	.882	.930	.933	.859	.890	.983	.861	.906
B9	99.2	243.	155.6	.841	.940	.874	.837	.931	.867	.758	.896	.826	.819	.910	.848
B10	119.	455.	0	1.155	1.001	-	1.103	.951	-	1.066	.963	-	1.014	.845	-
B11	60.7	0	165.5	.817	-	.929	.823	-	.929	.743	-	.890	.795	-	.910
B12	57.1	64.4	168.0	.756	.639	.854	.771	.638	.860	.670	.616	.809	.750	.627	.849
B13	53.2	252.	128.8	.942	.876	.915	.930	.861	.900	.836	.840	.875	.867	.819	.857
B14	58.4	372.	0	.800	.886	-	.799	.879	-	.747	.861	-	.737	.840	-
Mean Value				.877	.899	.905	.878	.879	.899	.807	.873	.868	.842	.836	.867
Std. Deviation				.105	.108	.055	.097	.099	.051	.102	.105	.048	.094	.090	.057
Coeff Variation				.011	.011	.003	.009	.009	.002	.010	.011	.002	.008	.008	.003

1 K. = 4.5 kN 1 K-ft = 1.37 kN-m.

TABLE 1.2.3.1 : Observed loads and loads computed from strains.

Inclination of the N.A.	Curvature	Inclination of the N.A.	Curvature
0	4.13	180	4.53
15	3.63	195	3.85
30	3.38	210	3.51
45	3.34	225	3.34
60	3.51	240	3.37
75	3.86	255	3.62
90	4.13	270	4.53
105	4.09	285	4.16
120	4.24	300	3.98
135	4.62	315	3.91
150	4.24	330	3.98
165	4.10	345	4.15

TABLE 2.4.3.1 : The ultimate biaxial curvature for Pu=6500KN

and 0.003 maximum allowable concrete strain

Inclination of the N.A.	Curvature	Inclination of the N.A.	Curvature
0	6.09	180	6.32
15	5.47	195	5.58
30	5.13	210	5.14
45	5.03	225	5.03
60	5.15	240	5.13
75	5.59	255	5.49
90	6.09	270	6.32
105	6.12	285	6.20
120	6.34	300	6.05
135	6.66	315	6.05
150	6.36	330	6.06
165	6.11	345	6.20

TABLE 2.4.3.2 : The ultimate biaxial curvature for Pu=6500KN and 0.004 maximum allowable concrete strain

Inclination of the N.A.	Curvature	Inclination of the N.A.	Curvature
0	4.90	180	5.47
15	4.30	195	4.62
30	4.03	210	4.16
45	3.98	225	3.98
60	3.98	240	4.02
75	4.62	255	4.29
90	4.90	270	5.47
105	5.96	285	5.00
120	6.27	300	4.73
135	6.85	315	4.63
150	5.05	330	4.74
165	4.87	345	4.99

TABLE 2.4.3.3 : The ultimate biaxial curvature for Pu=6000KN and 0.003 maximum allowable concrete strain

Inclination of the N.A.	Curvature	Inclination of the N.A.	Curvature
0	7.18	180	7.80
15	6.35	195	6.60
30	5.92	210	6.05
45	5.83	225	5.83
60	6.04	240	5.91
75	6.60	255	6.33
90	7.18	270	7.80
105	7.12	285	7.24
120	7.36	300	7.00
135	7.87	315	6.89
150	7.38	330	6.98
165	7.12	345	7.23

TABLE 2.4.3.4 : The ultimate biaxial curvature for Pu=6000KN and 0.004 maximum allowable concrete strain

Inclination of the N.A.	Curvature	Inclination of the N.A.	Curvature
0	5.98	180	7.01
15	5.25	195	5.78
30	4.94	210	5.15
45	4.90	225	4.90
60	5.16	240	4.92
75	5.78	255	5.23
90	5.98	270	7.01
105	4.86	285	6.23
120	5.06	300	5.81
135	5.45	315	5.65
150	6.28	330	5.81
165	5.94	345	6.24

TABLE 2.4.3.5 : The ultimate biaxial curvature for Pu=5000KN and 0.003 maximum allowable concrete strain

Inclination of the N.A.	Curvature	Inclination of the N.A.	Curvature
0	8.48	180	9.69
15	7.44	195	8.17
30	6.99	210	7.36
45	6.98	225	6.95
60	7.35	240	7.00
75	8.13	255	7.47
90	8.48	270	9.69
105	8.47	285	8.77
120	8.92	300	8.30
135	9.86	315	8.13
150	8.95	330	8.30
165	8.49	345	8.76

TABLE 2.4.3.6 : The ultimate biaxial curvature for Pu=5000KN and 0.004 maximum allowable concrete strain

Inclination of the N.A.	Curvature	Inclination of the N.A.	Curvature
0	7.03	180	8.75
15	6.13	195	7.11
30	5.77	210	6.21
45	5.77	225	5.77
60	6.20	240	5.78
75	7.13	255	6.14
90	7.03	270	8.75
105	7.05	285	7.47
120	7.49	300	6.75
135	8.17	315	6.57
150	7.43	330	6.77
165	7.02	345	7.43

TABLE 2.4.3.7 : The ultimate biaxial curvature for Pu=4000KN and 0.003 maximum allowable concrete strain

Inclination of the N.A.	Curvature	Inclination of the N.A.	Curvature
0	9.83	180	11.83
15	8.51	195	9.93
30	8.09	210	8.67
45	8.14	225	8.14
60	8.67	240	8.10
75	9.88	255	8.54
90	9.83	270	11.83
105	9.84	285	10.35
120	10.44	300	9.48
135	11.57	315	9.26
150	10.47	330	9.49
165	9.80	345	10.41

TABLE 2.4.3.8 : The ultimate biaxial curvature for Pu=4000KN and 0.004 maximum allowable concrete strain

Inclination of the N.A.	Curvature	Inclination of the N.A.	Curvature
0	8.40	180	****
15	7.19	195	8.70
30	6.72	210	8.70
45	6.84	225	6.84
60	7.42	240	6.72
75	8.69	255	7.21
90	8.40	270	****
105	8.37	285	8.89
120	8.80	300	7.86
135	9.89	315	7.56
150	8.74	330	7.84
165	8.34	345	8.93

TABLE 2.4.3.9 : The ultimate biaxial curvature for Pu=3000KN and 0.003 maximum allowable concrete strain

Inclination of the N.A.	Curvature	Inclination of the N.A.	Curvature
0	11.53	180	14.65
15	9.82	195	11.93
30	9.22	210	10.31
45	9.51	225	9.51
60	10.34	240	9.22
75	11.98	255	9.86
90	11.53	270	14.65
105	11.44	285	12.13
120	12.18	300	10.90
135	13.66	315	10.46
150	12.11	330	10.82
165	11.42	345	12.07

TABLE 2.4.3.10: The ultimate biaxial curvature for Pu=3000KN and 0.004 maximum allowable concrete strain

Inclination of the N.A.	Curvature	Inclination of the N.A.	Curvature
0	10.10	180	14.42
15	8.59	195	10.64
30	8.04	210	8.93
45	8.00	225	8.08
60	8.91	240	8.02
75	10.64	255	8.60
90	100.1	270	14.42
105	9.94	285	10.69
120	10.49	300	9.17
135	11.98	315	8.73
150	10.45	330	9.19
165	9.93	345	10.60

TABLE 2.4.3.11: The ultimate biaxial curvature for Pu=2000KN and 0.003 maximum allowable concrete strain

Inclination of the N.A.	Curvature	Inclination of the N.A.	Curvature
0	13.47	180	18.78
15	11.45	195	14.68
30	10.98	210	12.39
45	11.09	225	11.09
60	12.34	240	10.92
75	14.59	255	11.51
90	13.47	270	18.78
105	13.55	285	14.58
120	14.50	300	12.62
135	16.21	315	11.88
150	14.37	330	12.59
165	13.46	345	14.64

TABLE 2.4.3.12: The ultimate biaxial curvature for Pu=2000KN and 0.004 maximum allowable concrete strain

Inclination of the N.A.	Curvature	Inclination of the N.A.	Curvature
0	12.93	180	*****
15	10.83	195	13.38
30	9.88	210	10.73
45	9.87	225	9.87
60	10.75	240	9.87
75	13.41	255	10.76
90	12.93	270	*****
105	12.32	285	13.39
120	12.85	300	10.93
135	14.68	315	10.32
150	12.77	330	10.93
165	12.30	345	13.33

TABLE 2.4.3.13: The ultimate biaxial curvature for Pu=1000KN and 0.003 maximum allowable concrete strain

Inclination of the N.A.	Curvature	Inclination of the N.A.	Curvature
0	17.62	180	*****
15	14.44	195	18.24
30	13.36	210	15.00
45	13.63	225	13.63
60	14.86	240	13.38
75	18.42	255	14.49
90	17.62	270	*****
105	16.96	285	18.39
120	17.51	300	14.84
135	20.27	315	14.10
150	17.34	330	14.81
165	17.07	345	18.17

TABLE 2.4.3.14: The ultimate biaxial curvature for Pu=1000KN and 0.004 maximum allowable concrete strain

Inclination of the N.A.	Curvature	Inclination of the N.A.	Curvature
0	18.52	180	*****
15	14.67	195	17.54
30	13.04	210	13.98
45	12.86	225	12.86
60	14.01	240	13.11
75	17.72	255	14.84
90	18.52	270	*****
105	16.41	285	17.67
120	15.92	300	13.97
135	19.37	315	12.81
150	16.01	330	14.03
165	16.12	345	17.45

TABLE 2.4.3.15: The ultimate biaxial curvature for Pu=0000KN and 0.003 maximum allowable concrete strain

Inclination of the N.A.	Curvature	Inclination of the N.A.	Curvature
0	23.26	180	*****
15	19.56	195	24.78
30	17.72	210	18.64
45	16.89	225	16.89
60	18.90	240	17.68
75	24.77	255	19.92
90	23.26	270	*****
105	22.20	285	24.68
120	21.80	300	18.85
135	25.82	315	16.83
150	21.85	330	18.70
165	22.08	345	24.65

TABLE 2.4.3.16: The ultimate biaxial curvature for Pu=0000KN and 0.004 maximum allowable concrete strain

Load level (KN)	Maximum allowable concrete strain			
	0.003		0.004	
	Ultimate biaxial curvature			
	Mean	Standard deviation	Mean	standard deviation
0	15.52	2.13	20.90	3.00
1000	11.77	1.48	16.10	2.06
2000	9.95	1.74	13.50	2.18
3000	8.05	0.88	11.30	1.53
4000	6.91	0.87	9.63	1.14
5000	5.71	0.64	8.21	0.88
6000	4.61	0.47	6.82	0.65
6500	3.92	0.39	5.82	0.51

TABLE 2.4.3.17 : The ultimate biaxial curvatures

load level (KN)	percent increase in the ultimate biaxial curvature
0	34.6
1000	36.8
2000	35.7
3000	40.4
4000	39.5
5000	43.8
6000	47.9
6500	48.5

TABLE 3.5.1 : The effect of increasing the maximum allowable concrete strain from 0.003 to 0.004 on the ultimate biaxial curvature

ultimate load (KN)	percent increase in the ultimate biaxial curvature	
	maximum allowable concrete strain	
	0.003	0.004
0		
1000	31.9	29.8
2000	18.4	19.3
3000	23.5	19.5
4000	16.6	17.7
5000	20.9	17.3
6000	23.9	20.4
6500	17.6	17.2

TABLE 3.5.2 : The change in the ultimate biaxial curvature between successive load levels

Appendix D

FIGURES

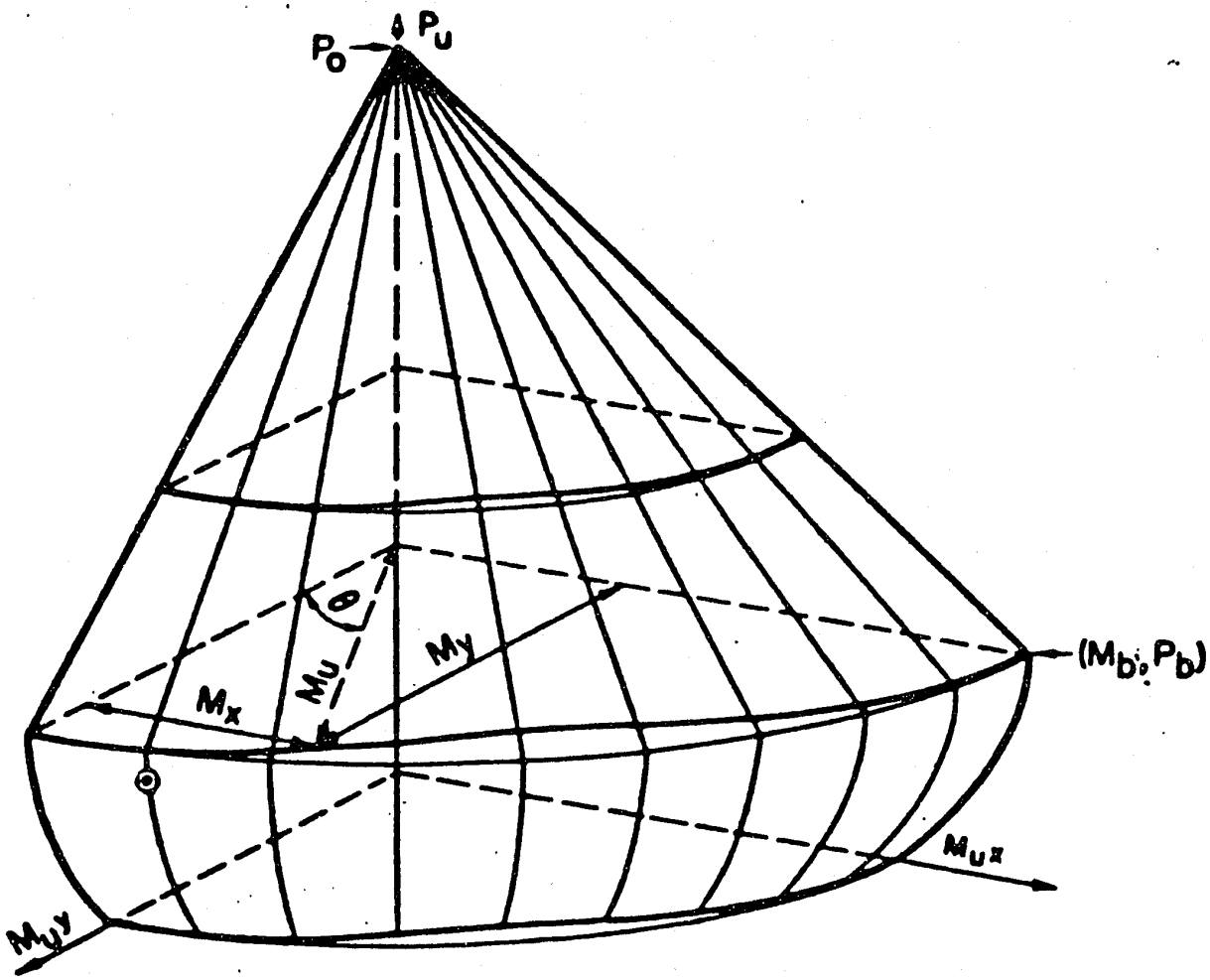

FIGURE 1.1.1 : Interaction surface for a reinforced concrete column with biaxial bending.

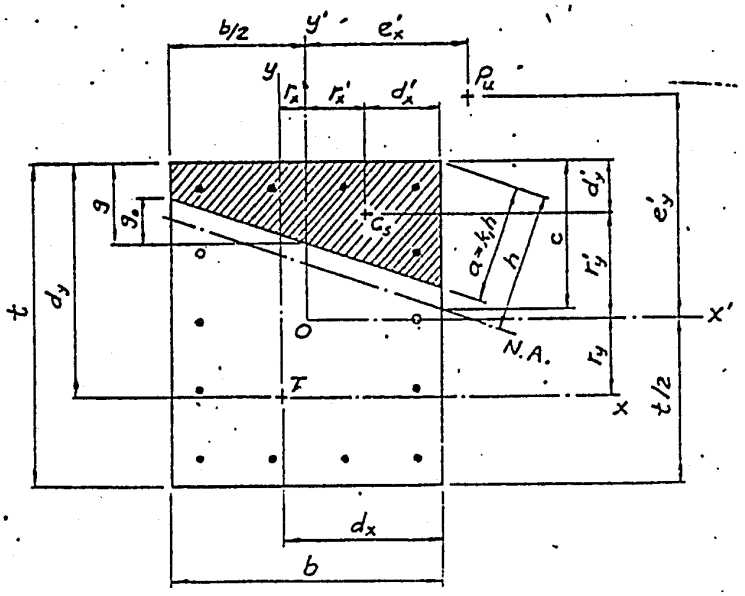

a

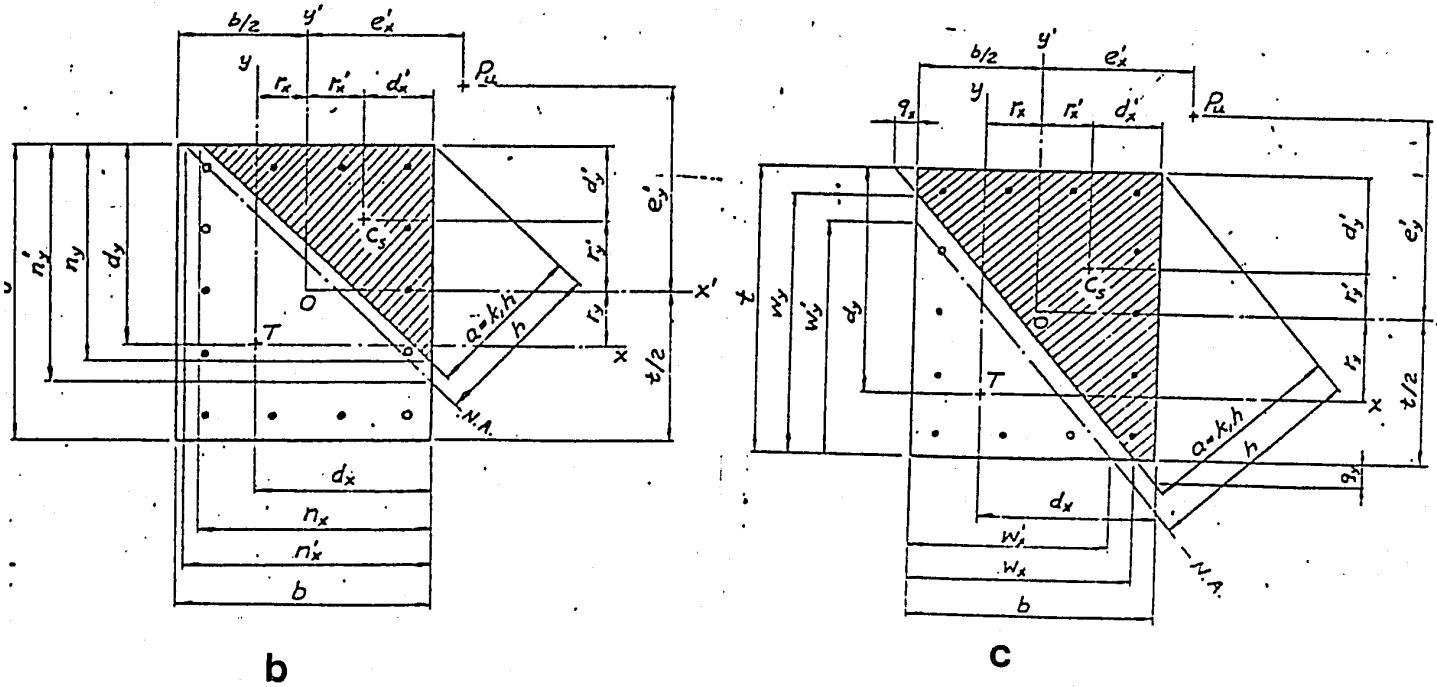

b c

FIGURE 1.2.2.1 : The three posible cases of the location of the neutral axis.

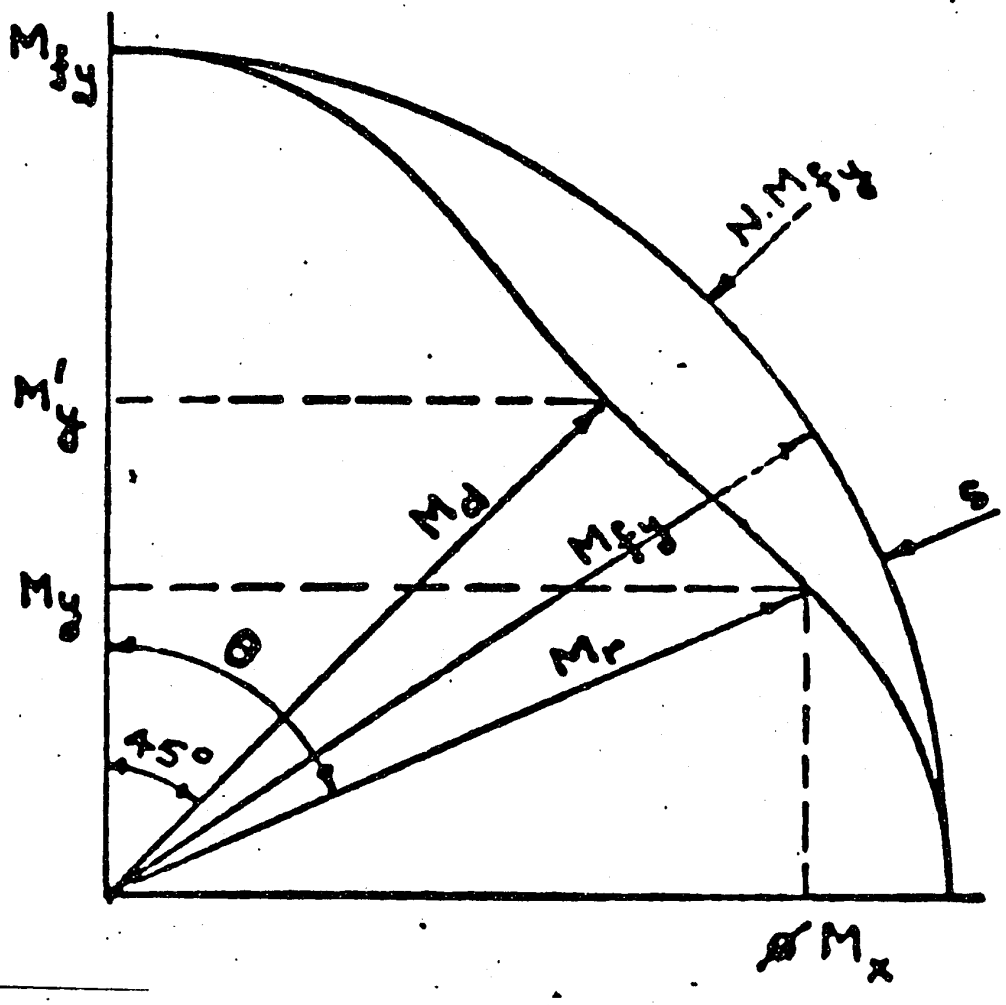

FIGURE 1.2.2.2 : Horizontal section of quadrant of actual failure surface and surface of revolution.

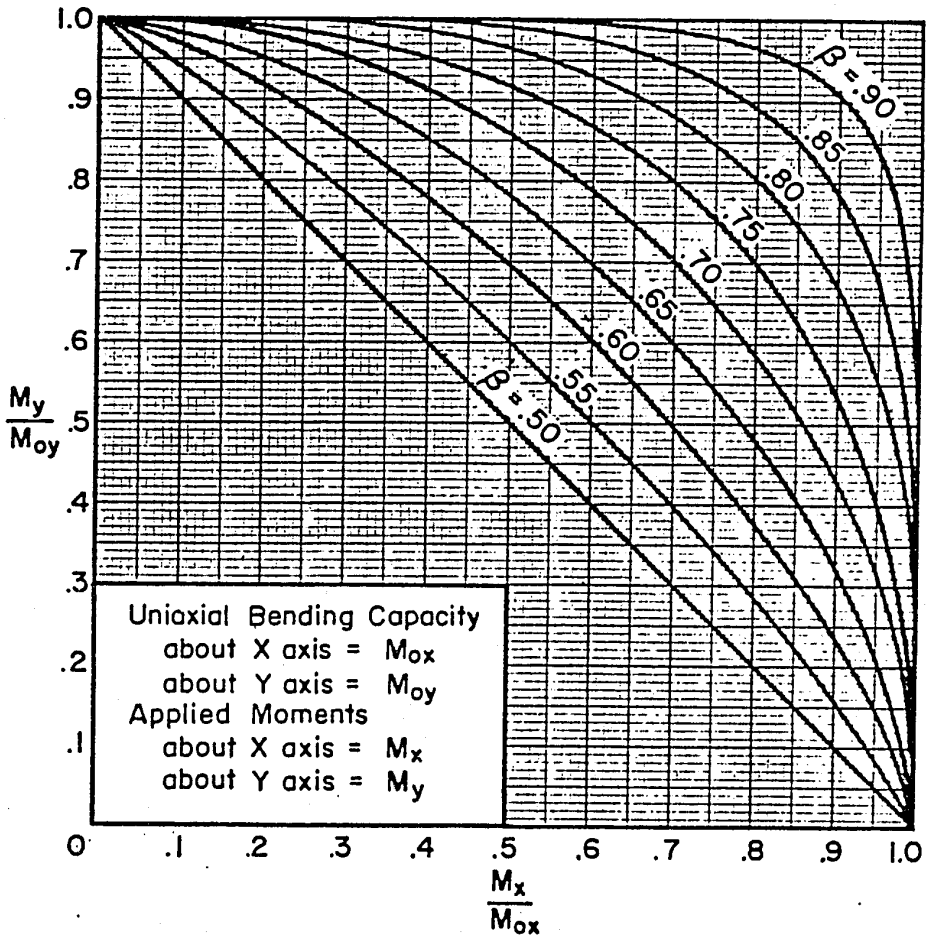

FIGURE 1.2.2.3 : Biaxial moment relationship.

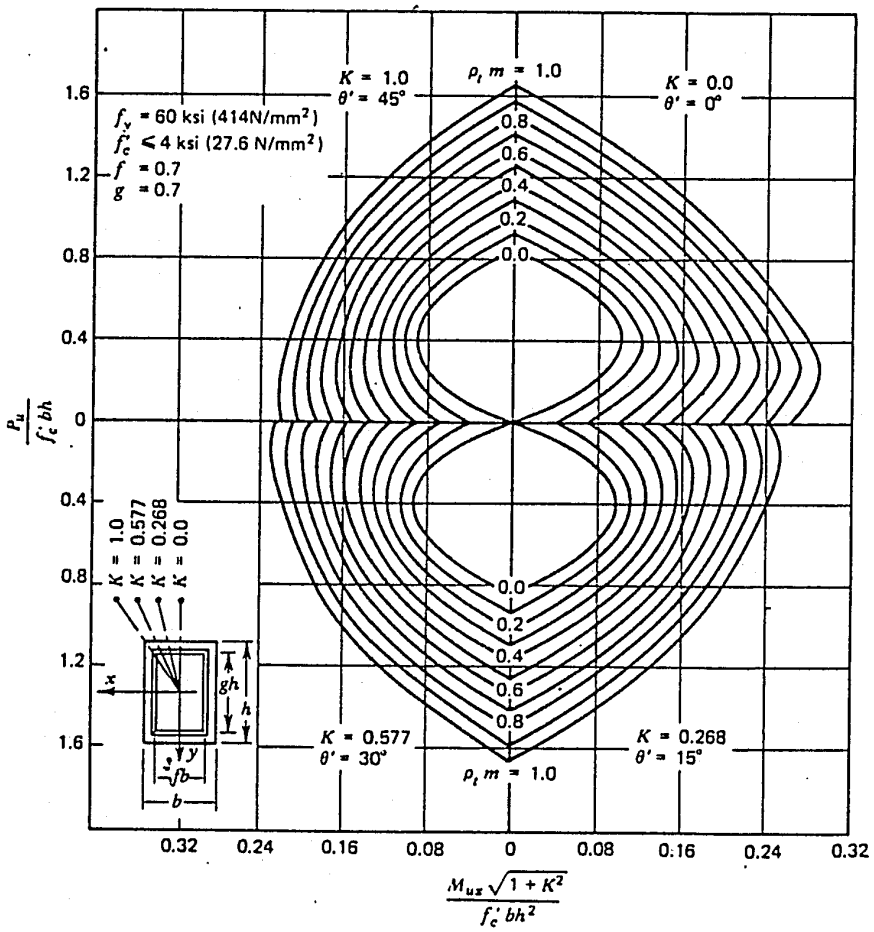

FIGURE 1.2.2.4 : Design chart for a reinforced concrete column section with load applied at various angles of eccentricity.

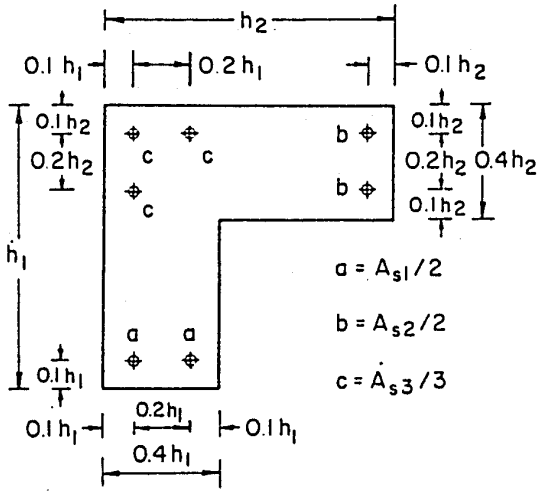

FIGURE 1.2.2.5 : Arrangement of reinforcement.

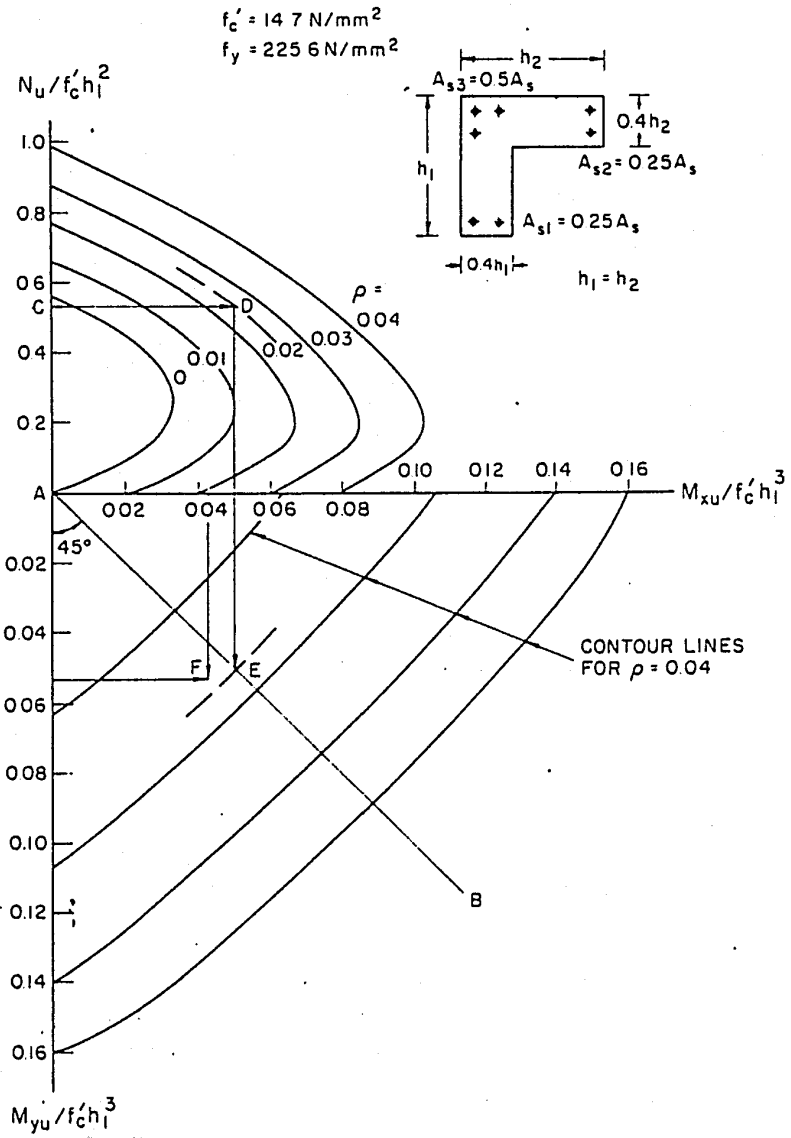

FIGURE 1.2.2.6 : Typical design chart.

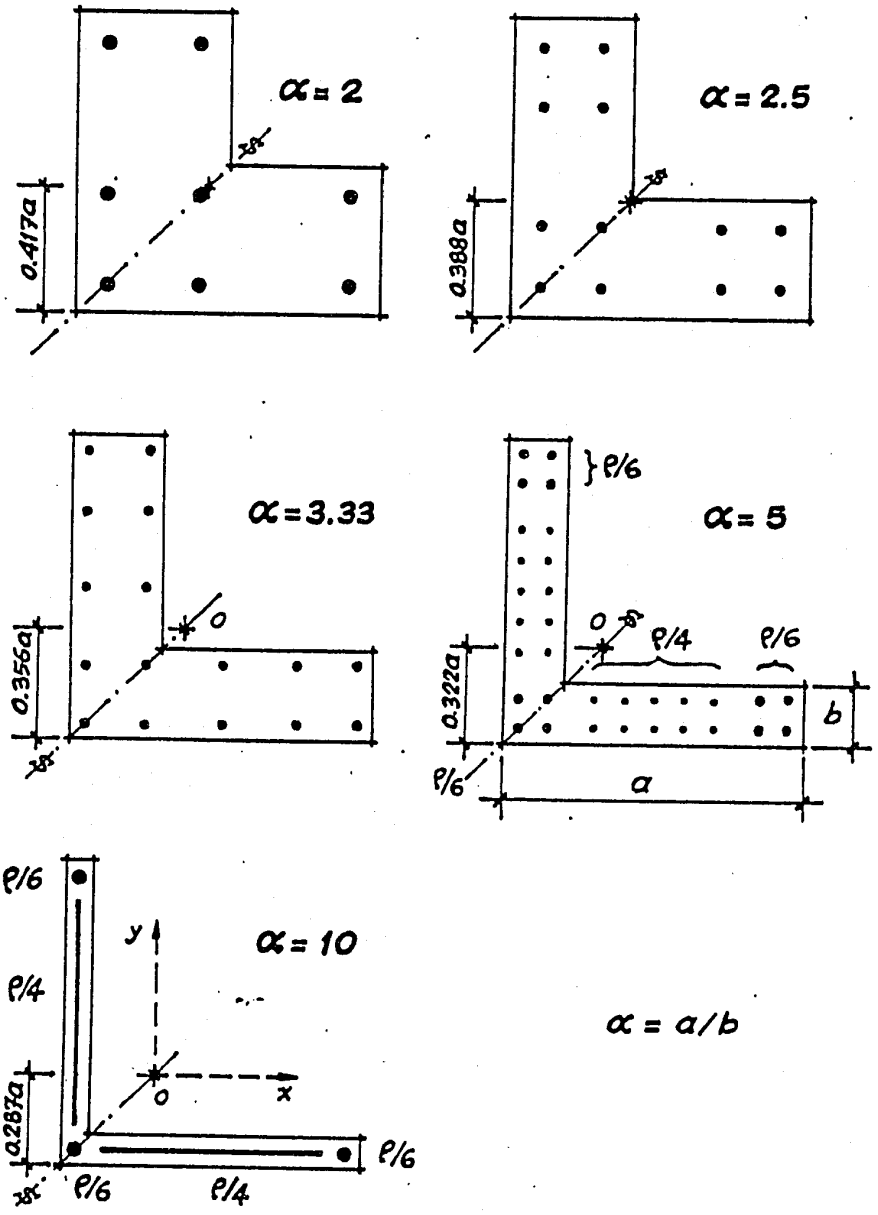

FIGURE 1.2.2.7 : Cross section geometry and steel distribution selected for the analysis.

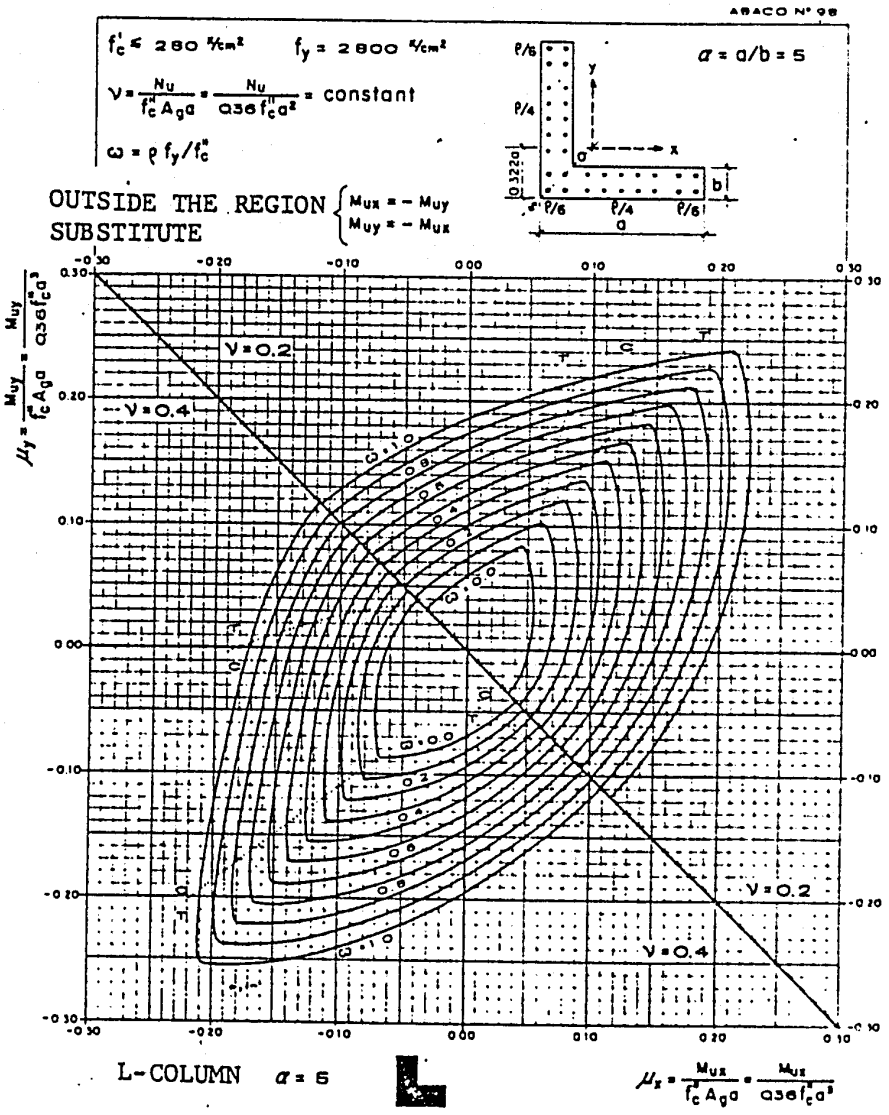

FIGURE 1.2.2.8 : Typical isobaric curves corresponding to all isoloads.

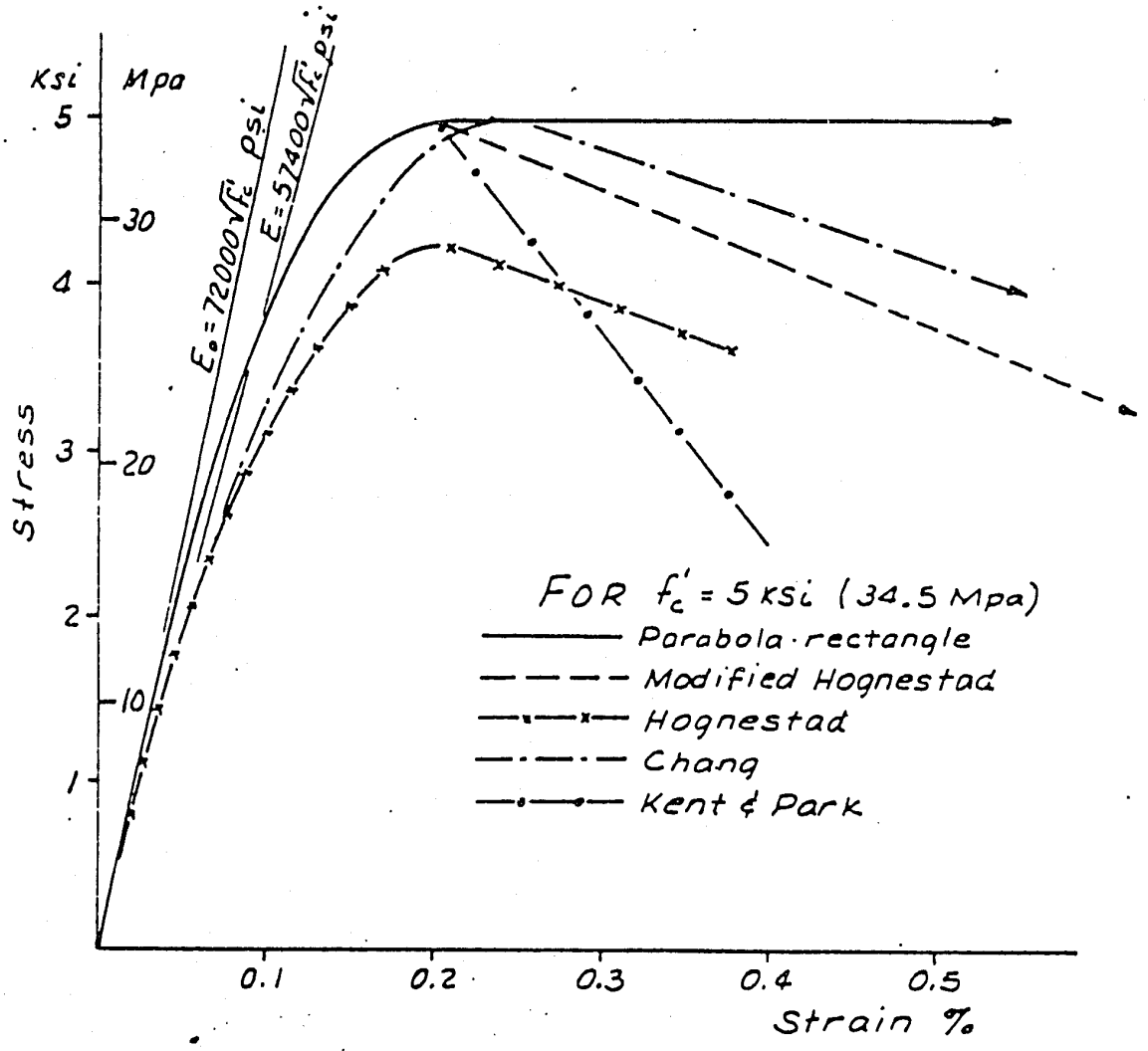

FIGURE 1.2.3.1 : Typical stress-strain representations.

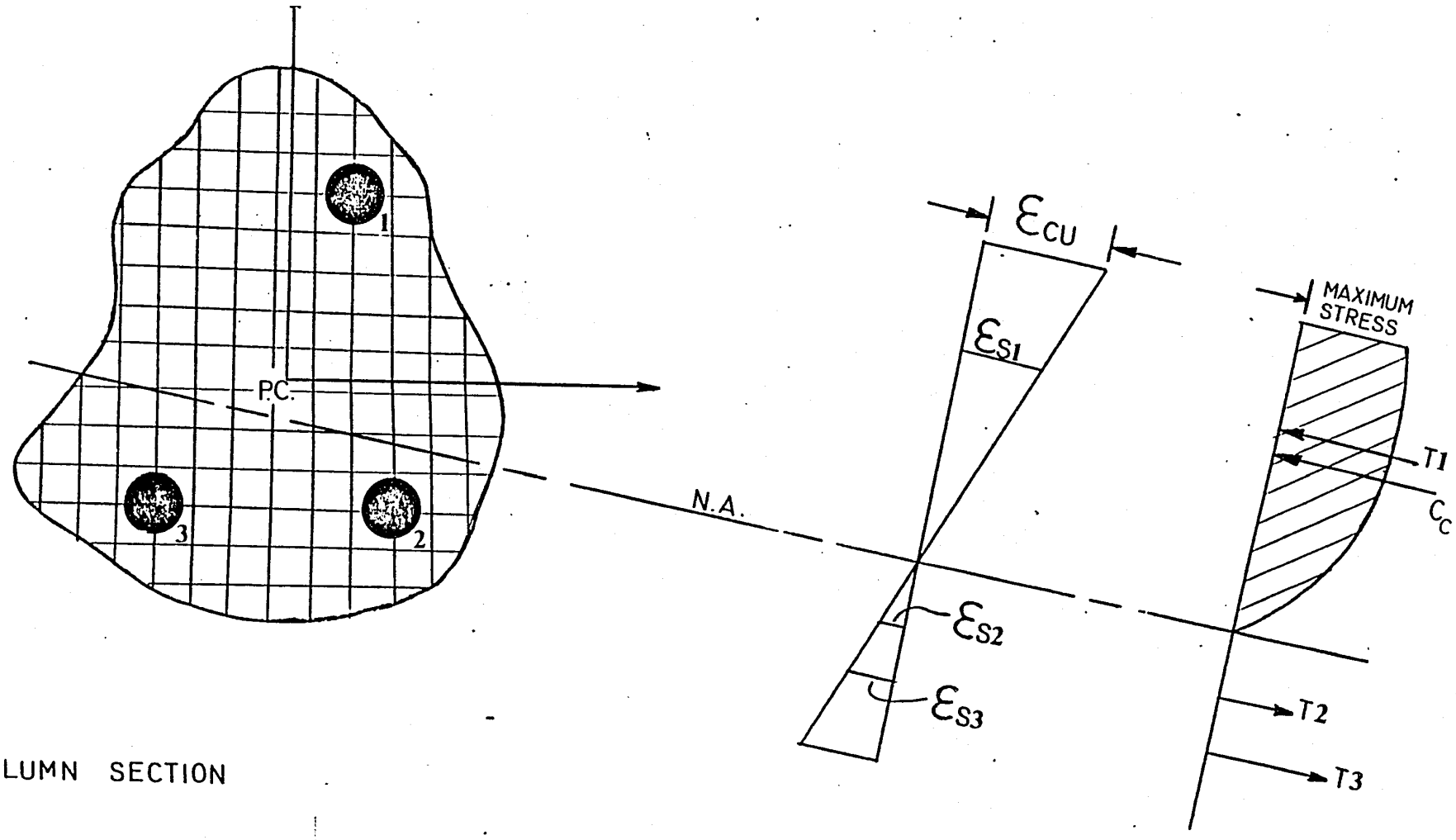

FIGURE 2.3.1 Column Section Subjected to Biaxial Bending

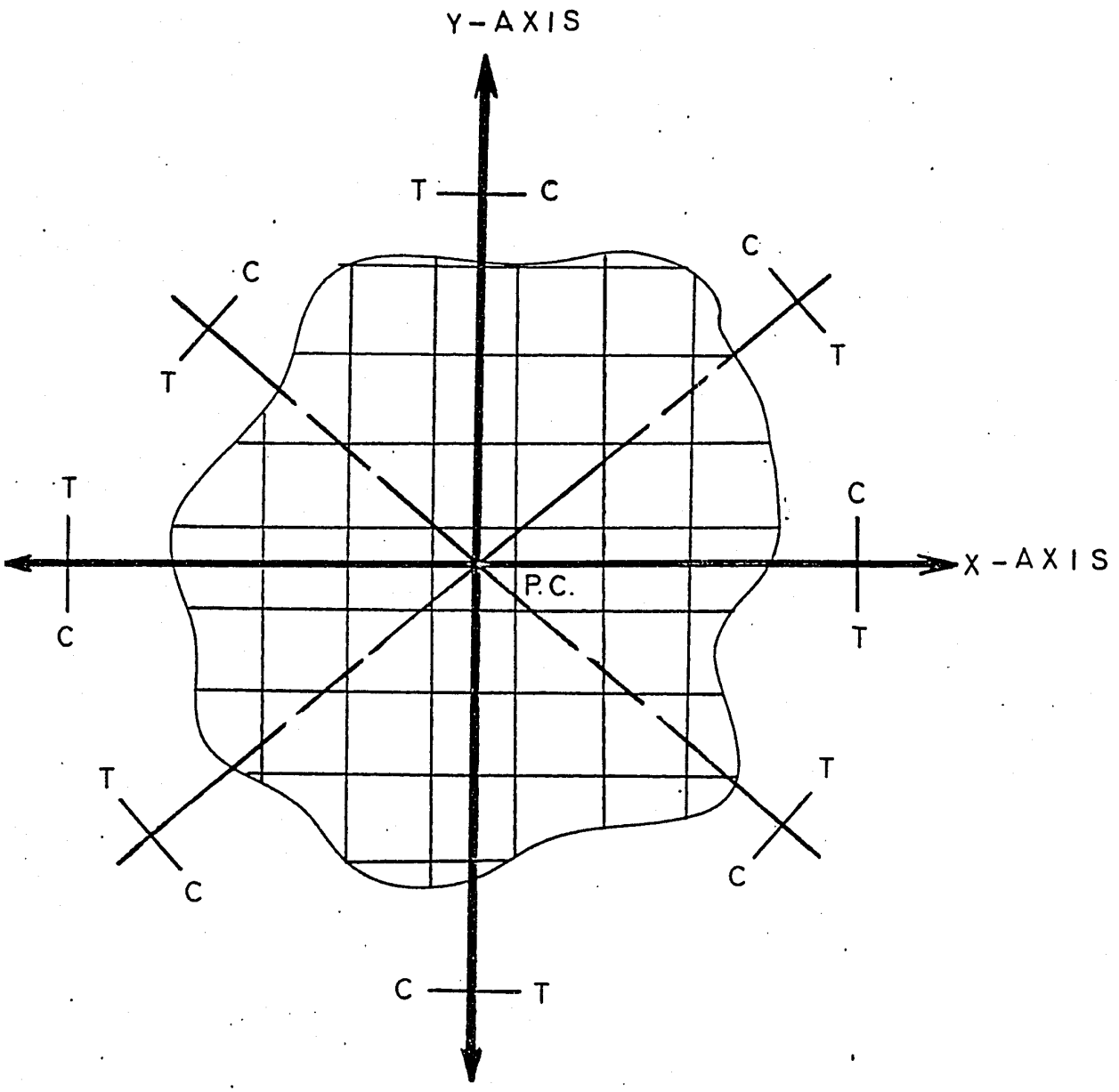

FIGURE 2.3.2 : Notation of the neutral axis inclination used in the computer model.

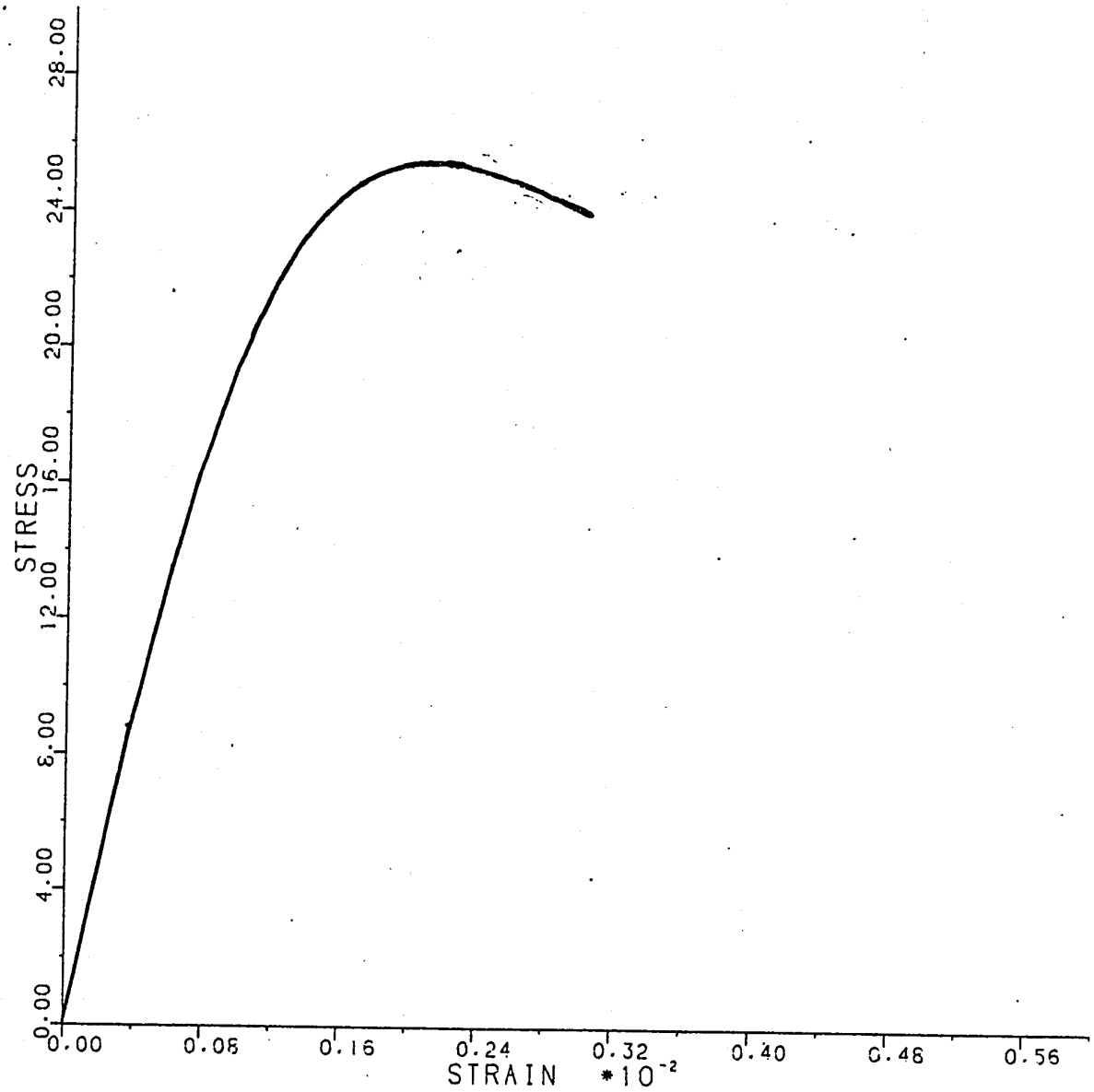

FIGURE 2.4.1.1 : The concrete stress-strain relationship.

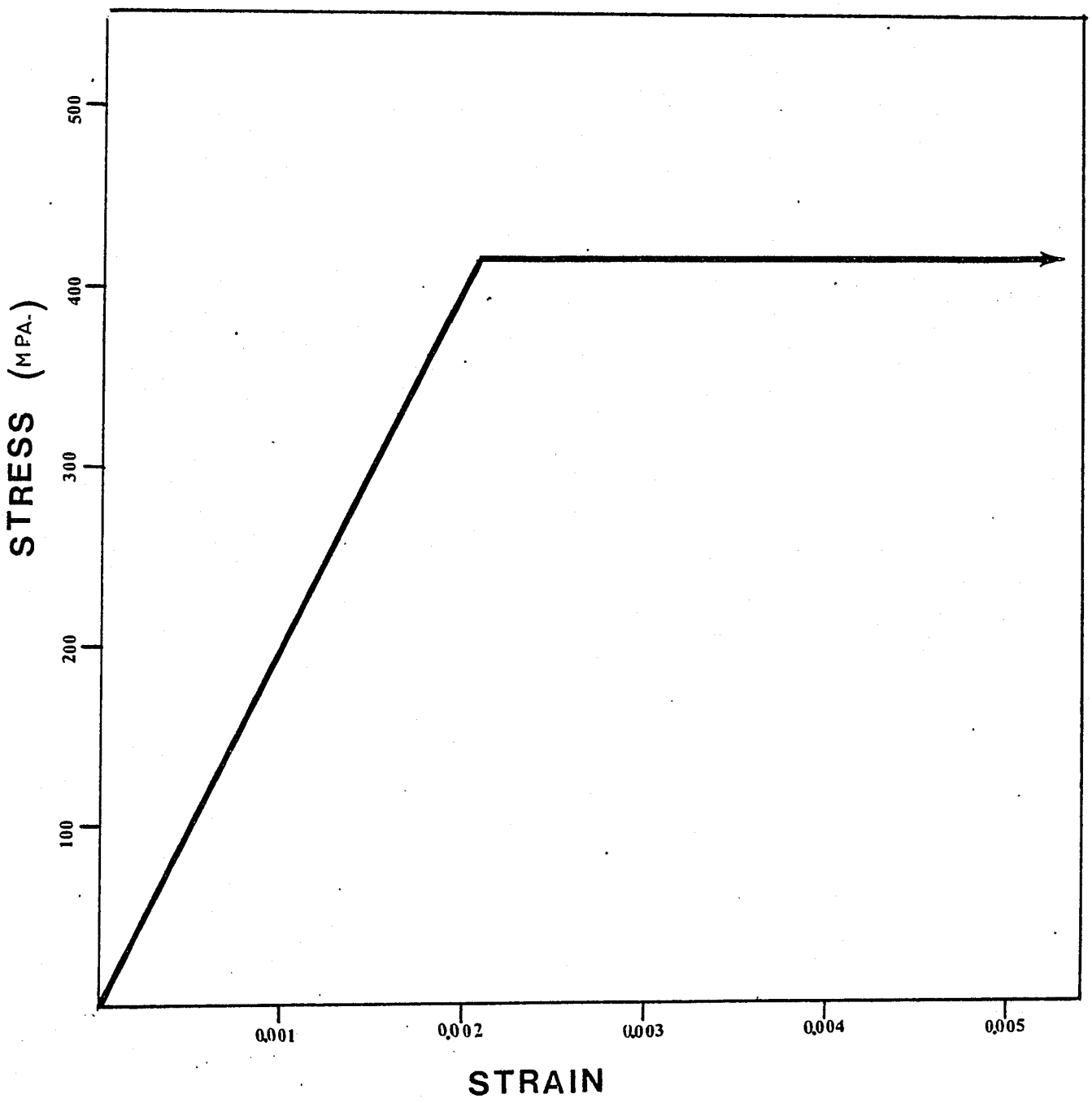

FIGURE 2.4.2.1 : The steel stress-strain relationship.

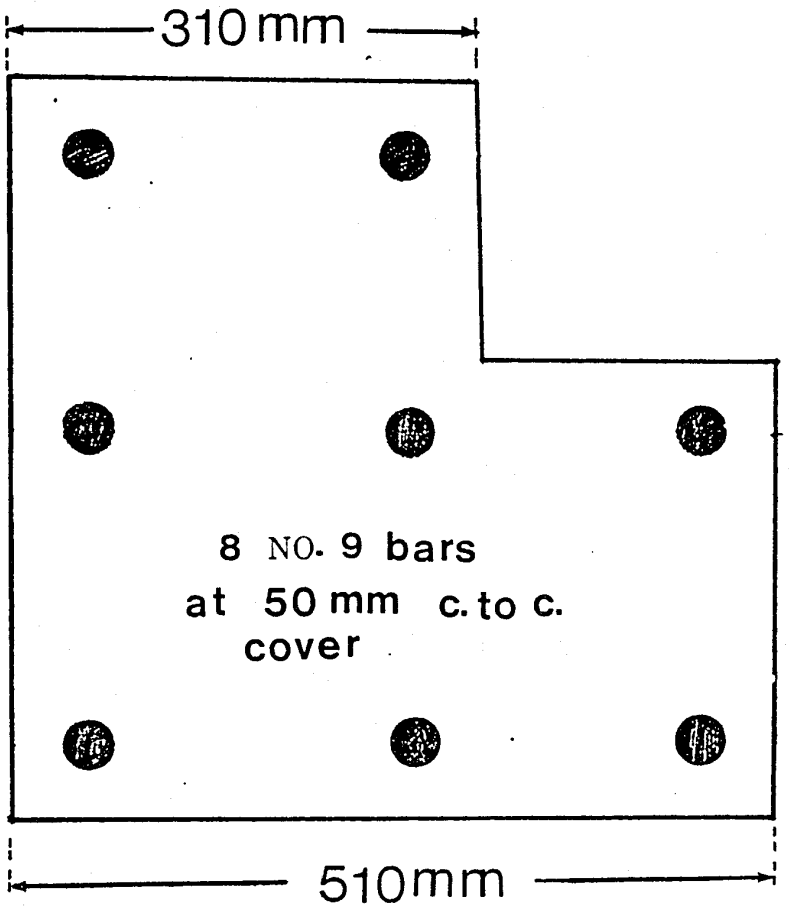

FIGURE 2.4.3.1 : The geometry and steel arrangement of the L-Shaped section used in the analysis.

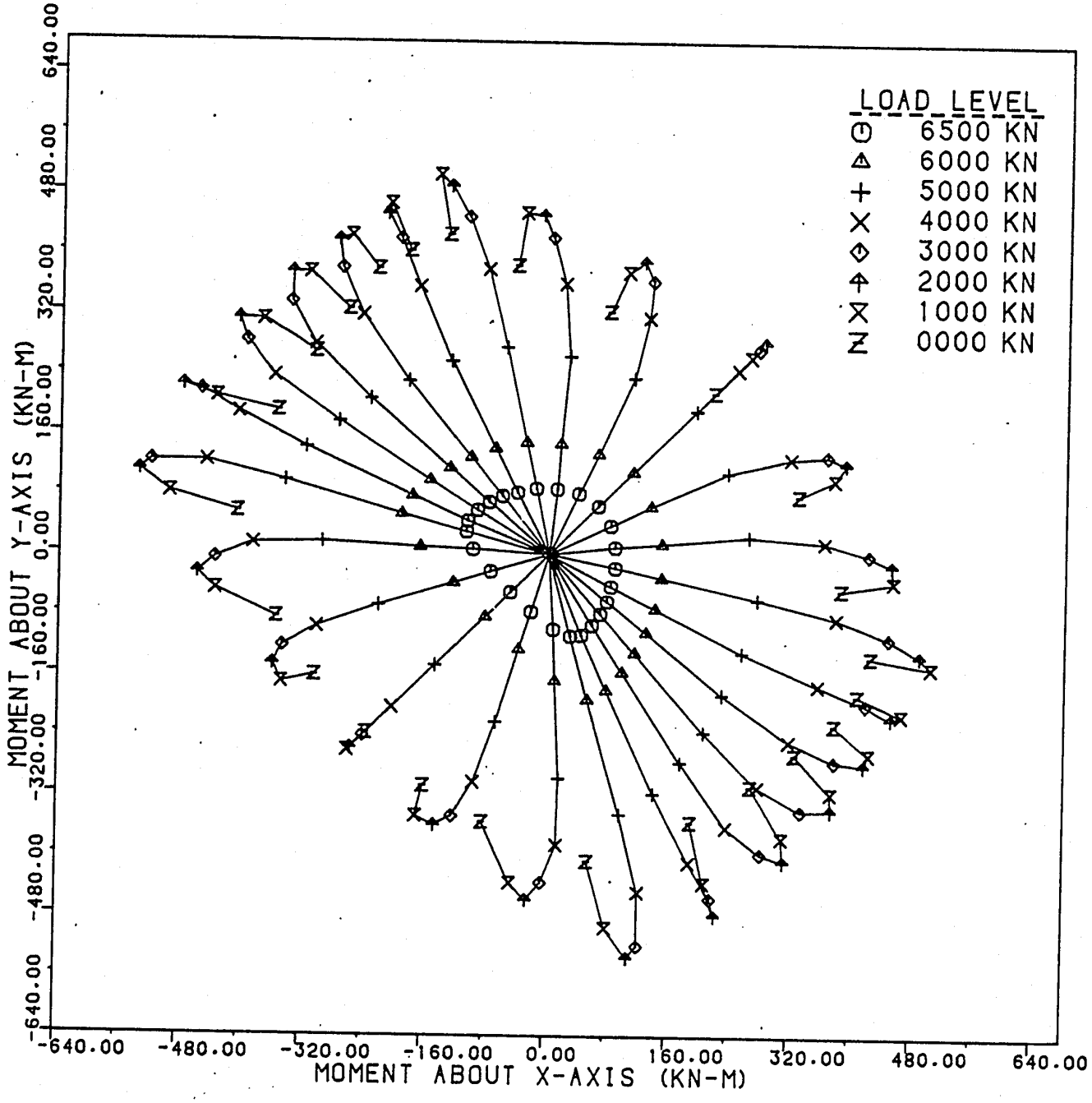

FIGURE 2.4.3.2 : Plan view of the interaction curve using 0.0025 as the maximum allowable concrete strain.

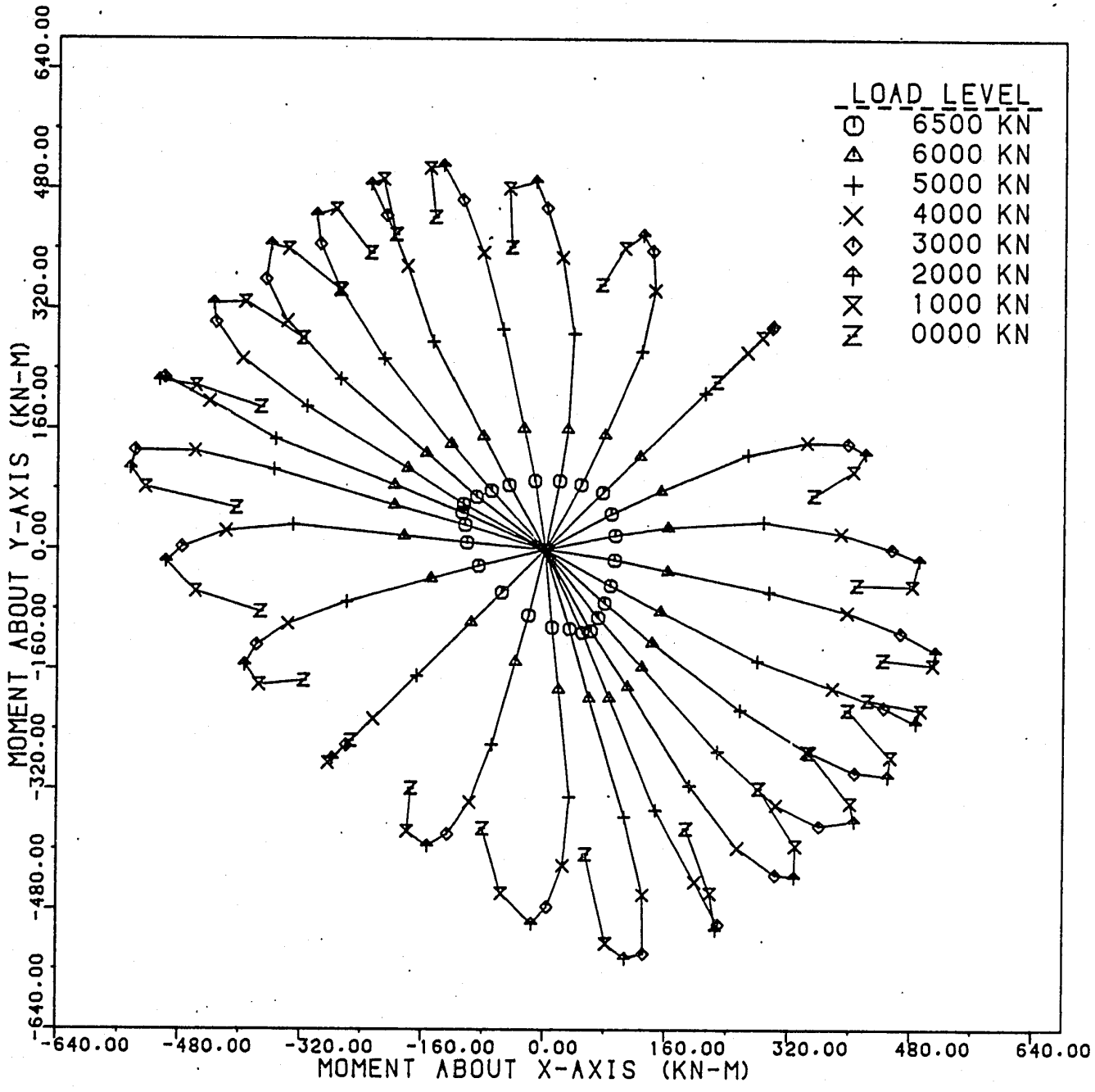

FIGURE 2.4.3.3 : Plan view of the interaction curve using 0.0030 as the maximum allowable concrete strain.

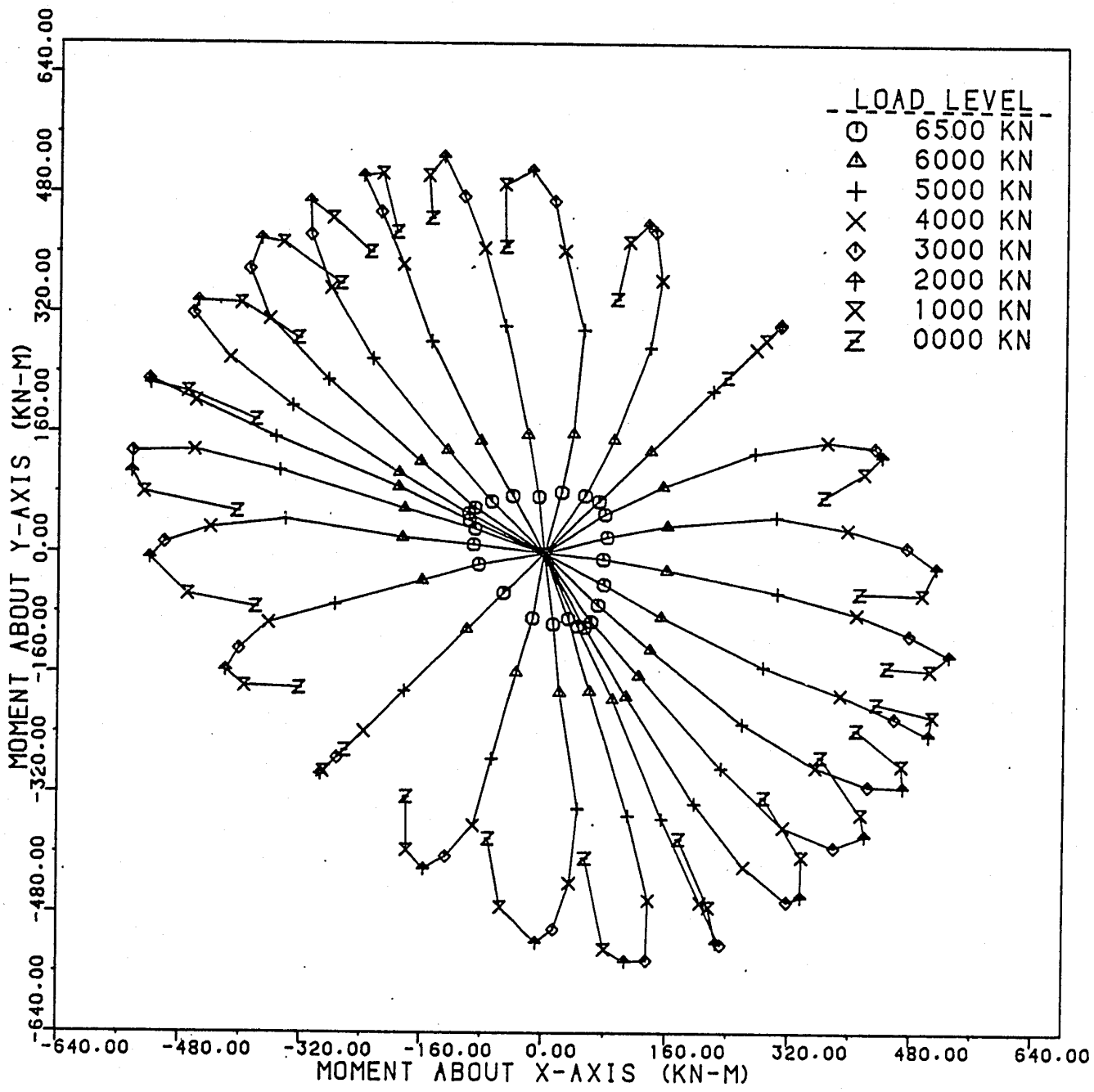

FIGURE 2.4.3.4 : Plan view of the interaction curve using 0.0035 as the maximum allowable concrete strain.

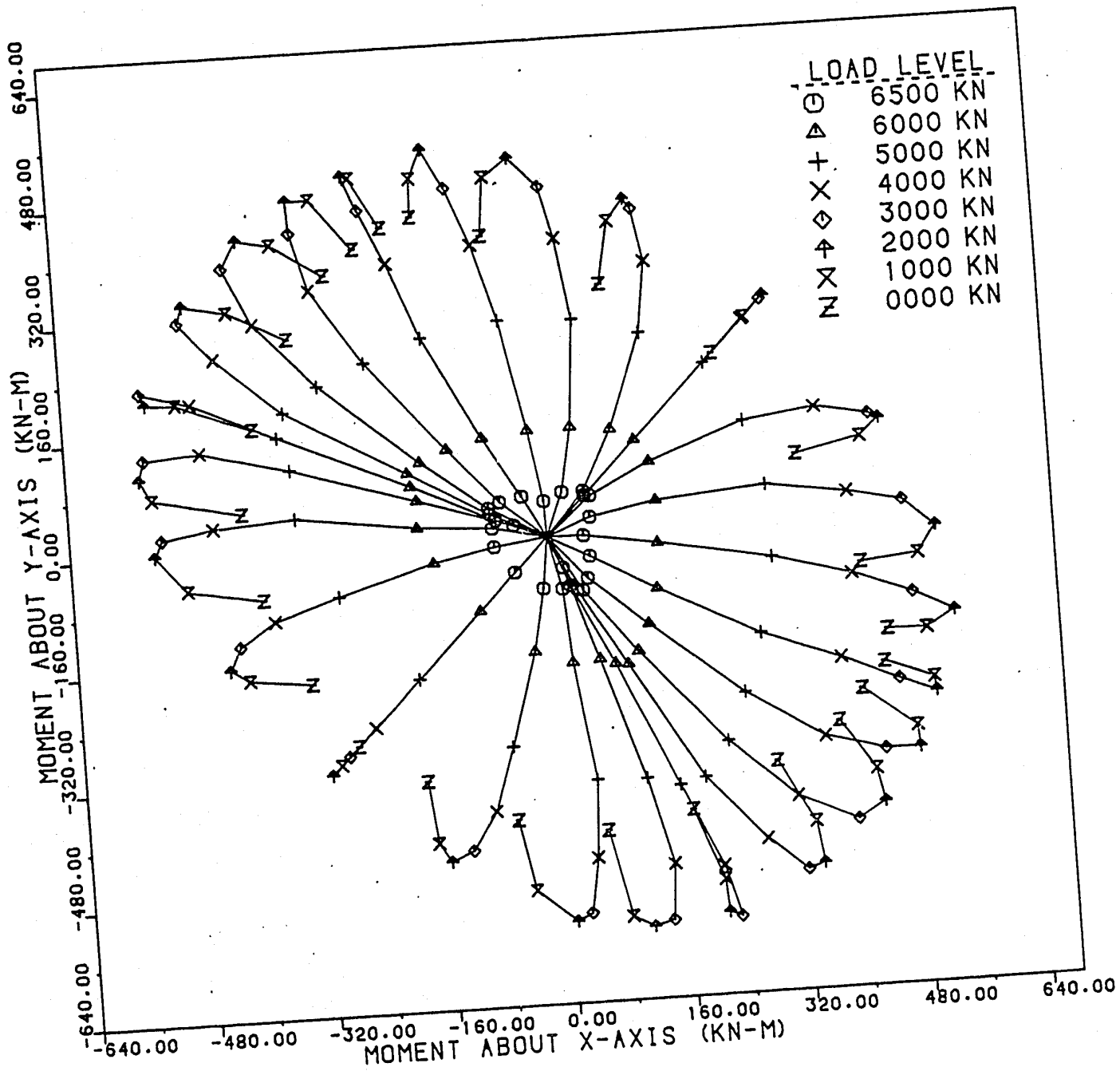

FIGURE 2.4.3.5 : Plan view of the interaction curve using 0.0040 as the maximum allowable concrete strain.

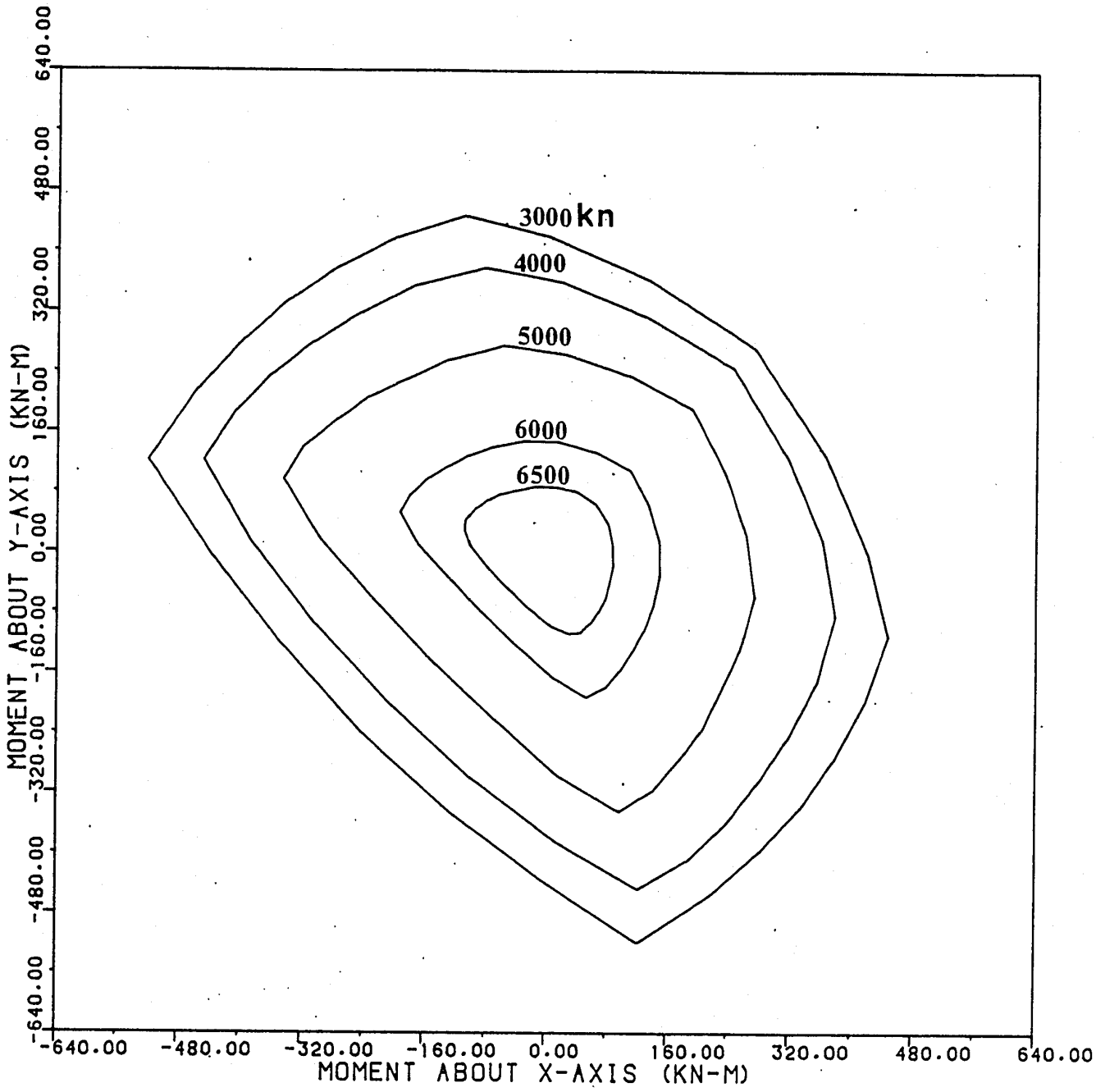

FIGURE 2.4.4.6 A : The ultimate isoload contours using 0.0025 as the maximum allowable concrete strain.

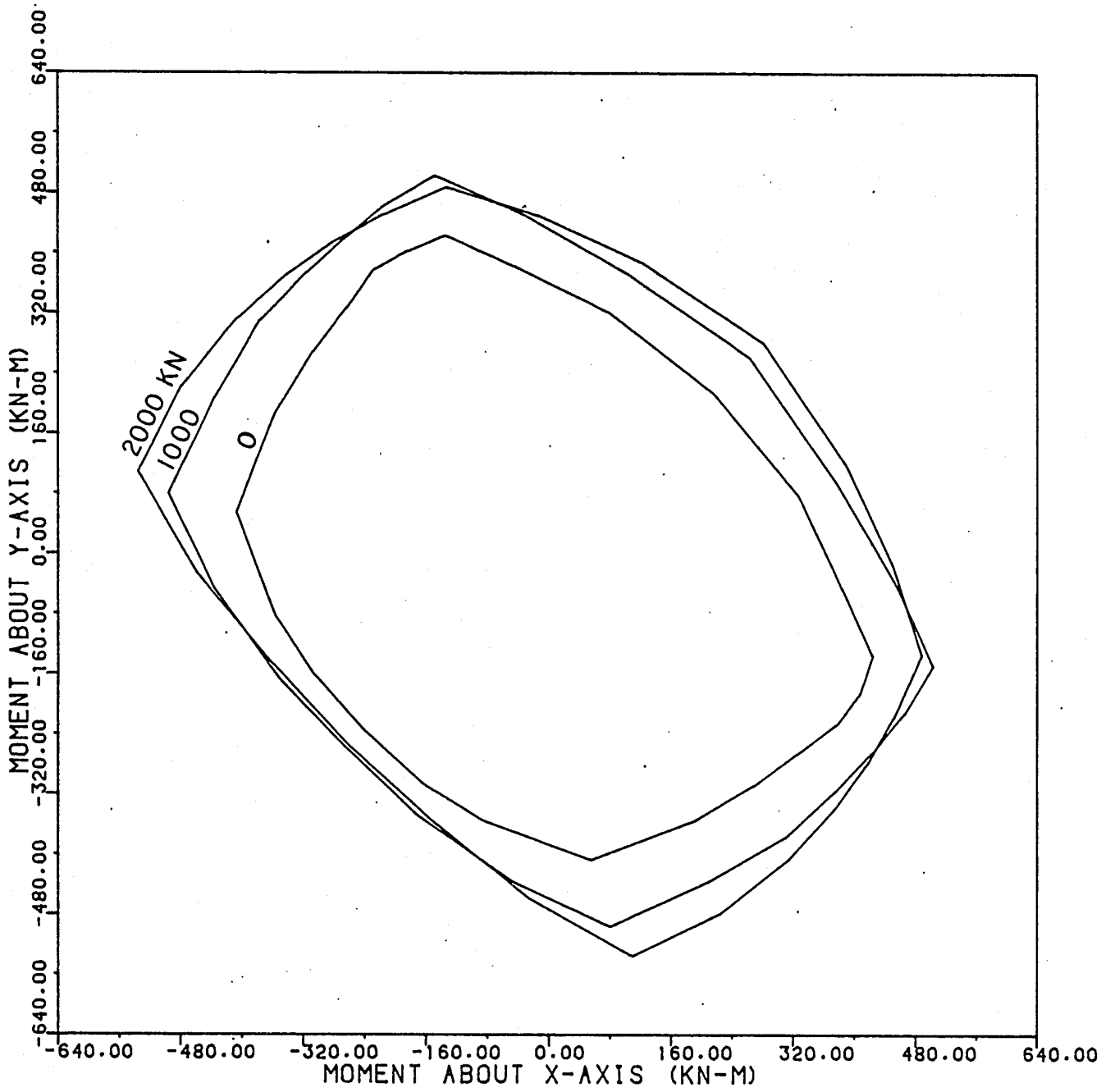

FIGURE 2.4.4.6 B : The ultimate isoload contours using 0.0025 as the maximum allowable concrete strain.

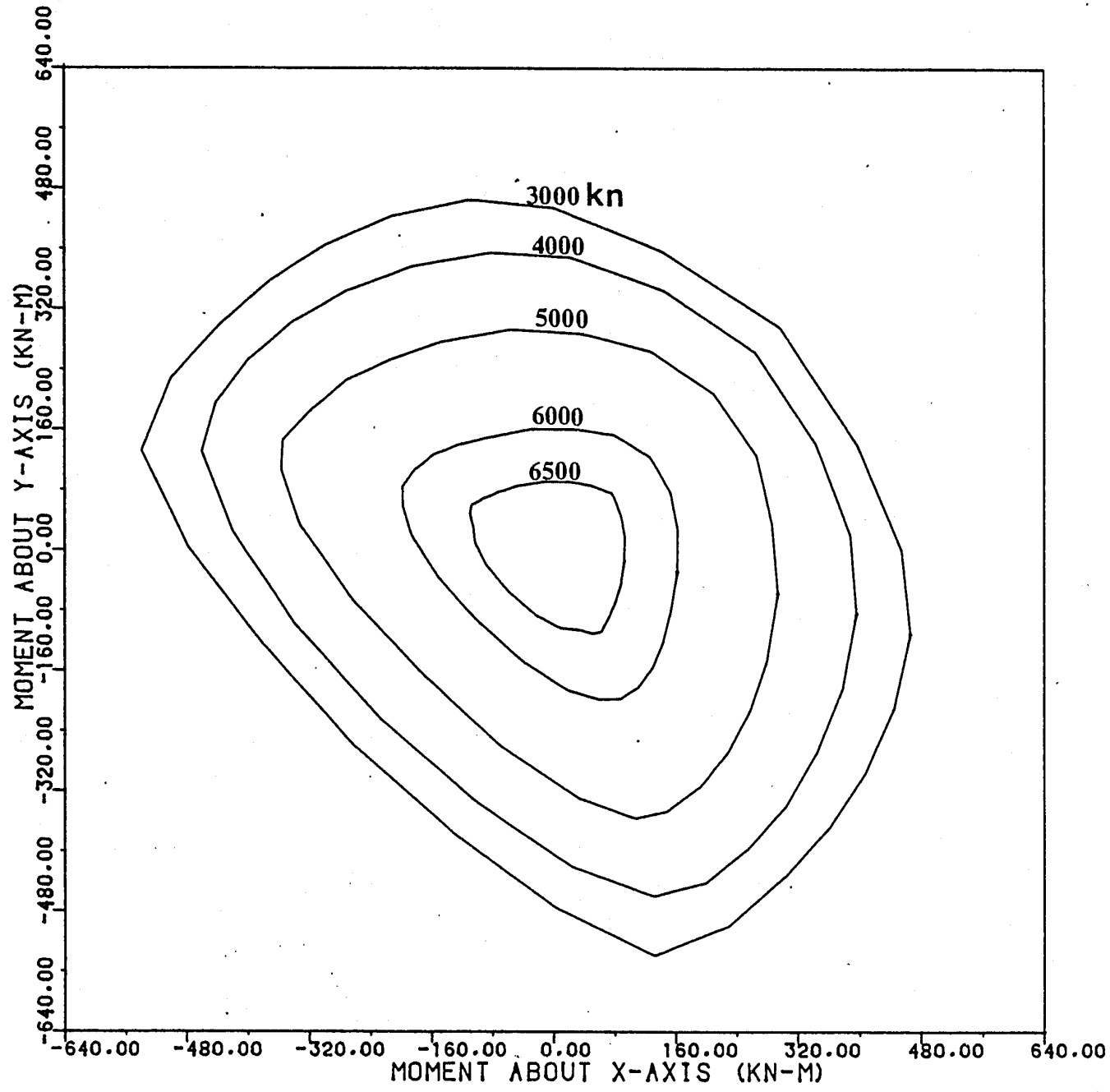

FIGURE 2.4.4.7 A : The ultimate isoload contours using 0.0030 as the maximum allowable concrete strain.

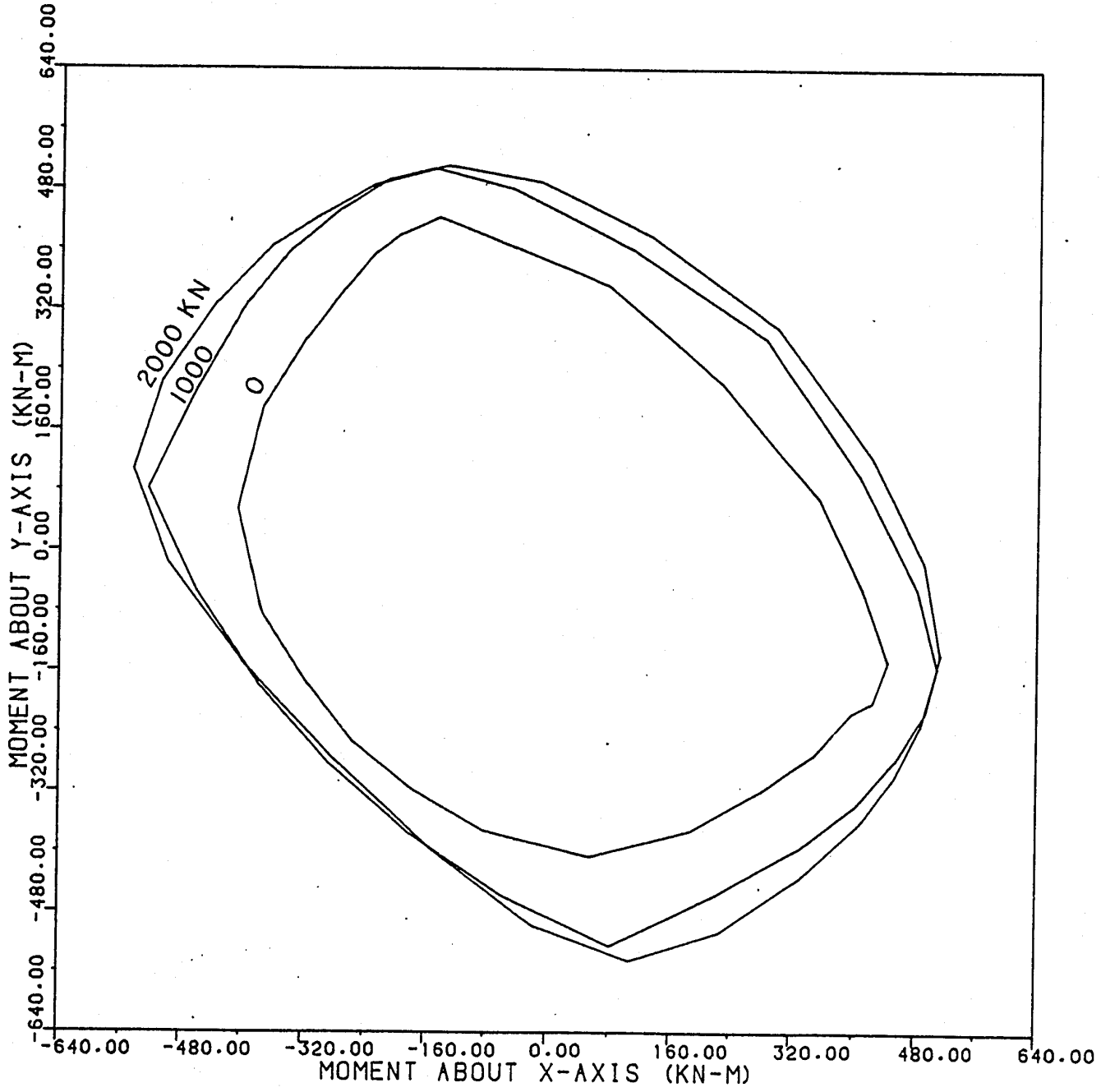

FIGURE 2.4.4.7 B : The ultimate isoload contours using 0.0030 as the maximum allowable concrete strain.

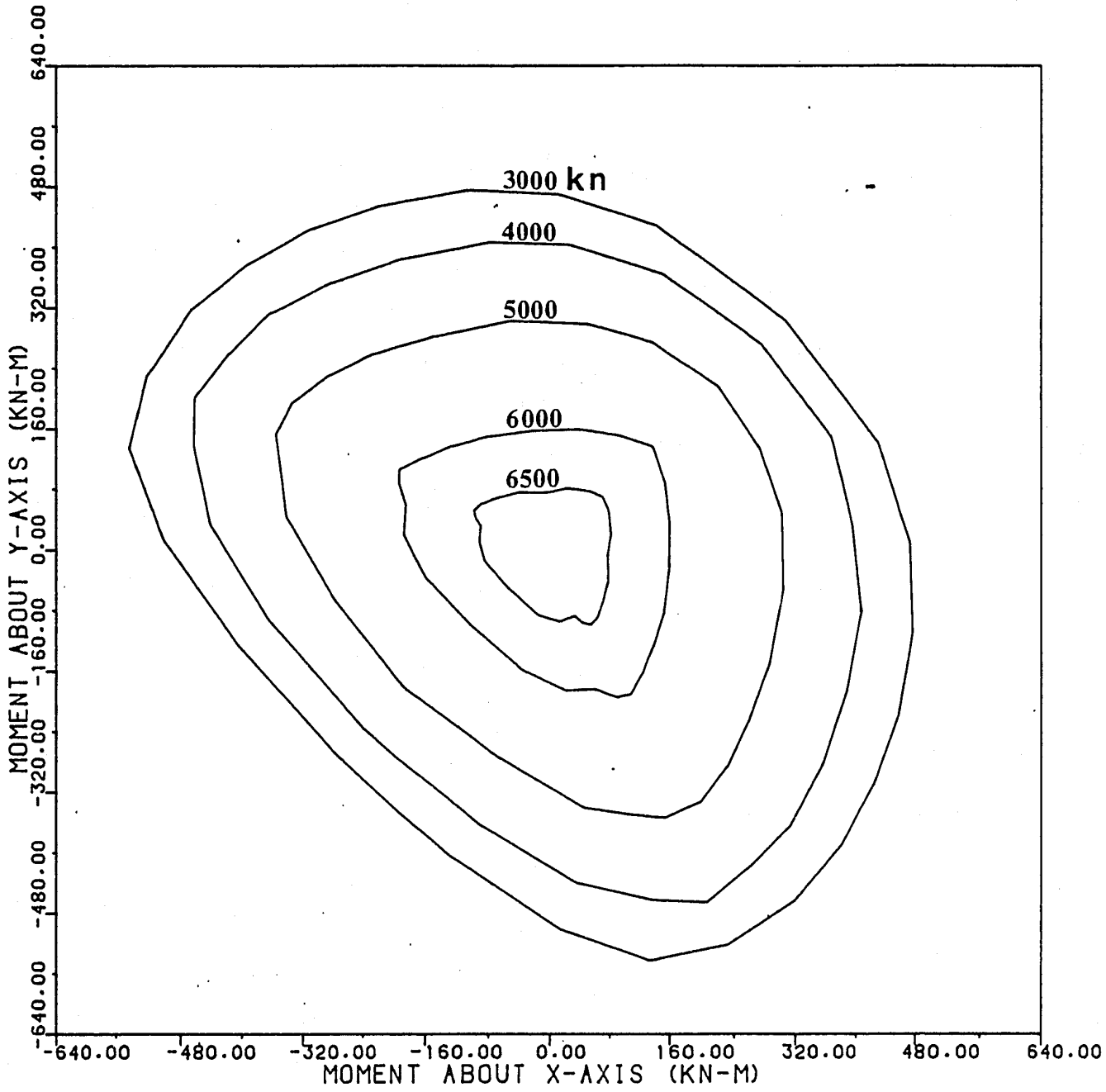

FIGURE 2.4.4.8 A : The ultimate isoload contours using 0.0035 as the maximum allowable concrete strain.

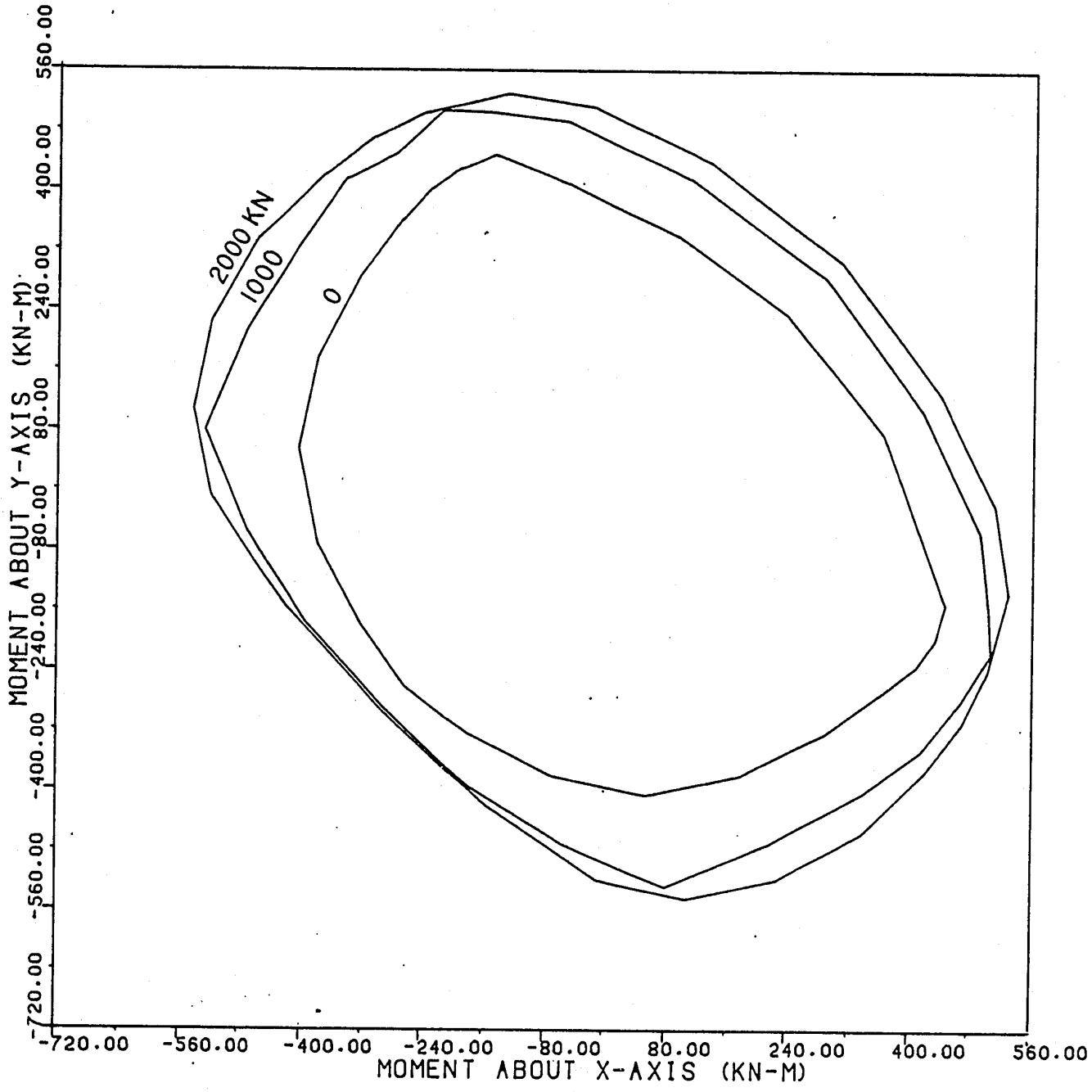

FIGURE 2.4.4.8 B : The ultimate isoload contours using 0.0035 as the maximum allowable concrete strain.

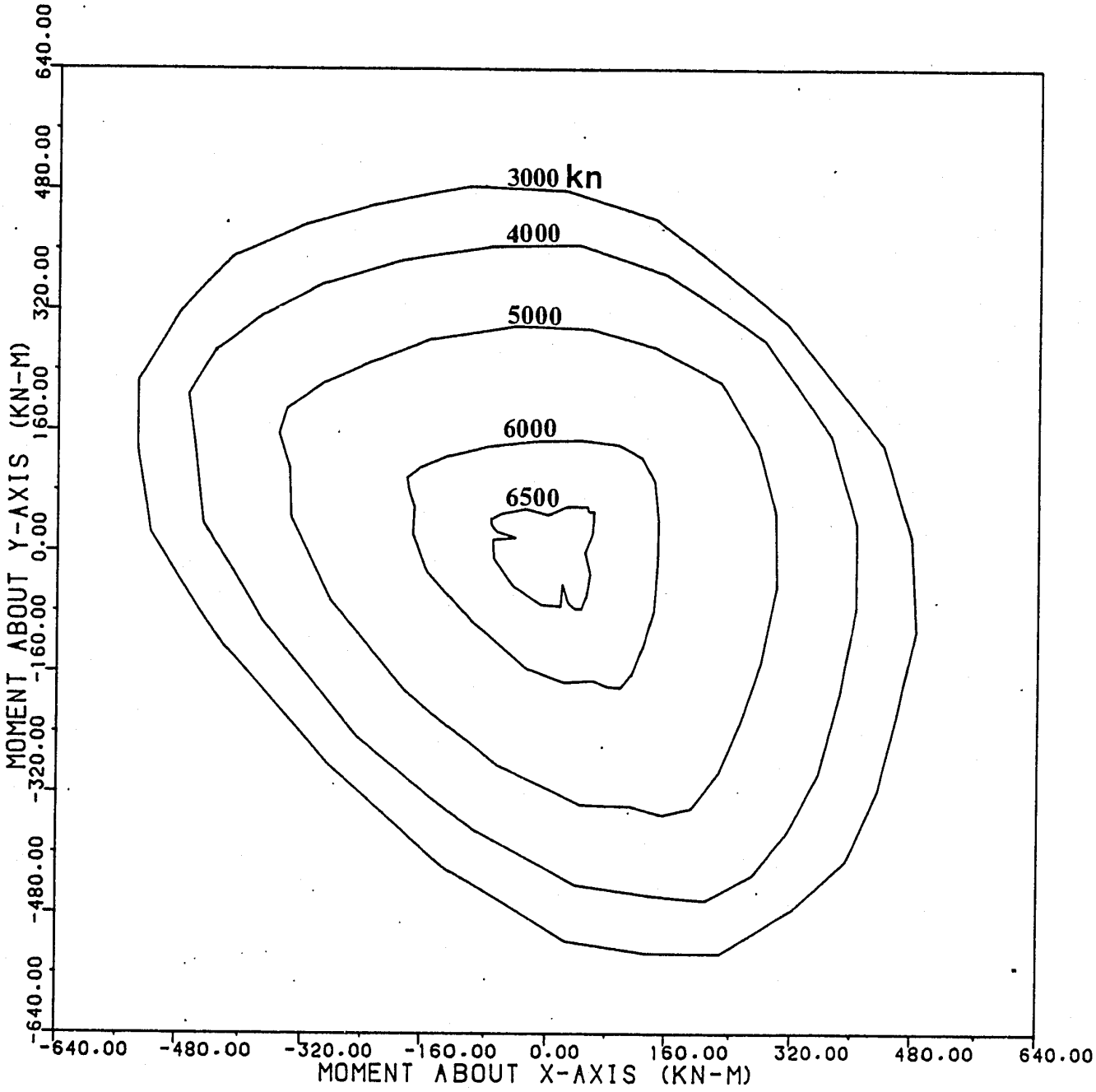

FIGURE 2.4.4.9 A : The ultimate isoload contours using 0.0040 as the maximum allowable concrete strain.

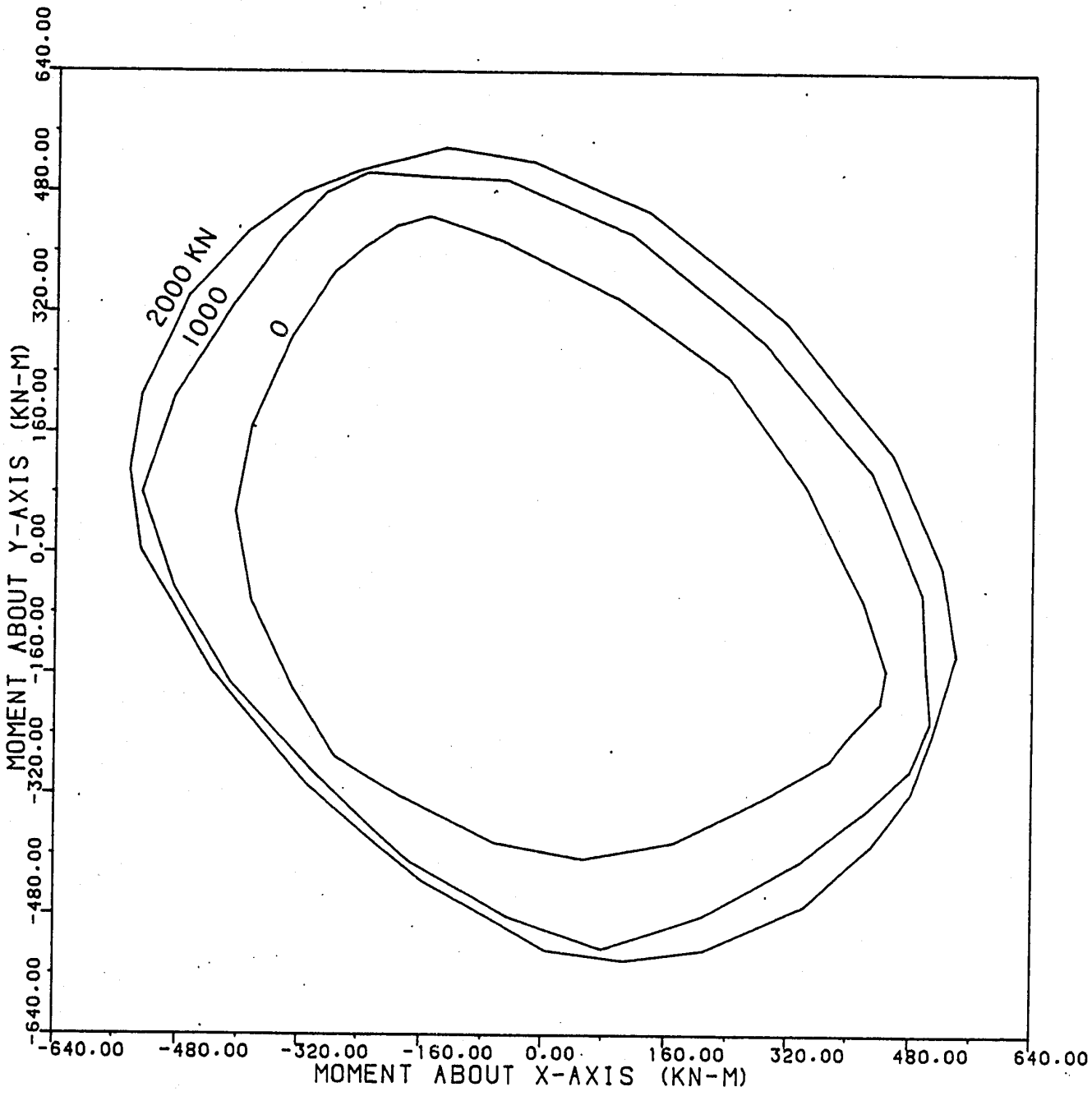

FIGURE 2.4.4.9 B : The ultimate isoload contours using 0.0040 as the maximum allowable concrete strain.

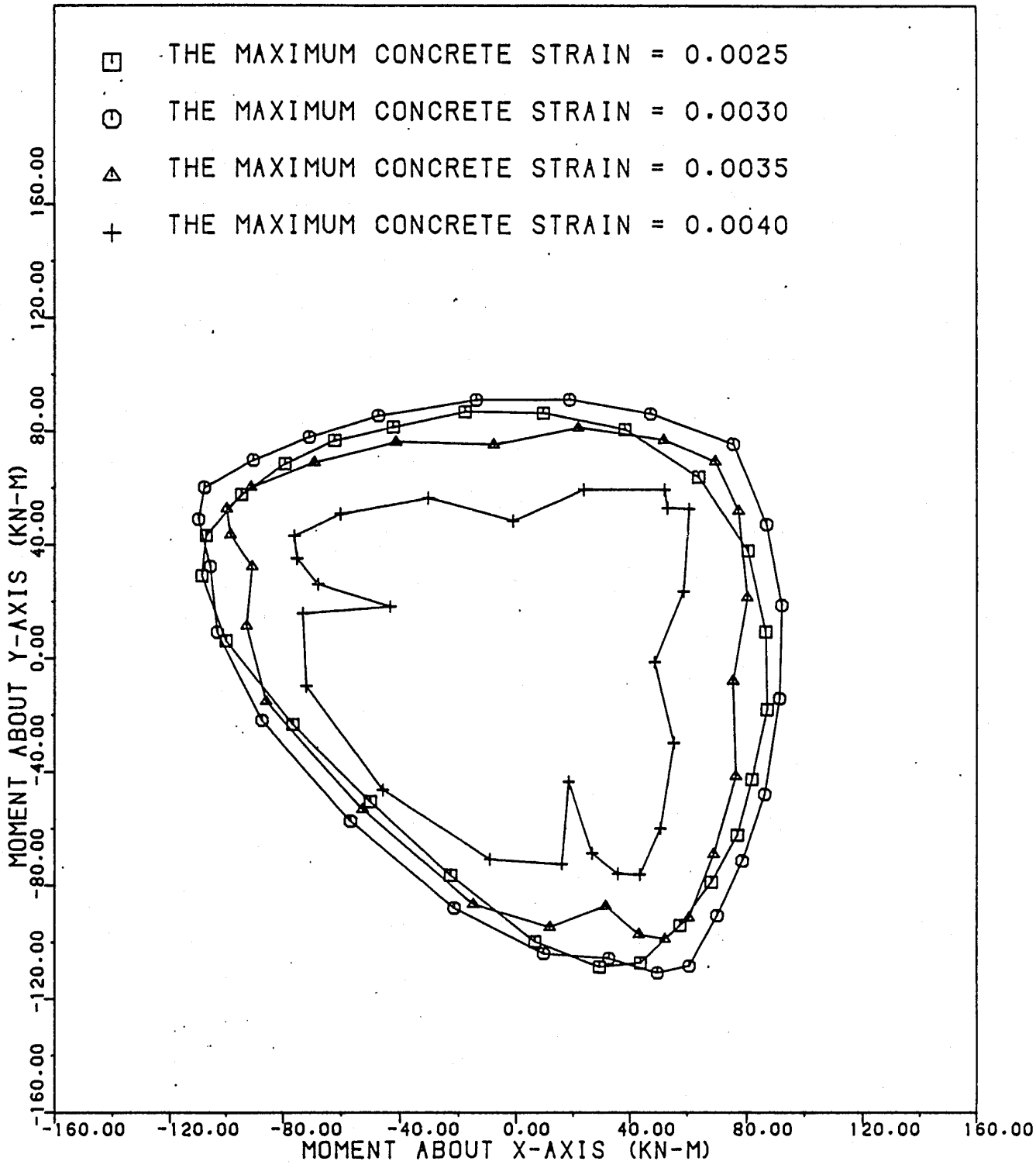

FIGURE 2.4.3.10 : The 6500 KN load isoload contours.

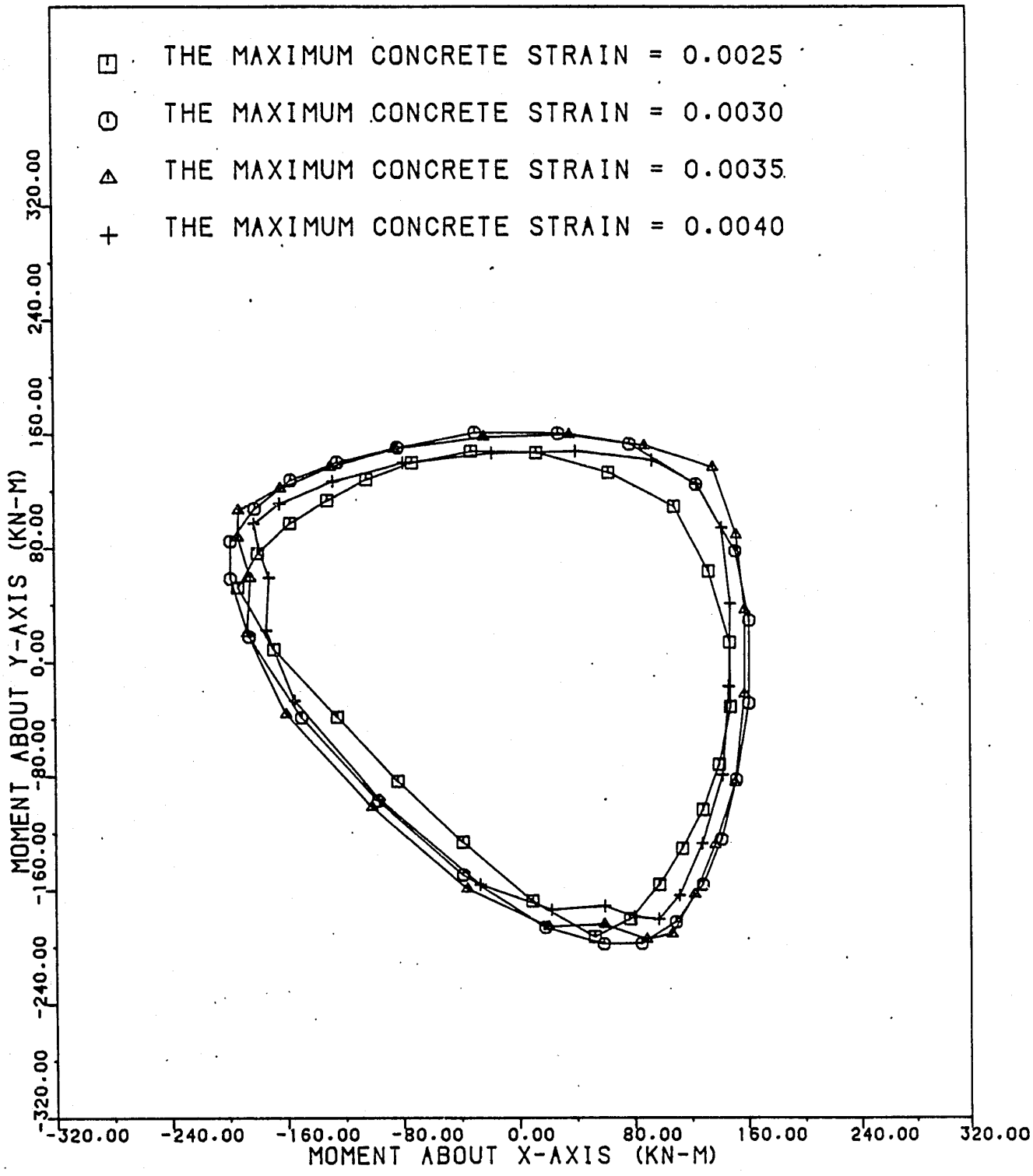

FIGURE 2.4.3.11 : The 6000 KN load isoload contours.

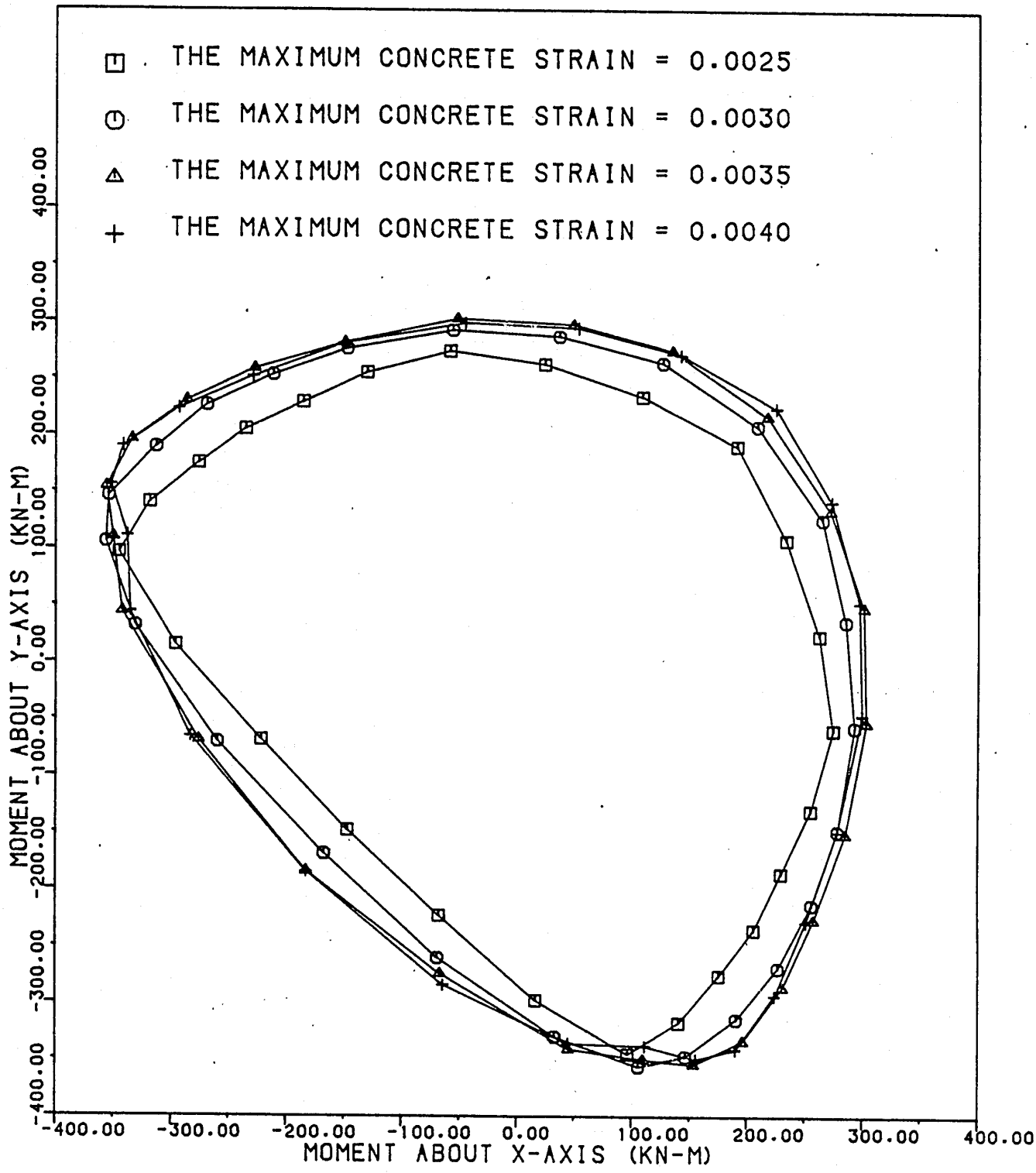

FIGURE 2.4.3.12 : The 5000 KN load isoload contours.

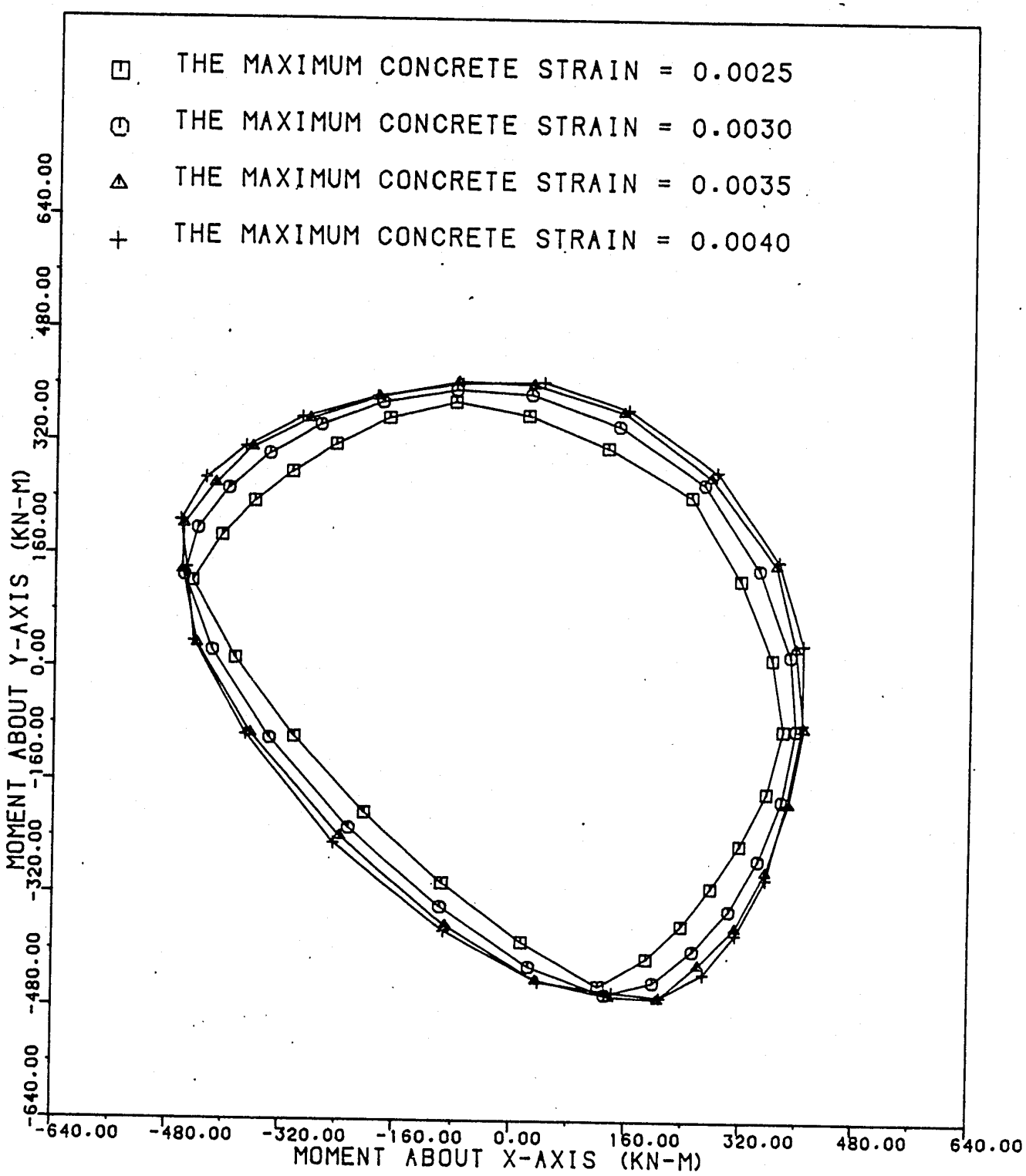

FIGURE 2.4.3.13 : The 4000 KN load isoload contours.

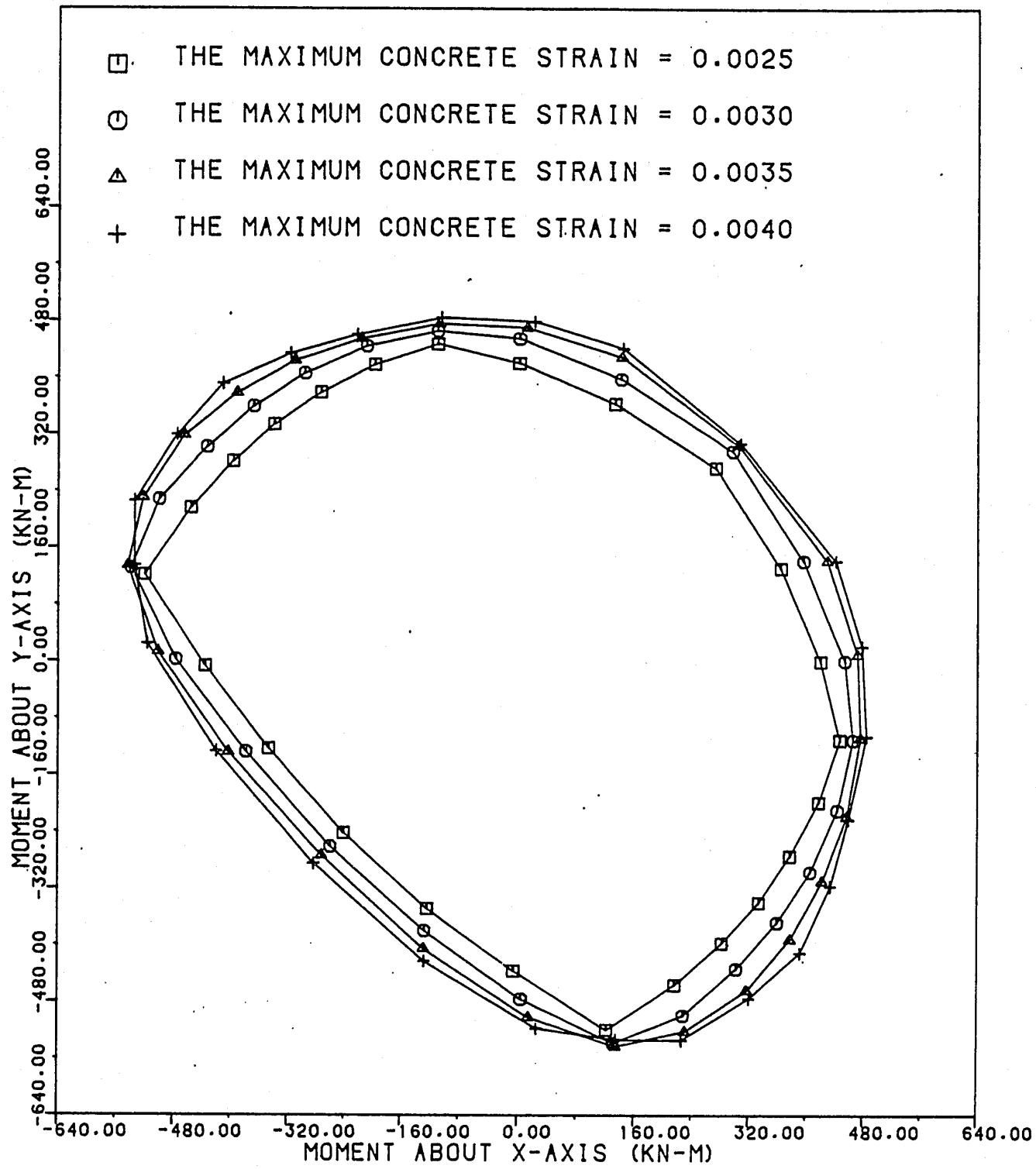

FIGURE 2.4.3.14 : The 3000 KN load isoload contours.

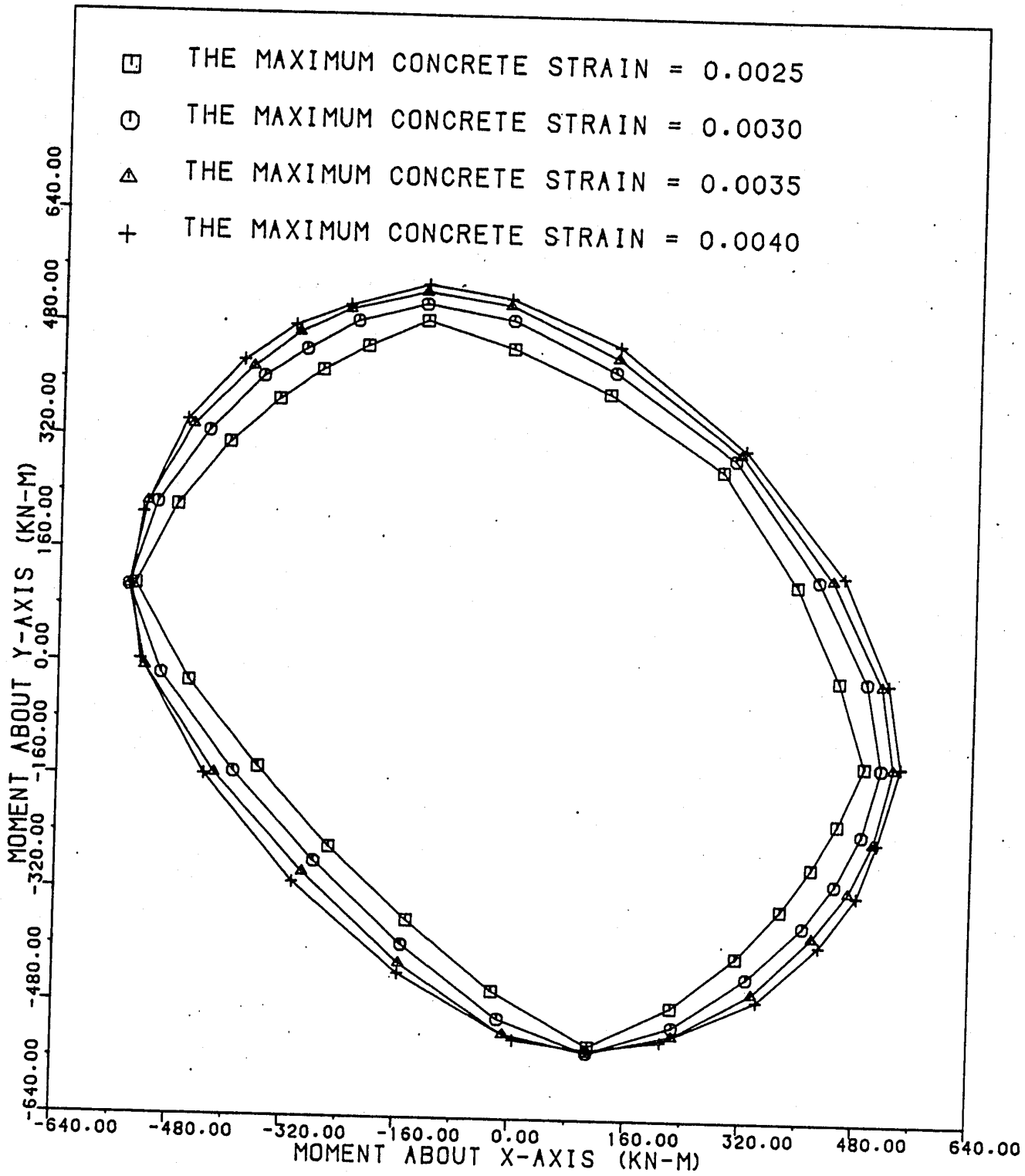

FIGURE 2.4.3.15 : The 2000 KN load isoload contours.

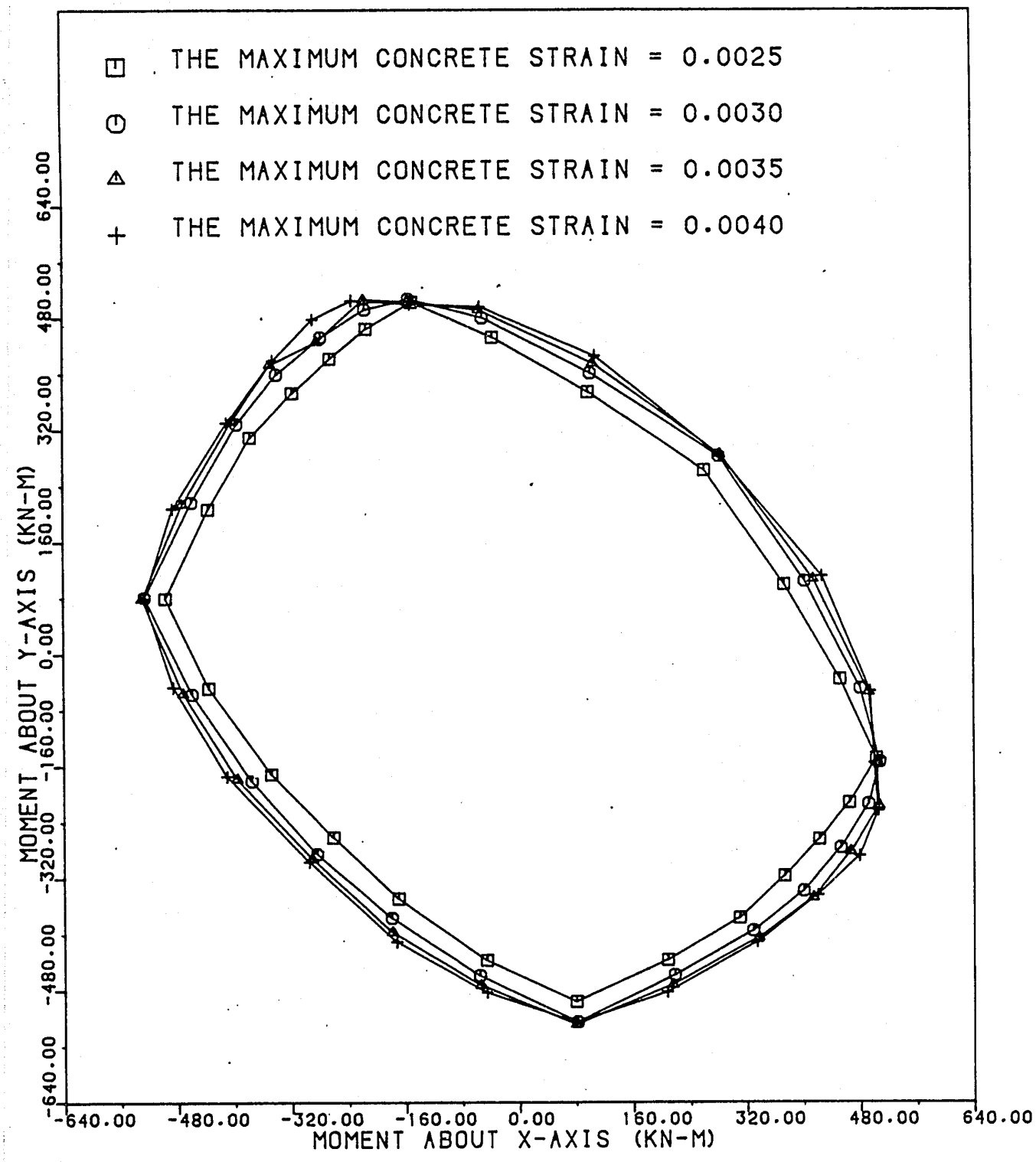

FIGURE 2.4.3.16 : The 1000 KN load isoload contours.

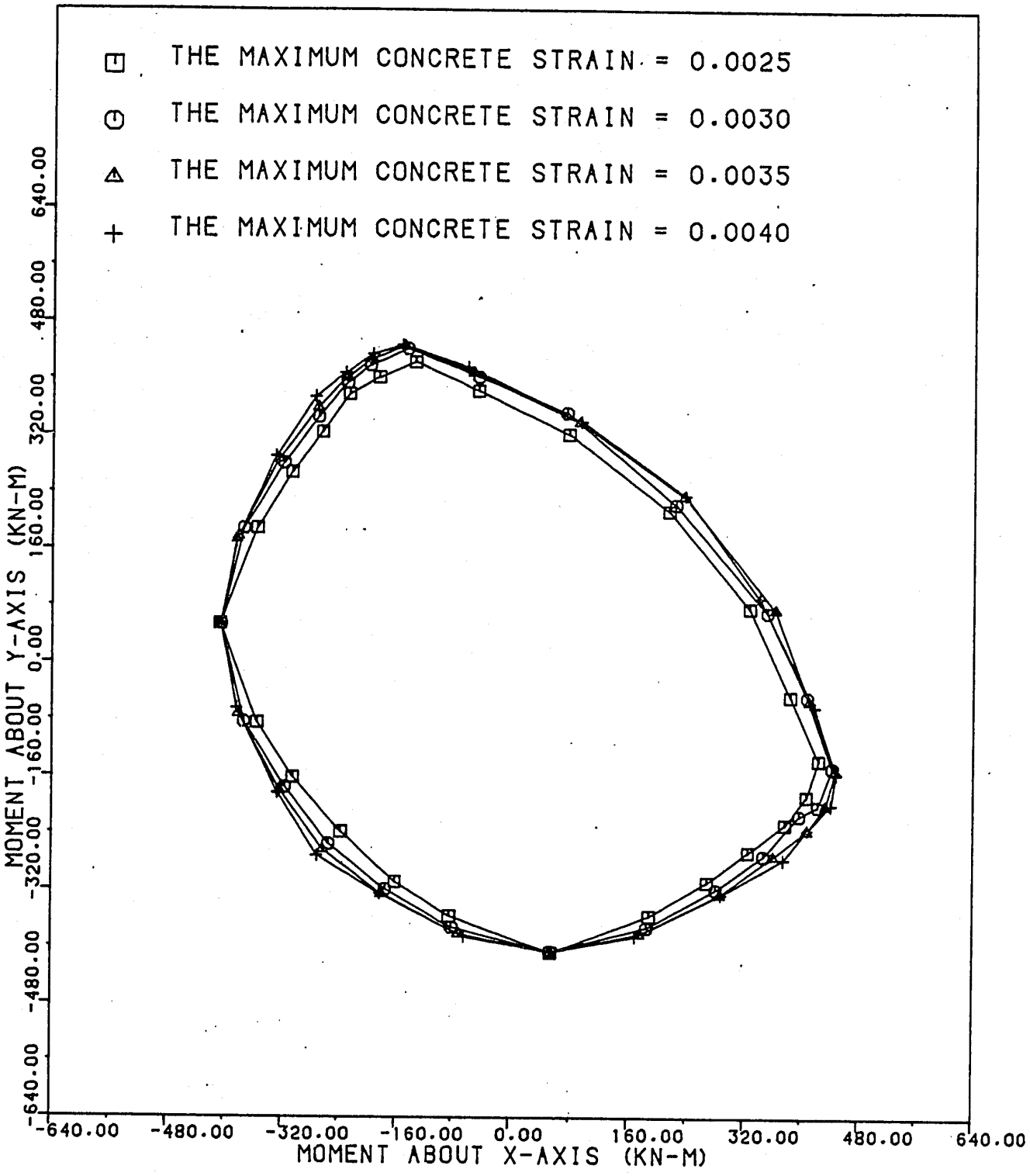

FIGURE 2.4.3.17 : The 0 KN load isoload contours.

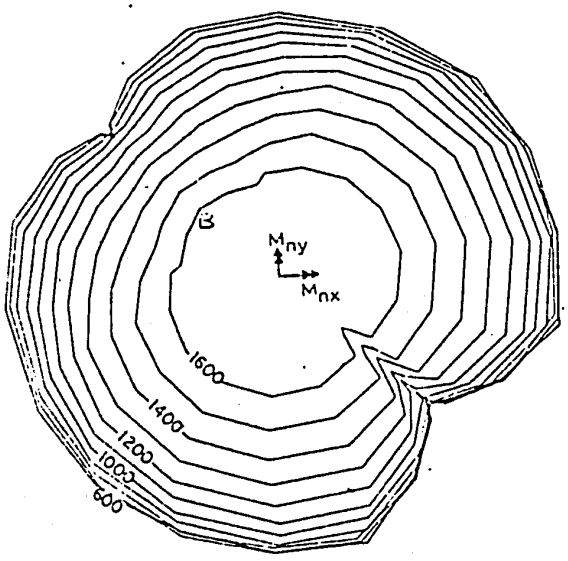

a

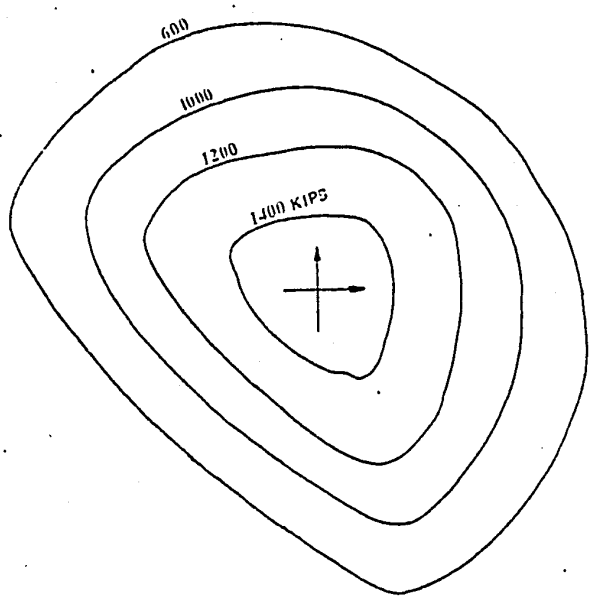

b

FIGURE 3.3.1 : Comparission between the isoload contours presented by Mr. M. Iqbal[A] with those obtained in the present study.[B]